

University of Kentucky

UKnowledge

University of Kentucky Doctoral Dissertations

Graduate School

2009

ROLE OF P33 IN TOMBUSVIRUS REPLICATION

Jozsef Stork

University of Kentucky

[Right click to open a feedback form in a new tab to let us know how this document benefits you.](#)

Recommended Citation

Stork, Jozsef, "ROLE OF P33 IN TOMBUSVIRUS REPLICATION" (2009). *University of Kentucky Doctoral Dissertations*. 684.

https://uknowledge.uky.edu/gradschool_diss/684

This Dissertation is brought to you for free and open access by the Graduate School at UKnowledge. It has been accepted for inclusion in University of Kentucky Doctoral Dissertations by an authorized administrator of UKnowledge. For more information, please contact UKnowledge@lsv.uky.edu.

ABSTRACT OF DISSERTATION

Jozsef Stork

The Graduate School

University of Kentucky

2009

ROLE OF P33 IN TOMBUSVIRUS REPLICATION

ABSTRACT OF DISSERTATION

A dissertation submitted in partial fulfillment of the requirements for the degree of Doctor of Philosophy in the College of Agriculture at the University of Kentucky

By
Jozsef Stork

Lexington, Kentucky

Director: Dr. Peter D. Nagy, Associate Professor of Plant Pathology

Lexington, Kentucky

2009

Copyright © 2009 ELSEVIER

ABSTRACT OF DISSERTATION

ROLE OF P33 IN TOMBUSVIRUS REPLICATION

Replication of the nonsegmented, plus-stranded RNA genome of Cucumber necrosis tomosvirus (CNV) requires two essential overlapping viral-coded replication proteins, the p33 replication co-factor and the p92 RNA-dependent RNA polymerase. In my thesis I describe (i) the effect of phosphorylation of p33, (ii) the RNA chaperone-like activity of p33, and (iii) the role of HSP70s a host proteins in the viral replication. To test the effect of phosphorylation on p33 function, I used in vitro phosphorylated p33. I found that phosphorylation inhibited the ability of p33 to bind to the viral RNA. Phosphorylation-mimicking mutations rendered p33 nonfunctional in plant protoplasts and in yeast.

Based on these results, I propose that the primary function of phosphorylation of p33 is to regulate its RNA binding capacity, which could affect the assembly of new viral replicase complexes, recruitment of the viral RNA template into replication and/or release of viral RNA from replication. Thus, phosphorylation of p33 might help in switching the role of the viral RNA from replication to other processes, such as viral RNA encapsidation and cell-to-cell movement. Small plus-stranded RNA viruses do not code for RNA helicases that would facilitate the proper folding of viral RNAs during replication. Instead, small RNA viruses might use RNA chaperones for replication as shown here for the p33 replication protein. In vitro experiments demonstrated that the purified recombinant p33 facilitated RNA synthesis on plus-stranded and double-stranded (ds)RNA templates up to 5-fold. In addition, p33 rendered dsRNA templates sensitive to single-strand specific S1 nuclease, suggesting that p33 can destabilize highly structured RNA. Altogether, the RNA chaperone activity of p33 might perform similar biological functions to the helicases. SSA a yeast HSP70 found in the viral replication complex and shown to facilitate viral replication (Serva and Nagy, 2006) To dissect the mode of action of SSA in the viral replication I used temperature sensitive and deletion mutants. Both showed miss localization of p33 compared to the wild type. Purified SSA rendered non functional bacterial expressed p92 functional in an in vitro replication assay. SSA might play a role in the transportation and assembly of viral replication proteins.

KEYWORDS: Tombusvirus, phosphorylation, RNA, chaperone, host factor.

Jozsef Stork

02/13/2009

ROLE OF P33 IN TOMBUSVIRUS REPLICATION

By

Jozsef Stork

Dr Peter Nagy 02/13/2009

Dr Lisa Vaillancourt 02/13/2009

RULES FOR THE USE OF DISSERTATIONS

Unpublished dissertations submitted for the Doctor's degree and deposited in the University of Kentucky Library are as a rule open to inspection, but are to be used only with the due regard to the rights of the authors. Bibliographical references may be noted, but quotations or summaries may be published only with the permission of the author, and with the usual scholarly acknowledgments.

Extensive copying or publication of the dissertation in whole or in part also requires the consent of the Dean of the Graduate School of the University of Kentucky.

A library that borrows this dissertation for the use by its patrons is expected to secure the signature of each user.

Name

Date

DISSERTATION

Jozsef Stork

The Graduate School
University of Kentucky

2009

ROLE OF P33 IN TOMBUSVIRUS REPLICATION

DISSERTATION

A dissertation submitted in partial fulfillment of the
requirements for the degree of Doctor of Philosophy in the
College of Agriculture
at the University of Kentucky

By
Jozsef Stork

Lexington, Kentucky

Director: Dr. Peter D. Nagy, Associate Professor of Plant Pathology

Lexington, Kentucky

2009

Copyright © 2009 ELSEVIER

Table of Contents

List of figures	v
CHAPTER I.....	1
General introduction	1
Goals and hypothesizes.....	6
CHAPTER II.....	10
Phosphorylation of the p33 replication protein of Cucumber necrosis tomosvirus adjacent to the RNA binding site affects viral RNA replication	10
Introduction.....	10
Results.....	13
Discussion.....	21
Materials and methods	24
CHAPTER III	40
Inhibition of in vitro RNA binding and replicase activity by phosphorylation of the p33 replication protein of Cucumber necrosis tomosvirus	40
Introduction.....	40
Results.....	41
Discussion.....	48
Materials and methods	53
CHAPTER IV	67
RNA chaperone activity of the tomosviral p33 replication protein facilitates initiation of RNA synthesis by the viral RdRp	67
Introduction.....	67
Results.....	69
Discussion.....	75
Materials and Methods.....	78
CHAPTER V	96
Role of a host HSP70 protein in viral replication	96
Introduction.....	96
Results.....	98
Discussion.....	102
Materials and methods	104
CHAPTER VI.....	117
Summary.....	117

Future directions	119
References	120
VITA.....	128

List of figures

Chapter II

Fig. 2.1 Location of the predicted phosphorylation sites in the CNV replication proteins.....	29
Fig. 2.2 Detection of in vivo phosphorylated replication proteins of CNV and TCV.....	30
Fig. 2.3 In vitro phosphorylation of p33 by a plant kinase.....	31
Fig. 2.4 In vitro phosphorylation at S210 and T211 residues of p33 by PKC.....	32
Fig. 2.5 Comparison of accumulation of CNV gRNA carrying phosphorylation-mimicking mutations adjacent to the RPR-motif in p33/p92 gene.....	33
Fig. 2.6 Effect of phosphorylation-mimicking mutations on accumulation of (A) CNV (+) RNAs and (B) p33 replication protein.....	35
Fig. 2.7 Effect of phosphorylation-mimicking mutations on accumulation of DI-72 RNA in trans.....	36
Fig. 2.8 Phosphorylation-mimicking mutations affect the function of p33, and a lesser extent, p92.....	37
Fig. 2.9 Effect of phosphorylation-mimicking mutations on DI RNA replication in yeast.....	38
Fig. 2.10 Nonphosphorylation-mimicking mutant of CNV shows delay in gRNA accumulation and symptom formation in <i>N. benthamiana</i> plants.....	39

Chapter III

Fig. 3.1 Proposed effect of CNV p33 phosphorylation on its ability to bind to the viral RNA.....	57
Fig. 3.2 Reduced RNA binding by the phosphorylation-mimicking p33 mutants in vitro.....	58
Fig. 3.3 The nonphosphorylated wt p33 binds both DI-72(+) and (-) RNA more efficiently than the phosphorylation-mimicking mutant.....	59
Fig. 3.4 Phosphorylation inhibits the ability of p33 to bind to the viral RNA and facilitates the release of bound RNA from the p33: RNA complex.....	61
Fig. 3.5 Phosphorylation-mimicking mutations in p33 inhibit the assembly of functional CNV replicase complexes in yeast.....	63
Fig. 3.6 Phosphorylation does not inhibit the activity of the preassembled functional CNV replicase complexes in vitro.....	64
Fig. 3.7 Effect of phosphorylation site mutations in p33 on in vitro asymmetrical RNA synthesis by the CNV replicase obtained from yeast.....	65
Fig. 3.8 A model on the role of phosphorylation of p33 in CNV replication.....	66

Chapter IV

Fig. 4.1 Unwinding of the ssDNA/ssRNA hybrid by p33 in a strand separation assay.....	82
Fig. 4.2 Increased sensitivity of dsRNA to single-strand specific S1 nuclease due to the RNA chaperone activity of p33.....	83
Fig. 4.3 Recombinant CNV p33 promotes the self cleavage activity of the satellite <i>Tobacco ringspot virus</i> ribozyme in vitro.....	85
Fig. 4.4 Recombinant p33 promotes initiation on RNA templates by the RdRp. (A) Schematic presentation of the ssDNA/ssRNA hybrid template used to program the TCV p88C RdRp preparation in vitro.....	86
Fig.4.5 Recombinant CNV p33 promotes initiation on dsRNA template by the recombinant TCV RdRp.....	88
Fig. 4.6 The lack of RNA chaperone activity of p33 mutant missing the N-terminus in vitro.....	90
Fig. 4.7 The RNA binding sequences are predicted to be present within intrinsically disordered (unstructured) regions in p33 replication proteins of five tombusviruse..	92
Fig. 4.8 A model on the possible role of the RNA chaperone activity of p33 in tombusvirus replication.....	94

Chapter V

Fig 5.1 RDRP activity of yeast cell free extract membrane fraction with added MBP p33 and p92	111
Fig 5.2 Effect of high concentration (1.2 M) salt washing during affinity purification of Flag tagged Ssa1 p on RDRP activity of yeast cell free extract membrane fraction with added MBP p33 and p92	112
Fig 5.3 RDRP activity of yeast cell free extract membrane fraction with added mutant and wt Ssa1 p.....	113
Fig 5.4 RDRP activity of membrane enriched fractions obtained from wt Ssa 1 ssa 2, 3, 4 and ts Ssa 1 ssa 2, 3, 4 yeast strains grown at permissive temperature.....	114
Fig 5.5 Northern blot analysis of the replicon RNA isolated from wt Ssa 1 ssa 2, 3, 4 and ts Ssa 1, ssa 2, ssa 3, ssa 4 yeast strains grown at different temperatures..	115
Fig 5.6 Western blot analysis of membrane fractions of yeast cell free extract membranes incubated with purified Ssa 1P with or without ATP.....	116

CHAPTER I

General introduction

Positive stranded RNA plant viruses

Plant viruses are intracellular pathogens. During their life cycle they replicate and encapsidate inside the infected plant cell. The majority of plant viruses are positive stranded RNA viruses. The life cycle of positive stranded RNA consists of entering the plant cell, disassembly (removal of the capsid proteins that leads to exposure of the viral RNA to the ribosomes), translation of the viral RDRP (RNA dependent RNA polymerase) and auxiliary replication proteins from the viral genomic RNA, genome replication and transcription using the genomic RNA as a template, encapsidation of the newly transcribed RNA, and cell-to-cell movement. Plant RNA viruses, however, have small genomes encoding only a few (4-10) proteins. To complete the multiple tasks during the infection cycle they utilize not only the viral-coded proteins but co-opt host encoded proteins as well, reprogramming the infected cell into, a virus producing mode.

The key event in a positive strand RNA infection cycle is genome replication. Since the positive strand RNA viruses use a unique enzyme for their replication (RNA dependent RNA polymerase), this unique event is a good target for future antiviral drugs. During the replication a (+) RNA virus uses its RNA for recruiting the replicase complex (RC), which consists of viral and host proteins (Pogany et al., 2005). The viral RNA contains cis-acting regulatory regions to control the replication process and subgenomic RNA synthesis (Pogany et al., 2003). The replication of the (+) RNA viruses is an asymmetric process that produces the positive (mRNA sense) strand progeny in 20-100 excess over the negative sense RNA (Nagy, 2008). The viral replication complexes utilize different subcellular membranes as “platforms” for replication, including endoplasmatic reticulum, mitochondria, vacuoles, Golgi, chloroplasts, and peroxisomal membranes (Salonen et al., 2004). During the course of my PhD work, I focused my research on positive strand (+) plant viral replication using the intensively-studied tombusviruses as model viruses.

Tombusviruses

Tombusviruses are emerging plant pathogens that are among the best characterized plant viruses (White and Nagy, 2004). Tombusviruses, such as Tomato bushy stunt virus (TBSV) and Cucumber necrosis virus (CNV), have monopartite, 4.8 kb long single-stranded RNA genomes with mRNA-sense polarity. They belong to supergroup 2 viruses that include important plant pathogens (luteoviruses, carmoviruses, and others), human and animal pathogens (hepatitis C virus, flaviviruses, pestiviruses), and bacteriophages (Qbeta). Tombusviruses have a nonsegmented genomic RNA with five open reading frames (ORF), two of which code for essential replication proteins, termed p33 and p92. P33 and p92 were shown to be essential for tombusvirus replication (Oster et al., 1998) and recombination (Panaviene and Nagy, 2003). Both p33 and p92 are directly translated from the genomic RNA and p92 is the result of translational readthrough of the translation stop codon at the end of the p33 ORF. Due to the protein expression strategy of tombusviruses, the N-terminal portion of p92 overlaps with p33 (Scholthof et al., 1995). p 92 contains the signature RdRp motifs and together with p33 is part of the tombusvirus replicase (Scholthof et al., 1995). The auxiliary p33 is a replication co-factor that plays a role in template selection (Pogany et al., 2005) and viral RNA recruitment into replication (Monkewich et al., 2005; Panavas and Nagy, 2005) via selectively binding to a conserved stem-loop element [RII-SL(+), a high-affinity binding sequence for p33, termed p33 recognition element, or p33RE] present within the p92 ORF. P33 binds to the viral RNA via its arginine–proline-rich (RPR) domain, which was shown to be essential for tombusvirus replication (Panaviene et al., 2003; Rajendran and Nagy, 2003), and it also affects subgenomic RNA synthesis and RNA recombination (Panaviene and Nagy, 2003). Together, with the viral RNA, p33 is required for the assembly of the functional replicase complex (Panaviene et al., 2004; Panaviene et al., 2005), which also contains the p92 RNA-dependent RNA polymerase and possibly host factors. In addition to protein: RNA interactions, the assembly of the replicase might be aided by interactions between p33 and other p33

and p92 molecules, which are essential for replication (Rajendran and Nagy, 2004). Altogether, p33 is likely involved in many essential replication functions, such as template RNA binding (Monkewich et al., 2005; Panavas and Nagy, 2005; Pogany et al., 2005), assembly/disassembly of the viral replicase complex (Panaviene et al., 2004; Panaviene et al., 2005), targeting and/or attaching the replicase complexes to subcellular membranes (Navarro et al., 2004; Panavas and Nagy, 2005), complementary RNA synthesis, release of the newly made viral RNA progeny from the site of replication, and so on. P33 seems to be a multifunctional protein affecting viral RNA replication and possibly other processes (Burgyan et al., 2000).

Posttranslational modifications of viral proteins

Posttranslational modification of proteins affects the functions and stability of many cellular proteins, such as those involved in the control of gene expression, signal transduction and cell cycle regulation. The most common posttranslational modification is reversible phosphorylation/dephosphorylation, which could serve as a switch between active and inactive forms of proteins (Hunter and Karin, 1992). For example, an important cellular antiviral defense system depends on dsRNA-triggered phosphorylation/activation of PKR, which then leads to phosphorylation of eIF2 α and inhibition of translation (Gunnery and Mathews, 1998). The Tat protein of Human immunodeficiency virus-1 (HIV) is known to inhibit PKR activity by competing with eIF2 for phosphorylation by the activated PKR. The interaction between Tat and PKR requires the RNA binding region of Tat (Brand et al., 1997; Gunnery and Mathews, 1998). Phosphorylation of serine/threonine residues is also known to regulate the formation of protein complexes (Pawson and Scott, 1997), and it can also be used as a signal to trigger ubiquitination and degradation of proteins (King et al., 1996). Phosphorylation of viral proteins is also common. Examples include regulation of function of the viral movement proteins (MP) in plants (Sokolova et al., 1997; Karpova et al., 1999; Waigmann et al., 2000; Trutnyeva et al., 2005). The phosphorylated MP binds to the viral RNA less efficiently than the nonphosphorylated form, which might be important in facilitating the release of the

bound RNA from the MP:RNA complex during cell-to-cell movement of viral RNAs (Waigmann et al., 2000; Lee and Lucas, 2001). Binding of coat protein to viral RNA is also inhibited by phosphorylation (Kann et al., 1999; Ivanov et al., 2001; Ivanov et al., 2003). Protein phosphorylation can also regulate the intracellular distribution of viral proteins (Kann and Gerlich, 1994). Another role of phosphorylation /dephosphorylation is to regulate virus replication. For example, protein: RNA interaction and replicase assembly of animal negative-strand RNA viruses are controlled by phosphorylation (Barik and Banerjee, 1992; Takacs et al., 1992; Gao and Lenard, 1995; Gao et al., 1996; Lenard, 1999). Rapid formation of an RNA binding site in the HIV Rev protein is promoted by phosphorylation of serine residues (Fouts et al., 1997). Similarly, phosphorylation of Rex protein of human T-cell leukemia virus (HTLV) alters the conformation of Rex and its ability to bind to viral RNA, which serves as a switch between the latent and productive phases of the HTLV infection cycle (Narayan et al., 2001; Younis and Green, 2005). Phosphorylation of replication proteins of animal and plant viruses has also been documented, which could regulate interaction between the replication proteins (Hericourt et al., 2000; Kim et al., 2002; Puustinen et al., 2002; Evans et al., 2004; Street et al., 2004). However, the role of phosphorylation /dephosphorylation of replication proteins in plus-strand RNA virus replication is currently poorly understood.

RNA chaperones in viral replication

RNA viruses utilize their genomes not only as templates to produce more viral RNA progeny during replication, but for many other processes, such as translation, regulation of replication, encapsidation and movement from cell to cell. The folding of viral RNAs in biologically relevant conformation is important because the RNA can be trapped in one of many incorrect structures. Therefore, RNA binding proteins, such as helicases and cofactors, have been proposed to play auxiliary roles in most steps during the viral infection process. However, unlike larger RNA viruses, small plus-strand (+)RNA viruses with genomes less than 6,000 nt do not code for RNA helicases (Koonin and Dolja, 1993). This suggest that these small RNA viruses might

not need helicases with robust unwinding functions for their replication or, alternatively, they might recruit RNA helicases(s) from the host. Another alternative possibility is that these RNA viruses might code for RNA chaperones, which are also capable of unwinding/destabilizing RNA structures (Cristofari and Darlix, 2002).

Role of host factors in viral replication

During the genome wide screen of yeast genes (Panavas 2005) a number of host factors were identified that alter viral replication. Recent studies deciphered the mechanism how these proteins affect the replication of positive strand RNA viruses.

Cdc34p ubiquitin-conjugating enzyme was identified as a component of the tombusvirus replicase complex and shown to ubiquitinate p33 replication protein (Li et al., 2008). Downregulation of the cdc34p level decreases the DI-72 accumulation in the yeast based viral replication system, and decreases the activity of the viral replicase purified from the yeast cells with downregulated level of cdc34p expression. The in vitro and in vivo assays demonstrated that cdc34p plays a crucial role in tombusvirus replication.

Tdh2p was shown to co-purify with the viral replicase complex from yeast (Serva and Nagy, 2006). A more recent publication reveals the role Tdh2p plays in tombusvirus replication (Wang and Nagy, 2008). The lack of the tdh proteins in the mutated yeast strain resulted in equal amount of + and – strand accumulation, suggesting that Tdh proteins promote + strand synthesis by selectively binding the negative strand replicon RNA and retaining it in the replicase complex.

In my studies I continued Dr Serva's work who identified HSP70 proteins (Ssa1/2p) in the viral replication complex and showed that downregulation of Ssa1/2p levels inhibited while upregulation of Ssa2p level facilitated viral replication (Serva and Nagy, 2006).

Goals and hypothesizes

The main objective of my research was identifying the role(s) p33 plays in tombusvirus replication. The close focus of my research was to understand the mechanism of the multiple roles of p33 in the viral replication process.

During my study two powerful tools were used extensively, the defective interfering RNA and the yeast replication system.

DI RNA a robust replicon

Tombusviruses are often associated with defective interfering (DI) RNAs (Havelda et al., 1995). The DI RNAs are often called “superparasites” because for their replication they completely rely on the viral replication machinery. They do not encode any functional genes. DI RNAs were discovered by their amelioration of the viral symptoms (Hillman et al., 1987).

A typical DI RNA, such as DI-72, consists of four noncontiguous RNA regions derived from the viral genome. These regions are essential for viral RNA replication. Due to the short length and lack of translation, DI RNAs are better templates for replication than the genomic RNA. DI-72 RNA competes for the replication machinery with the genomic and subgenomic RNA which leads to symptom attenuation and DI RNA accumulation (Hillman et al., 1987). These features make the DI-72 an excellent tool as a surrogate template to study tombusvirus replication.

Yeast as a model host to study viral replication

In recent studies, yeast has emerged as a powerful tool to study viral replication. Viral replication systems were established in yeast with plant viruses: Brome mosaic virus (Janda and Ahlquist, 1993), geminivirus (Raghavan et al., 2004), and with animal viruses (Naito et al., 2007), showing that several viruses can replicate in yeast cells. Dr Panavas in our lab established a novel yeast system (Panavas and Nagy, 2003) capable of supporting the replication of DI-72 replicon RNA when CNV p33 and P92 replication proteins were co-expressed.

The relatively small genome of the yeast (*Saccharomyces cerevisiae*) made it easier to perform genome wide screens identifying host genes which play a role in viral replication. The availability of a single gene deletion library (Yeast Knock Out), two hybrid libraries and, a commercially available yeast overexpression library makes yeast an ideal host to study viral replication (Nagy, 2008).

My studies were evolving around p33 including three major areas, phosphorylation of p33 and its effect on viral replication, the RNA chaperone activity of p33 and the role of a host hsp 70 in viral replication.

Phosphorylation of p33 and its effect on viral replication

The objectives of the phosphorylation study was to show the phosphorylation of p33 at a predicted phosphorylation site in the vicinity of the RNA binding motif, and test the effect of the phosphorylation on the tombusvirus replication.

My hypothesis was that either the 211 S or\and 210 T residue can be phosphorylated, and the negative charge introduced by the phosphorylation interferes with the RNA binding of the p33.

To test my hypothesis first I showed the phosphorylation of p33 in vivo by immunoprecipitating the protein from CNV infected *N. benthamiana* leaves and immunoblotted the p33 with antibodies raised against phosphorylated threonine. To show the phosphorylation of a conserved 210-211 site I developed an in vitro phosphorylation system using *N. benthamiana* leaf extract as a kinase source and a 60

amino-acid long portion of p33 which contains the phosphorylation sites and the RNA binding domain.

After showing the phosphorylation of the conserved 210 S 211 T sites, we mutated the phosphorylation sites and examined the effects of the phosphorylation\unphosphorylation mimicking pointmutations on viral RNA accumulation in infected plants and protoplasts In collaboration with Natalia Shapka. I used the same mutations to test the second part of the hypothesis. Using gel mobility assays I demonstrated that the phosphorylated form of p33 binds significantly lower amount of viral RNA.

RNA chaperone activity of p33

The objective of the chaperone project was to test the RNA chaperone activity of p33. Our hypothesis was that tombusviruses don't use host helicases and\or host RNA chaperones to complete the unwinding an RNA folding processes which can occur during replication because the p33 can act as an RNA chaperone and complete the RNA folding\unwinding tasks needed for replication.

To test this hypothesis I tested the chaperone activity of p33 with by testing the annealing\unwinding capability of the protein on short (15-17 nucleotide) complementary RNA strands. RNA chaperones facilitate unwinding in high concentrations and annealing in low concentrations. My results showed very weak chaperone activity. I used the other published general RNA chaperone test, whether p33 interferes with the shelf cleaving activity of a ribozyme. Again my results showed really weak interference.

To show unwinding facilitated by p33 I used s1 nuclease. When I added s1 nuclease to the unwinding reaction, it digested the unwound single stranded RNA freeing up p33 to unwind another double stranded RNA molecule. Finally I used double stranded RNA as a template in an in vitro RDRP reaction while adding p33 in an increasing concentration, and showed that p33 facilitates the initiation of p88c (TCV RDRP) on double stranded templates.

Role of a host HSP 70 in viral replication

The objective of this study was to show the role of a host HSP 70 (Ssa) in viral replication. My hypothesis was that Ssa facilitates the transportation and membrane insertion of p33 and p92.

To test the hypothesis I used temperature sensitive mutant Ssa p and in collaboration with Dr Robert Wang we showed that p33 localizes in the cytosol without the Ssa function. The membrane insertion was shown by western blott analysis of the yeast membrane fraction in the presence and in the absence of Ssa. While experimenting with the membrane insertion of p33 I was able activate the recombinant p33 p92- MBP proteins expressed in E. coli, which were inactive without the Ssa function.

CHAPTER II

Phosphorylation of the p33 replication protein of Cucumber necrosis tobravirus adjacent to the RNA binding site affects viral RNA replication

Introduction

Replication of plus-strand RNA viruses, which are the most abundant among plant, animal, and human viruses, is performed by viral replicases (Buck, 1996; Ahlquist, 2002; Ahlquist et al., 2003). The viral replicase consists of viral proteins, including the RNA-dependent RNA polymerase (RdRp), and putative host factors. In spite of their significance in virus replication, our current understanding of the roles of viral and host proteins is incomplete. These proteins are likely subject to posttranslational modification(s), which could affect/regulate their functions in viral replication. Indeed, reversible phosphorylation and other posttranslational modifications are important for the functions of many cellular and viral proteins. For example, protein phosphorylation/dephosphorylation is frequently used as an “on–off switch”, allowing regulation of protein function.

While considerable information is available for the role of phosphorylation of replication proteins in minus-strand RNA viruses, which code for P replication protein, a phosphoprotein (Barik and Banerjee, 1992; Takacs et al., 1992; Lenard, 1999), the role and significance of phosphorylation of replication proteins in plus-strand RNA viruses are currently poorly understood. The examples include phosphorylation and ubiquitinylation of Turnip yellow mosaic virus RNA-dependent RNA polymerase (RdRp) (Hericourt et al., 2000) and the Vpg of potyviruses (Puustinen et al., 2002). Also, phosphorylation of CMV 2a RdRp protein was shown to occur late in infection, affecting its interaction with the 1a replication protein (a methyltransferase and helicase-like protein) (Kim et al., 2002). Phosphorylation of the NS5A replication protein of hepatitis C virus (HCV) has been indicated to affect HCV replication and cellular signaling, likely facilitating establishment of chronic infections (Huang et al., 2004; Macdonald et al., 2004; Street et al., 2004). Phosphorylation of the NS5B RdRp protein of HCV has been proposed to play

critical role in HCV replication, based on enhanced HCV replication in cells overexpressing protein kinase C-related kinase 2 (PRK2, a host kinase), which is known to interact with NS5B (Kim et al., 2004). In addition to the proposed role of phosphorylation in virus replication, posttranslational modification also affects the functions of other viral proteins, as demonstrated for movement (MP) and coat proteins (CP) of plus-stranded RNA viruses of plants (Waigmann et al., 2000; Ivanov et al., 2003).

Because posttranscriptional modifications of the replication proteins might play roles as molecular switches in the replication process by altering the properties of the replication proteins, we tested if the tombusvirus p33 is phosphorylated in infected plants. This study establishes that phosphorylation of the p33 replication protein takes place both *in vivo* and *in vitro*. Using kinase-containing plant extract, the phosphorylation sites were mapped to threonine/serine (T/S) residues located in the vicinity of the RNA-binding site, suggesting the possible role of phosphorylation in modulating the RNA-binding activity of p33. Using phosphorylation-mimicking aspartic acid (D) mutants of p33, we demonstrate that phosphorylation of the T/S residues in p33 could influence subgenomic versus genomic RNA synthesis and the ratio between plus- and minus-stranded RNAs. Phosphorylation incompetent alanine (A) mutants of CNV replicated slower than wild type in plant protoplast and showed less severe symptoms in *Nicotiana benthamiana* plants. In summary, our data promote a regulatory role for phosphorylation of p33 in tombusvirus replication.

Rationale

Sequence comparison of p33 replication proteins of tombusviruses (Fig. 2.1A) revealed the presence of conserved S and T residues (i.e., T205, S210, and T211) adjacent to the previously identified arginine (R) and proline (P)-rich RNA-binding site (termed RPR-motif, R213P214R215R216R217P218) (Fig. 2.1B). These S and T residues are likely phosphorylated in cells based on NetPhos analysis (i.e., they showed the probability of 0.8–0.9 relative value on a scale of 0.0–1.0 for phosphorylation) (software: NetPhos, version 2.0, Technical University of Denmark) (Fig. 2.1B). Possible phosphorylation of these S and T residues in p33 would introduce negative charge in the vicinity of the positively charged RPR-motif, thus likely decreasing the RNA-binding capacity of p33. In support of this model, substitutions of A for arginines (R), which reduced the overall positive charge of the RPR motif, inhibited the ability of p33 to bind to the viral RNA as well as decreased tombusvirus replication in plant protoplasts (Panaviene and Nagy, 2003). Based on these observations, we predicted that phosphorylation of p33 adjacent to the RPR-motif could be a regulatory “switch”, affecting its biological function(s) in tombusvirus-infected cells.

The experiments in this chapter were done in collaboration with Natalja Shapka. She did the plant and protoplast experiments (fig 2.5; 2.6; 2.7; 2.10). See enclosed letter from DGS.

Results

In vivo phosphorylation of CNV p33 and the related TCV p28 replicase proteins

To test if the CNV p33 and the related TCV p28 replication proteins are phosphorylated in plants, first I enriched p33 and p28, respectively, in our samples by isolating membrane-enriched fractions from CNV and TCV-infected *N. benthamiana* plants [10 days postinoculation (dpi)]. This approach is based on previous findings that the membrane-fraction contains the active CNV and TCV replicases (Song and Simon, 1994; Nagy and Pogany, 2000) and the viral replication proteins (Fig. 2.2A (Panaviene et al., 2004)). The obtained fractions were treated with SDS, followed by SDS-PAGE electrophoresis and blotting on PVDF membranes for Western blot analysis. I used antibody specifically recognizing either phosphorylated T or S residues for the Western blot assays (Kim et al., 2004). Data obtained with the anti-phosphothreonine antibody (Fig. 2.2B) showed that membrane-enriched fraction from CNV and TCV-infected plants contained phosphorylated T residues in p33 and p28, whereas healthy plants lacked similar proteins. In contrast, the anti-phosphoserine antibody-based assay was not sensitive enough to detect phosphorylated p33 and p28 (not shown). In addition, we also captured p33 with anti-p33 antibody from CNV-infected plants (using isolated membrane-enriched fraction, which was treated with 2% Triton X-100 to solubilize p33) on a protein A column, followed by elution. The recovered proteins were analyzed by SDS-PAGE, followed by staining with Pro-Q Diamond (Molecular Probes), a phosphoprotein-specific dye. This assay showed the presence of phosphorylated CNV p33 in plants (Fig. 2.2C). Overall, both the Western blot with phosphothreonine-specific antibody and the staining assay with phosphoprotein-specific dye demonstrated that the CNV p33 (and the related TCV p28) replication protein is phosphorylated at T residue(s) in infected cells.

In vitro phosphorylation of serine and threonine residues adjacent to the RNA-binding domain in p33

To determine if the conserved T205, S210, and T211 residues located adjacent to the RNA-binding site in p33 (Fig. 2.1A) can be phosphorylated, as predicted by NetPhos program, I developed an in vitro phosphorylation assay based on partially-purified kinase preparation obtained from healthy *N. benthamiana* plants. First, I prepared a membrane-enriched fraction from uninfected plants using the procedure developed for isolation of p33 (see above) and the CNV replicase (Panaviene et al., 2004). Then, I performed a phosphorylation assay including the kinase in the membrane-enriched preparation, ³²P-labeled ATP, and purified peptides including or lacking the predicted phosphorylation sites adjacent to the RPR-motif in p33 (Fig. 2.3). After the kinase reaction, the radioactively-labeled peptides were detected using SDS-PAGE/PhosphoImager analysis. This assay demonstrated that the peptide p33C181–240 containing the predicted T205, S210, and T211 phosphorylation sites could be efficiently phosphorylated in vitro by the partially-purified plant kinase (Fig. 2.3A). The second peptide (p33C211–240), which was not phosphorylated in this assay, lacked T205, S210 residues and contained only T211 residue in an unfavorable context (Fig. 2.3A). Overall, these experiments demonstrated that healthy *N. benthamiana* plants contain a membrane-associated kinase capable of phosphorylating p33 in vitro at one or more of the conserved T205, S210, and T211 residues.

Based on NetPhos analysis, the probable kinase involved in phosphorylation of T205, S210, and T211 residues in p33 is a protein kinase C (PKC)-like kinase. Interestingly, PKC-like kinase activity has been detected in plants (Sokolova et al., 1997; Lee and Lucas, 2001). Therefore, I tested if purified PKC preparation (Sigma) could phosphorylate p33-derived peptides in vitro. The in vitro kinase assay revealed efficient phosphorylation of a 30 aa-long peptide p33C205–234 carrying wt sequences and less efficient phosphorylation of mutant D210, where as mutants A210A211 and D211 (in the context of p33C205–234) were not phosphorylated at a detectable level (Fig. 2.4A). Thus, these experiments demonstrated that T211 residue can be phosphorylated by PKC, but no data for phosphorylation of S210 residue was

obtained. The lack of phosphorylation of S210 residue in mutant D211 (Fig. 2.4A) could be due to the sequence change at position 211, because the sequence context of the phosphorylation site is known to affect the efficiency of phosphorylation. To circumvent this problem, I treated the wt p33C205–234 peptide with PKC, followed by detection of phosphorylated serine with anti-phosphoserine antibody (Fig. 2.4C). This experiment demonstrated that S210 residue could be phosphorylated by PKC in vitro. Therefore, we conclude that both S210 and T211 residues can be phosphorylated by PKC in vitro.

Effect of phosphorylation of CNV p33 on virus replication based on the use of phosphorylation-mimicking mutants

Because phosphorylation of neutral S and T residues introduces negative charge around these residues, effect of phosphorylation on protein function can be tested by mutating these residues to D, which is negatively-charged. In contrast, the non-phosphorylated status of S and T residues can be mimicked by mutating S and T residues to A, which is neutral. Thus, D mutation mimics the phosphorylated, while A mutation mimics the nonphosphorylated forms of S and T residues as previously demonstrated in numerous assays (Waigmann et al., 2000; Jabbur et al., 2001; Kim et al., 2002; Freye-Minks et al., 2003; Jia et al., 2004). Another advantage is that both D and A residues are similar in sizes to S and T residues, thus likely minimizing the sterical/structural changes caused by these mutations. In spite of the above advantages, D mutations only “mimic” phosphorylation, thus results obtained with D mutants could possibly cause problems unrelated to phosphorylation.

A set of 12 single, double, and triple A/D mutations was introduced at T205, S210, and T211 within the p33/p92 open reading frame in an infectious cDNA clone of CNV (Rochon, 1991). Note that the above mutations changed the sequences of the overlapping p33 and p92 replication proteins (Fig. 2.1A). I then generated CNV RNA transcripts in vitro, followed by electroporation to *N. benthamiana* protoplasts to test the replication features of the mutated CNV proteins. Total RNA was extracted 12 and 24 h after electroporation and analyzed by Northern blotting. These experiments

demonstrated that single and double D for S/T substitutions (at positions S210 and T211) reduced the ability of CNV to replicate to detectable levels (constructs with single mutations, such as D210, and D211, and double mutation, D210D211, Fig. 2.5A). In addition, mutant D205 replicated poorly (<1% at 12, and 7% of wt at 24 h time points, lanes 18 and 26, Fig. 2.5A). These data suggest that negative charge(s) at positions S210, T211, and, to a less extent, at T205 inhibits CNV replication.

All single and double A mutants (at T205, S210, and T211) mimicking the nonphosphorylated form of p33/p92 supported replication, albeit with reduced efficiency (34–58% of wt CNV gRNA) when compared to wt (Fig. 2.5A). Even the triple A mutant (construct A205A210A211, accumulation level of 13–21% of wt, lanes 19 and 27, Fig. 2.5A) was replication competent, suggesting that nonphosphorylated residues at positions 205, 210, and 211 are important for the function(s) of replicase proteins *in vivo*. However, because all these A mutants replicated less efficiently than wt, it is likely that phosphorylation of p33/p92 plays a regulatory role during virus replication (see below).

To demonstrate that the above mutations at T205, S210, and T211 in CNV affected replication due to changes in the p33/p92 replication proteins, but not due to altered CNV RNA structure, I tested the ability of the mutated CNV replication proteins to support replication *in trans*, using a model template, DI-73 RNA (Fig. 2.5B). Co-electroporation of DI-73 RNA with the CNV helper (wt or D210D211) into plant protoplasts demonstrated that CNV D210D211 did not support replication of DI-73 RNA *in trans*, indicating that the phosphorylation-mimicking replication protein(s) is not functional *in vivo*.

To test if the above CNV mutants expressed p33 in comparable amounts, I performed Western blotting on total protein extracts obtained from protoplasts 12, 18, and 24 hpi with an antibody specific for the C-terminal portion of p33 (outside the mutagenized domain of p33). We found that D210D211 p33 was not detectable (Fig. 2.5C), whereas the amount of D210A211 was only 10% of wt p33 (Fig. 2.6B). The accumulation of A210A211 p33 was comparable to wt p33. The reduced accumulation of phosphorylation-mimicking p33 mutants in plant protoplasts can be explained by several alternative models including decreased stability and/or

production of these p33 forms. To exclude some of these explanations we further analyzed the mutants in a yeast system.

Hypophosphorylation-mimicking p33 mutants affected plus-strand RNA and subgenomic RNA synthesis in vivo

To test for possible regulatory roles of phosphorylation of p33/p92 in replication, we performed time-course experiments in protoplasts with a viable nonphosphorylation-mimicking mutant, a hypophosphorylation mutant (i.e., D210A211 carrying only a single D mutation), and the wt (Fig. 2.6). Total RNA samples were prepared from protoplasts and analyzed with Northern blotting as described above. These experiments revealed that nonphosphorylation-mimicking A210A211 and the partial (hypo)-phosphorylation-mimicking D210A211 mutants generated 5–6 times more subgenomic (sg) RNA2 than sgRNA1 at early time points, whereas sgRNA2 was approximately 3-fold more abundant than sgRNA1 in the wt CNV infections (Fig. 2.6A). Altogether, sgRNA2 was the most abundant viral RNA species in A210A211 and D210A211 infections, in contrast to wt CNV, which produced the gRNA in the largest amount (except at the early time point, Fig. 2.6A). These data suggest that phosphorylation status of S210 and T211 in p33/p92 could affect the level and ratio of sgRNA1 and sgRNA2 synthesis in CNV infections.

To test if mimicking mutations could also affect minus- versus plus-strand synthesis during CNV replication, we took advantage of DI-72 RNA replicon, which produces minus-strand RNA at easily detectable levels (Monkewich et al., 2005). In this assay, *N. benthamiana* protoplasts were co-electroporated with wt or mutated (A210A211, A205A210A211, and D210A211) CNV RNA and DI-72 RNA, followed by detection of plus- and minus-strand DI-72 RNA levels in total RNA samples by Northern blotting (Fig. 2.7). We observed that DI-72 minus-strand synthesis took place at low levels (10–20%) between 4 and 12 h postinfection (hpi), followed by increased synthesis between 12 and 24 h in the presence of wt or any of the mutated helper CNV. On the contrary, plus-strand RNA synthesis showed remarkable differences depending on the wt and mutated helper CNV (Fig. 2.7A). For example,

detectable level of DI-72 plus-strands was observed as early as 6 and 8 hpi in the presence of wt CNV helper, whereas A205A210A211 and D210A211 mutants of CNV accumulated DI-72 plus-strands at a detectable level only at 12 hpi (Fig. 2.7A). Interestingly, the relative level of minus-strand accumulation (when compared to wt level of minus strands representing 100%) supported by A205A210A211 and D210A211 mutants was 20% higher than the relative level of plus-strand accumulation (Fig. 2.7C). The altered ratio between minus and plus-strand accumulation means that the RNA synthesis was less asymmetrical with the above mutants than in the case of wt CNV replicase. Overall, these observations indicate that the phosphorylation status of p33 at positions 205, 210, and 211 might affect the level of asymmetry between plus-versus minus-strand synthesis.

Phosphorylation-mimicking mutations inhibit the function of p33 more than p92 in protoplasts

To test if phosphorylation-mimicking mutations inhibit p33 and/or p92 functions in plant cells, we utilized a two-component complementation-based replication assay developed by Oster et al. (Oster et al., 1998), which allows separate mutagenesis of p33 and p92. Expression of p33 and p92 (the p92 ORF contains a tyrosine mutation to suppress termination at the end of p33 ORF, Fig. 2.8A) from two separate RNAs leads to efficient replication of DI-p33, whereas CNV-Y replicates poorly in *N. benthamiana* protoplasts (Figs. 2.8B–C and (Panaviene et al., 2003; Panaviene and Nagy, 2003)). We found that co-expression of the unmodified p92Y with D210D211 mutation in p33 led to undetectable level of DI-p33 replication (Fig. 2.8B), suggesting that phosphorylation renders p33 nonfunctional. On the contrary, the D210D211 mutation in p92Y inhibited wt DI-p33 replication by only 50% (Fig. 2.8C), suggesting that phosphorylation of p92 RdRp protein at 210–211 positions interfered with its replication function to a lesser extent than phosphorylation of p33.

Yeast-based tombusvirus replication assay confirms a role for the phosphorylation status of p33 replication protein in tombusvirus replication

To test if the phosphorylation status of p33 affects its stability and/or functions, I took advantage of the availability of TBSV replicon-based replication assay in yeast expressing the CNV p33 and p92 replication proteins, which supports efficient replication of DI-72 RNA (Panavas and Nagy, 2003). In the yeast system, the expression of p33 and p92 is driven from separate expression vectors via the constitutive ADH1 promoter. The advantage of the yeast replication system is that we can study the replication of the DI-72 RNA without the need of replication and gene expression of the helper virus. This allowed us to re-test if several mimicking mutants of p33 could support tombusvirus replication in yeast.

I found that co-expression of wt p92 together with p33 carrying D for T211 mutation (see constructs D211, D210D211, A210D211, D205D210D211, Figs. 2.9A–C) did not result in DI-72 RNA replication, based on undetectable levels of DI-72 plus- and minus-strands in yeast. Similar mutations at T205 and S210 (see constructs D205 and D210, Figs. 2.9A–C) also reduced replication of DI-72 RNA (down to 12 and 8% of wt levels), but to a lesser extent than observed in plant cells. Western blot analysis of total protein extracts of yeast strains revealed that, unlike in the plant protoplast-based replication assay, the p33 levels in yeast were similar for wt and the mutated p33 (Fig. 2.9D), suggesting that the stability of p33 is not altered by these mutations. Instead, these data indicate that the phosphorylation-mimicking D mutations make p33 less functional/nonfunctional in tombusvirus replication. On the contrary, the nonphosphorylatable A mutations had less pronounced effects on p33 functions (16–57% level of replication, see constructs A210A211, A205A210A211, Figs. 2.9A–C).

I also tested the ability of p33 mutants to support plus- versus minus-strand synthesis of the replicon RNA in yeast. Northern blot analysis of total RNA samples revealed that the relative levels of minus-strand (as compared to wt level representing 100%) versus plus-strand accumulation were 2-to-5-fold higher in case of four out of

five functional p33 mutants (i.e., A210A211; A205A210A211; D210A211; and D205, Figs. 2.9B–C) than that observed with wt p33. However, one p33 mutant (i.e., D210) showed lower relative level of minus-strand versus plus-strand synthesis (Figs. 2.9B–C). Altogether, these data indicate that nonphosphorylation or partial phosphorylation-mimicking mutations in p33 at positions 205, 210, and 211 selectively decrease the level of plus-strand RNA accumulation, likely resulting from less asymmetrical RNA synthesis.

Delayed accumulation of a nonphosphorylation-mimicking mutant in *N. benthamiana* plants

To test if CNV expressing the nonphosphorylation-mimicking A210A211 p33 mutant could replicate with similar efficiency as the wt CNV (expressing phosphorylation-competent p33) in whole plants, I extracted total RNA from CNV-infected leaves 5, 7, and 14 days after inoculation (dpi). I found that wt CNV accumulated viral-specific RNAs to higher levels than A210A211 did at 5 and 7 dpi (Fig. 2.10A), suggesting that virus replication/accumulation is more robust in wt CNV infections. Interestingly, the difference in accumulation level between wt and A210A211 gRNA was more significant in plants than in protoplasts (2-to-2.5-fold difference in plants at 5 and 7 dpi versus 5% in protoplast at 24 hpi). This might be due to an indirect effect of phosphorylation of wt p33 on cell-to-cell movement and/or stability of gRNA. The symptoms caused by the wt CNV infection were also more intensive than in A210A211 infections (Fig. 2.10B), and led to the death of most leaves by 14 dpi. On the contrary, symptoms caused by A210A211 were mild and did not lead to necrosis. Interestingly, viral RNA accumulation was 3-fold higher in A210A211-infected than in wt CNV-infected plants at 14 dpi, likely due to the sickness of wt CNV-infected plants (Fig. 2.10A). Altogether, these data demonstrate that the nonphosphorylatable A mutations at positions 210 and 211 in p33 have pronounced effects on the pathogenicity of CNV in *N. benthamiana*.

Discussion

Detection of phosphorylated replication proteins in plus-strand RNA virus-infected hosts is a challenging task due to the low abundance of viral replication proteins, their localization to less amenable cellular membranes, the dynamic and reversible nature of phosphorylation, and temporally existence of some phosphorylated proteins. By using both anti-phosphothreonine antibody-based Western blot and phosphoprotein-specific staining assays, I demonstrated the accumulation of phosphorylated CNV p33 (and the related TCV p28) replication protein in plants, while I could not detect phosphorylated CNV p92, possibly due to its very low abundance (approximately 20-fold less than p33; (Scholthof et al., 1995). In addition, I obtained a partially-purified kinase preparation from solubilized membrane-enriched fraction of *N. benthamiana*, which was able to phosphorylate the CNV p33 replication protein at conserved S/T residues (likely at T205, S210, and T211) adjacent to the RPR motif, an RNA-binding site (Panaviene et al., 2003; Rajendran and Nagy, 2003). On the contrary, the soluble (cytoplasmic) fraction of cells did not contain kinases capable of phosphorylation of the same region in p33 in vitro (not shown). Because p33 is membrane-associated in cells and tombusvirus replication occurs in membrane-containing compartments (Scholthof et al., 1995; Rubino and Russo, 1998; Navarro et al., 2004; Panaviene et al., 2004; Panavas et al., 2005) it is likely that phosphorylation of p33 takes place in cellular membranes (peroxisomal membrane for CNV; (Panavas et al., 2005) in infected cells. Thus, the kinase(s) present in the membrane-enriched fraction is likely responsible for in vivo phosphorylation of p33. This host kinase is functionally similar to PKC, based on phosphorylation site prediction and demonstration that purified PKC preparation could also phosphorylate recombinant p33 at residues S210 and T211 in vitro (Fig. 2.4). Altogether, I conclude that p33 gets phosphorylated in CNV-infected plants by a membrane-associated host kinase.

The effects of p33 phosphorylation during CNV infection were studied using phosphorylation-mimicking mutants (see rationale in the results section). The advantage of using mimicking mutants is that it simplifies the interpretation of data due to the presence of p33 representing either the “nonphosphorylated” (i.e., alanine

mutants) or “phosphorylated” (aspartic acid mutants) forms of p33 during the entire infection. Disadvantage is that the dynamics of phosphorylation cannot be fully examined with these mutants. Nevertheless, based on data obtained with the mimicking mutants, the model predicting that the nonphosphorylated form of p33 (I refer only to phosphorylation of T205, S210, and T211 in the text below) is the functional form is supported, while the fully phosphorylated form of p33 seems to be nonfunctional in replication. Accordingly, in vitro phosphorylation of p33 and phosphorylation-mimicking mutations in p33 (at S210 and T211 positions) both inhibited the ability of p33 to bind to the viral RNA in vitro (see (Stork et al., 2005), suggesting that phosphorylation and mimicking mutations had similar effect on p33 function. However, I cannot completely exclude that results obtained with D mutants could possibly cause changes in the structure of p33 unrelated to phosphorylation.

The mimicking mutants were also useful to demonstrate that similar phosphorylation of p92 RdRp protein (at T205, S210, and T211), which overlaps with p33 within its N-terminus, had only limited effect on its activity in protoplasts. Thus, I suggest that phosphorylation at T205, S210, and T211 mainly affects p33 function(s) during CNV infections.

In addition to the nonphosphorylated and fully phosphorylated forms of p33, I suggest that hypophosphorylation of p33 at either T205, S210, or T211 positions might affect its activity/function. For example, I observed changes in the ratio of sgRNA1 versus sgRNA2 and of plus- versus minus-strand levels (i.e., strand asymmetry was reduced) with mimicking mutants affecting only one or two of the predicted phosphorylation sites. These observations open up the possibility that hypophosphorylation of p33 might be involved in (i) timing and/or fine tuning of subgenomic RNA synthesis (sgRNA1 versus sgRNA2) and (ii) controlling the timing and/or ratio of plus- versus minus-strand synthesis. For example, hypophosphorylation of p33 might modify the activity of the CNV replicase, affecting the timing of production of different viral RNA species and the ratio of replication products. In contrast, full phosphorylation of p33 (especially phosphorylation of T211 seems to be the most critical) might shut down replication, which could be beneficial for viral RNA encapsidation, cell-to-cell movement, and

other processes by releasing the viral RNA from replication (see the accompanying paper by Stork et al., 2005). Indeed, the nonphosphorylated A210A211 mutant showed delay in gRNA accumulation in systemically infected leaves when compared to the wt CNV, suggesting less efficient virus spread in plants and/or decreased stability of mutant A210A211 gRNA.

The amount of p33 replication protein was not the same in infections with wt and phosphorylation-mimicking CNV mutants in *N. benthamiana* protoplasts (Fig. 2.5 and Fig. 2.6). For example, protoplasts containing a replication incompetent mutant (D210D211) and an inefficiently replicating mutant (D210A211) accumulated p33 at undetectable and reduced levels, respectively (Fig. 2.5 and Fig. 2.6). This suggests that phosphorylation-mimicking aspartic acid mutations (and analogously phosphorylation) might promote rapid p33 degradation, thus affecting the stability of p33. Although I cannot fully exclude that the above D mutations facilitate p33 degradation, this model is not supported by the observation that the amounts and stability of wt and phosphorylation-mimicking D mutants of p33 were comparable in yeast, expressing these proteins constitutively from plasmids (Fig. 2.9D).

Alternatively, it is possible that reduced accumulation of p33 carrying the phosphorylation-mimicking mutations is due to the production of a limited amount of new CNV RNA progeny in cells. I propose that some of the new CNV RNA progeny could participate in new rounds of translation to boost p33/p92 production, and thus replication, in infected cells. The proposed translational boost might not take place for CNV RNA expressing p33 with the phosphorylation-mimicking mutations that produce only limited amount of new progeny plus-strands.

The phosphorylation sites studied in this paper are located adjacent to the positively charged RNA-binding domain in p33 (Fig. 2.1B). Therefore, it is possible that the observed effects of the phosphorylation-mimicking mutants on CNV replication are due to altered RNA-binding capacity of p33. Accordingly, I show in the next chapter the inhibitory effect of phosphorylation of these sites on RNA-binding by the recombinant p33. Thus, phosphorylation of p33 is likely an important step in CNV replication by affecting replicase and template interactions.

Materials and methods

Detection of phosphorylated p33 and p28 replication proteins by Western blotting using phosphothreonine specific antibody or by staining with phosphoprotein-specific dye

Leaves (2 g) of *N. benthamiana* plants systemically infected with CNV and TCV, respectively, were used to obtain the membrane-enriched and soluble fractions as described (Panaviene et al., 2004), except that I included phosphatase inhibitor mix containing 25 mM NaF, 10 mM benzamidine, 10 mM sodium orthovanadate. 1/10th of the obtained membrane-enriched fraction was loaded on a 10% SDS-PAGE gels, electrophoresed, transferred to PVDF membranes, followed by using anti-phosphothreonine and anti-phosphoserine antibodies as recommended by the manufacturer (Research Diagnostic, Inc).

The second method to detect phosphorylated p33 in CNV-infected *N. benthamiana* was based on using the phosphoprotein specific Pro-Q Diamond dye from Molecular Probes. First, I prepared the membrane-enriched fraction (see above), followed by solubilization of membrane-bound proteins with 2% Triton X-100 as described (Nagy and Pogany, 2000; Panaviene et al., 2004). Anti-p33 antibody (prepared against CVGYLKNTPENRLIY peptide, Sigma-Genosys) was then added to the sample, followed by incubation in the cold room and then addition of protein A (Sigma) and further incubation for 60 min. The pellet was recovered after centrifugation, washed three times, and then loaded on an SDS-PAGE gel. The gel was then fixed overnight with 200 ml 10% acetic acid (glacial) and 50% methanol, followed by three time wash with 200 ml deionized water for 15 min. Staining of the gel was done overnight in the dark with 50 ml Pro-Q Diamond dye as recommended by the manufacturer (Molecular Probes). Destaining was done with 200 ml 10% methanol and 7% acetic acid for 30 min. Images of gels were taken when illuminated with 302 nm UV light.

Preparation of host kinase-containing fraction from *N. benthamiana* and in vitro phosphorylation of p33

Young leaves (5 g) of uninfected *N. benthamiana* were used to obtain the membrane-enriched fraction (see above), followed by solubilization with 4% Triton

X-100 exactly as described for preparation of CNV replicase (Panaviene et al., 2004). The solubilized membrane-enriched preparation was passed through Sephadex G-25 resin (Amersham). To reduce the background in subsequent assays, the obtained host kinase preparation was mixed with phosphorylation buffer (0.1 M HEPES pH 7.4, 10 mM EDTA, 5 mM DTT, 50 mM MgCl₂) in the presence of 1 mM ATP to allow phosphorylation of any phosphorylatable proteins that might be present in the preparation for 20 min at room temperature (RT). This was followed by removal of ATP on a Sephadex G-25 column.

To test phosphorylation of CNV p33 *in vitro* by the above kinase-containing plant membrane preparation, I selected two purified recombinant p33-derived peptides, termed C10 (p33181–240) and C11 (p33211–240) (Rajendran and Nagy, 2003), expressed in *E. coli*. The cleavage of the proteins was done with Factor Xa protease (NEB) as described (Rajendran and Nagy, 2003). The *in vitro* phosphorylation reaction was made in 20 μ l volume in the phosphorylation buffer (see above), plus 1 μ l γ ³²P-ATP (7000 Ci/mmol, 0.05 mCi), 2 μ l kinase-containing plant membrane fraction, and 3 μ g of p33-derived peptide. After incubation for 20 min, the samples were run in SDS-PAGE gels, stained with coomassie blue, dried and exposed to a phospho-storage screen, and imaged with a PhosphorImager.

In vitro phosphorylation of p33 with PKC

The affinity-purified p33 mutants (200 μ g/ml, expressed in *E. coli*) (Rajendran et al., 2002), carrying or lacking the T205, S210, and T211 positions, were phosphorylated in 20 μ l volume containing PKC-phosphorylation buffer (20 mM HEPES, 0.03% triton X-100, 4 mM MOPS, 5 mM β -glycerol phosphate, 1 mM EGTA, 0.2 mM Na-orthovanadate, 0.2 mM DTT), 0.1 mM ATP (unlabeled), 5 μ l PKC lipid activator (Upstate), 1 μ l 2 mM CaCl₂, 2.5 μ l γ ³²P-ATP (7000 Ci/mmol, 0.125 mCi), and 0.5 μ l PKC (Sigma), for 15 min at room temperature. Afterwards, the samples were boiled in SDS-PAGE running buffer for 3 min and loaded onto a

large 10% SDS-PAGE gel (Bio-Rad protean II xi). The electrophoresis was performed at 200 V for 6 h, followed by staining with coomassie blue, drying, and then scanning by a PhosphorImager.

Construction and testing of the phosphorylation-mimicking mutants of CNV p33 in *N. benthamiana* protoplasts and plants

To make site-directed mutations that replaced S/T residues with A/D residues, I used standard Quick Change XL Site-Directed Mutagenesis Kit (Stratagene) as described before (Panaviene et al., 2003) based on an infectious CNV clone (Rochon, 1991). The mutant clones were confirmed by sequencing, using Beckman Coulter DTCS Quickstart Kit and primer #958 (5' - CCGGCACGGGAGCTCAAGGGTAAGGA).

Full-length RNA transcripts of CNV (Rochon, 1991), DI-72, and DI-73 (White and Morris, 1994, 1994) were prepared using standard in vitro transcription reaction with T7 RNA polymerase on SmaI linearized DNA templates. *N. benthamiana* protoplasts were prepared as described before (Panaviene et al., 2003). Protoplasts were divided into aliquots (5×10^5 protoplasts) and electroporated with 5 μ g of wt or mutated CNV gRNA and 1 μ g of DI RNA (when the goal was to test DI RNA replication). After electroporation, protoplasts were incubated in the dark at 22 °C.

N. benthamiana plants were rub inoculated with 3 μ g of wt or mutated CNV gRNA. Inoculated plants were kept in the green house. Samples were taken after 5, 7, and 14 dpi.

CNV RNA extraction and Northern blotting

Total RNA was prepared from protoplast or plants using a standard phenol/chloroform method (Kong et al., 1997; Nagy et al., 2001) and the samples were electrophoresed in 1.2% agarose (in case of gRNA) or 4% polyacrylamide/8 M urea gels (for DI-72 RNA). The RNA was then transferred from the gels to Hybond

XL membrane (Amersham-Pharmacia) by electrotransfer and hybridized with CNV-specific probes for the 3' noncoding region as described (Panaviene et al., 2003). Hybridization was done in ULTRAhyb hybridization buffer at 68 °C as recommended by the supplier (Ambion). The riboprobes were made in an in vitro transcription reaction with T7 RNA polymerase in the presence of [32P]UTP as described. The CNV DNA template was obtained using PCR with pair of primers #16 (GTAATACGACTCACTATAGGGCTGCATTTCTGCAATGTTC) and #312 (GCTGTCAGTCTAGTGGA) for detection of plus-strands, and with #31 (GTAATACGACTCACTATAGGAAATTCTCCAGGATTTC) and #806 (CCGTCTAGAGTCGTCGTTTACTGGAAGTTAC) for detection of minus-strands. The template for detection of DI-72 RNA (+) and (-) strands (corresponding to RIII/RIV) was obtained with PCR using primers #1165 (AGCGAGTAAGACCAGACTCTTCA) and #22 (GTAATACGACTCACTATAGGGCTGCATTTCTGCAATGTTCC) versus #157 (GGGTTTCATAGAAAAGAAAACAAAACC) and #18 (GTAATACGACTCACTATAGGAGAAAGCGAGTAAGACAG), respectively.

The two component, trans-complementation assay was performed in *N. benthamiana* protoplasts with selected mutants as described earlier (Panaviene et al., 2003). The mutant clones were confirmed by sequencing, as described above.

Western blot analysis

Total proteins from *N. benthamiana* plant or protoplasts infected with CNV were prepared as described (Panaviene et al., 2004). The samples were run in 10% SDS-PAGE, followed by transfer onto PVDF membrane (Bio-Rad). Immunodetection of p33 protein in the Western blot was performed by using anti-p33 antibody (generous gift of H. Scholthof).

Analysis of replicon RNA accumulation in yeast

S. cerevisiae strain INVSc1 (Invitrogen) transformed with three plasmids [i.e., pGAD-His92, pGBK-His33 and pYC-DI-72(+)*Rz*; (Panaviene et al., 2004)] Purification of the cucumber necrosis virus replicase from yeast cells: role of coexpressed viral RNA in stimulation of replicase activity, *J. Virol.* 78 (2004) (15), pp. 8254–8263. (Panaviene et al., 2004) was grown in SC-ULT-medium containing 2% galactose for 24 h at 30 °C (Panavas and Nagy, 2003). To extract total RNA from yeast, equal volumes of RNA extraction buffer (50 mM sodium acetate, pH 5.3, 10 mM EDTA, 1% SDS) and water-saturated phenol were added to the pelleted cells (Panavas and Nagy, 2003). Agarose gel electrophoresis and Northern blotting were as described above (Pogany et al., 2005).

Western blot to detect accumulation levels of His-tagged p33 was performed as described earlier (Pogany et al., 2005) using monoclonal anti-His antibodies (Amersham) and secondary alkaline phosphatase-conjugated anti-mouse antibody (Sigma). Western blots were developed using BCIP and NBT (Sigma).

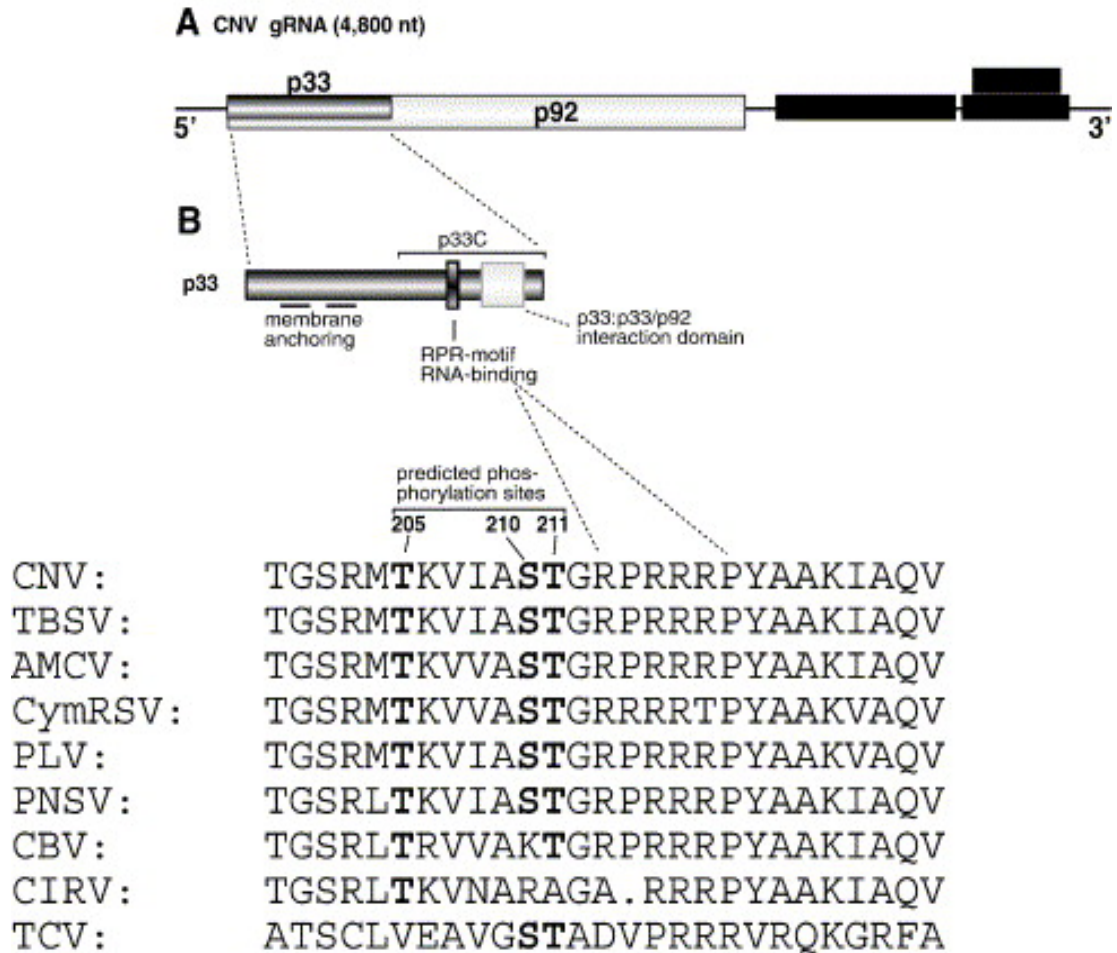


Fig. 2.1 Location of the predicted phosphorylation sites in the CNV replication proteins. (A) The CNV genomic RNA containing five open reading frames (indicated with boxes) and noncoding sequences (solid lines) is shown schematically. (B) The known functional domains in p33 are shown schematically at the top. The amino acid sequence of the RPR-motif and the predicted phosphorylation sites are shown for selected members of Tombusviridae. The following abbreviations were used: TBSV, Tomato bushy stunt virus (cherry strain); CNV, Cucumber necrosis virus; AMCV, Artichoke mottled crinkle virus; CymRSV, Cymbidium ringspot virus; PLV, Pear latent virus; PNSV, Pelargonium necrotic spot virus; CBV, Cucumber Bulgarian virus; CIRV, Carnation Italian ringspot virus; and TCV, Turnip crinkle virus (Carmovirus, Tombusviridae).

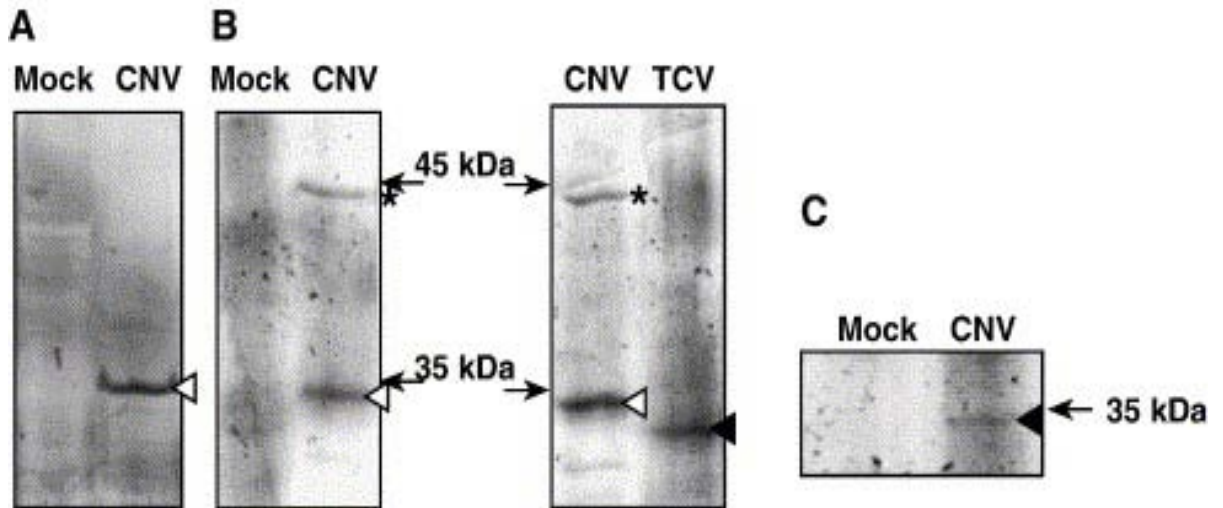


Fig. 2.2 Detection of in vivo phosphorylated replication proteins of CNV and TCV. (A) Detection of CNV p33 in the enriched membrane fraction by using anti-p33 antibody. (B) Detection of phosphorylated CNV p33 and TCV p28 proteins in membrane-enriched fractions prepared from mock-, CNV-, and TCV-infected *N. benthamiana* plants by Western blotting with anti-phosphothreonine antibody. Replication proteins p33 of CNV and p28 of TCV are indicated by arrowheads, whereas a band of unknown origin (present only in samples from CNV-infected plants) is marked with an asterisk. (C) Detection of CNV p33 in membrane-enriched fraction of *N. benthamiana* by staining with phosphoprotein-specific Pro-Q Diamond dye. The CNV p33 was captured on protein A column with anti-p33 antibody from the membrane-enriched fraction prior to loading to SDS-PAGE.

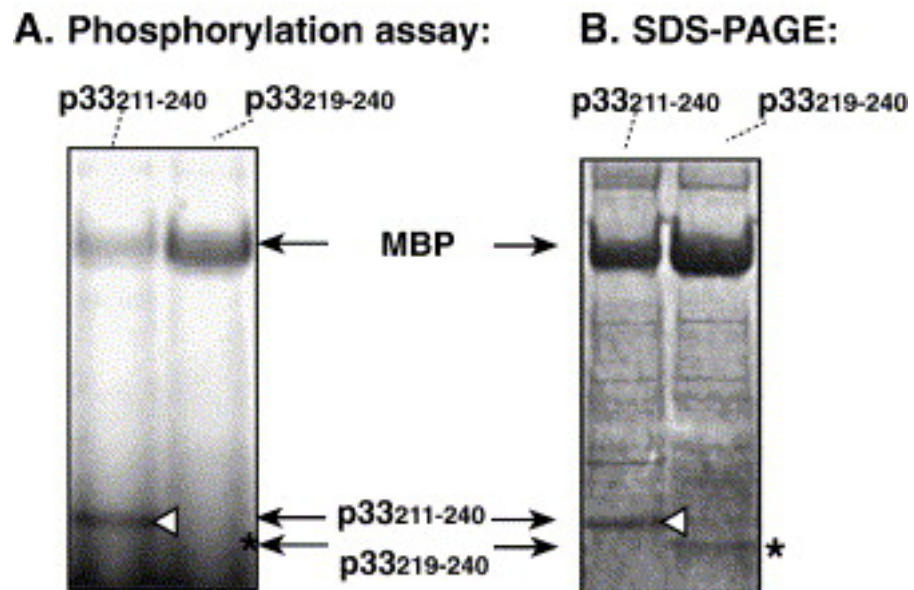


Fig. 2.3 In vitro phosphorylation of p33 by a plant kinase. (A) Two peptides derived from p33 were expressed as an MBP fusion in *E. coli*, affinity-purified, cleaved off from MBP with Factor Xa, and treated with a membrane-enriched preparation obtained from healthy *N. benthamiana* plants in the presence of γ -[^{32}P]ATP. The arrowhead shows the phosphorylated peptide (p33²¹¹⁻²⁴⁰), whereas asterisk pinpoints the nonphosphorylated peptide (p33²¹⁹⁻²⁴⁰). (B) Coomassie blue-stained SDS-PAGE shows the migration of the two peptides used in the phosphorylation assay

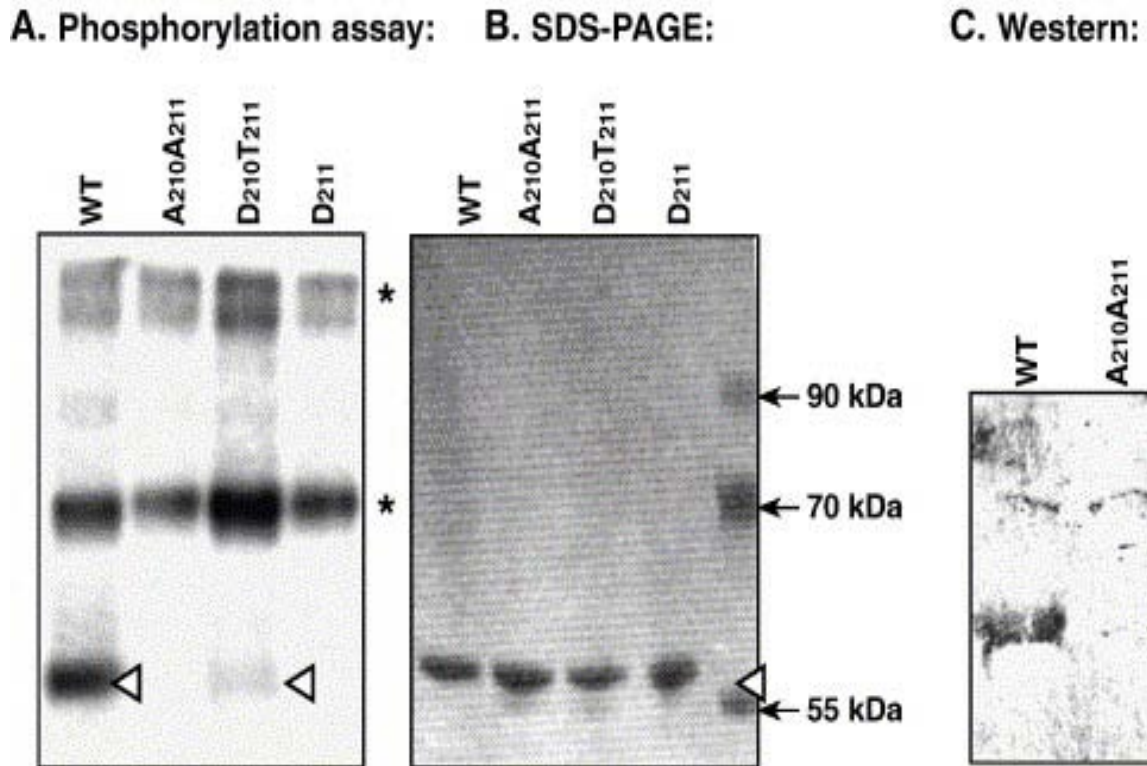


Fig. 2.4 In vitro phosphorylation at S210 and T211 residues of p33 by PKC. (A) A p33-derived peptide (p33205–234) and its derivatives with the shown mutations were expressed as MBP fusions in *E. coli*, affinity-purified and treated with PKC in the presence of γ -[³²P]ATP. The arrowheads show the phosphorylated peptides, whereas asterisks pinpoint phosphorylated PKC and high molecular weight proteins of unknown origin (B) Coomassie blue-stained SDS-PAGE shows the migration of the peptides (marked with an arrowhead) used in the phosphorylation assay. (C) Detection of PKC-mediated phosphorylation of S210 using anti-phosphoserine antibody. The reagents used in this assay were the same as in panel A. After the in vitro phosphorylation assay, the samples were loaded on an SDS-PAGE gel, blotted to a PVDF membrane, and treated with anti-phosphoserine antibody. Additional details are as described in panel A.

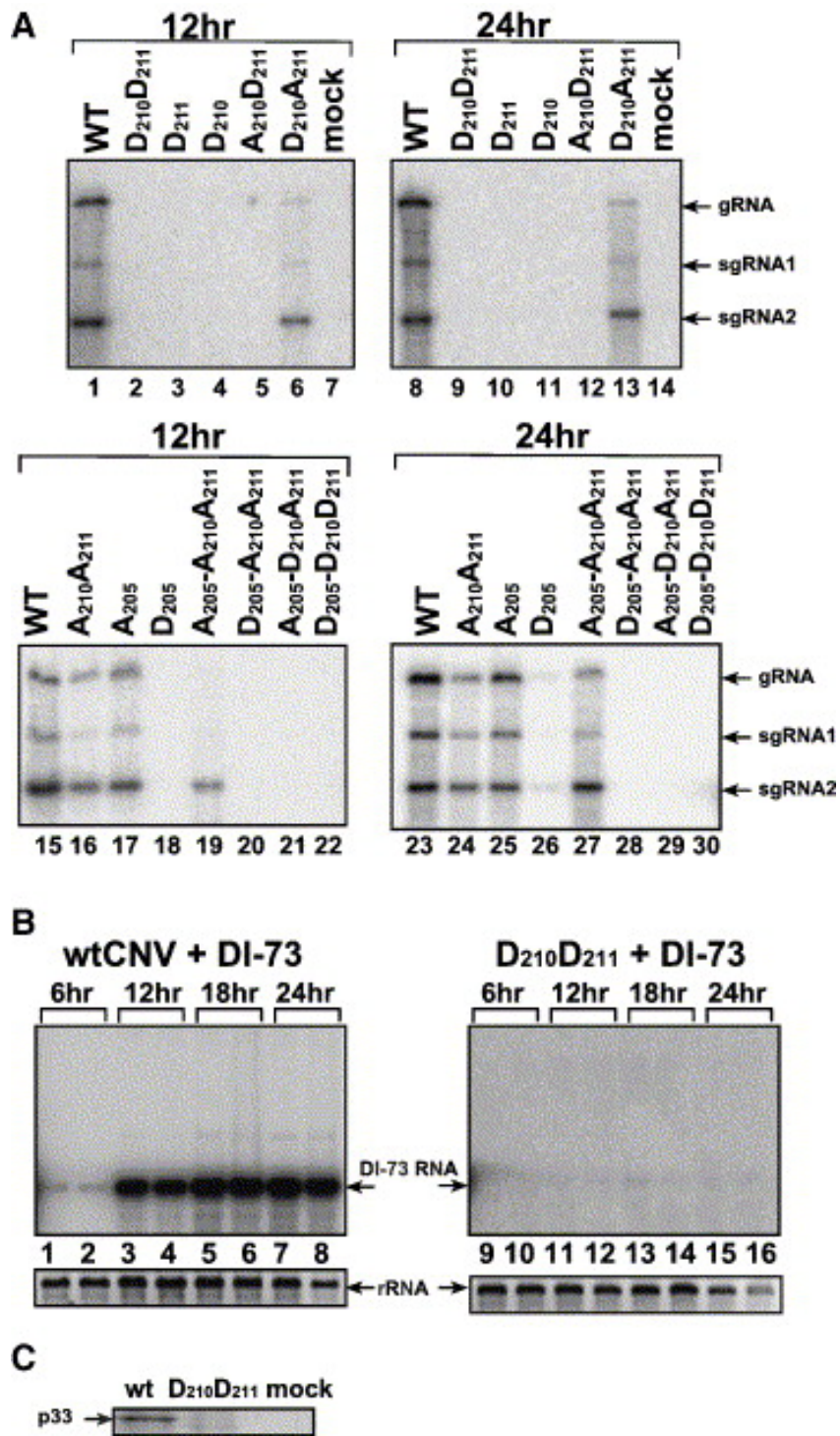


Fig. 2.5 Comparison of accumulation of CNV gRNA carrying phosphorylation-mimicking mutations adjacent to the RPR-motif in p33/p92 gene. The full-length, infectious CNV gRNA (2 μ g) was electroporated into *N. benthamiana* protoplasts (5 \times 10⁵ cells per experiment). Total RNA was isolated, electrophoresed and blotted onto a nylon membrane, followed by probing with ³²P-labeled RNA specific for gCNV (see Materials and methods). The same amount (5 μ g) of total RNA was used for loading onto the gels (based on the estimation of the host ribosomal RNA in ethidium bromide-stained gels). The positions of the CNV gRNA, sgRNA1, and sgRNA2 are depicted on the right. The names of the constructs are shown on the top. The samples were taken 12 and 24 h after electroporation. The experiment was repeated three times. (B) The ability of CNV mutants to support DI-73 RNA replication in trans. The full-length DI-73 RNA (1 μ g) was co-electroporated with the infectious CNV gRNA (2 μ g, mutated or wt) into *N. benthamiana* protoplasts (5 \times 10⁵ cells per experiment). Sample preparation and Northern blotting was done as described in the legend to panel A, except the probing was done with ³²P-labeled RNA specific for DI-73 RNA (see Materials and methods). (C) Accumulation of CNV p33 at 24 hpi. Western blot of total protein extracts was done with anti-p33 antibody.

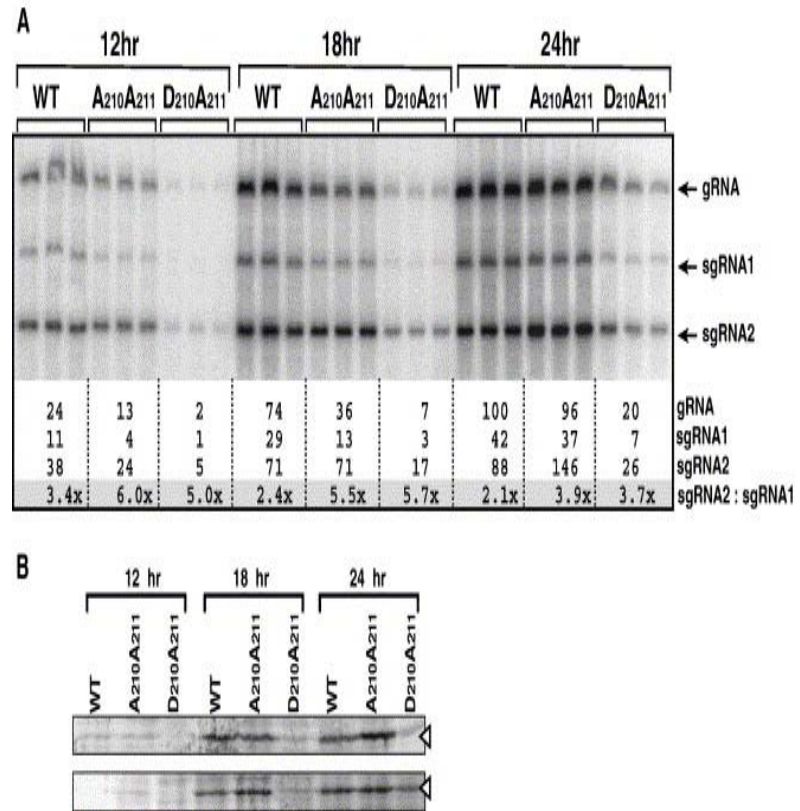


Fig. 2.6 Effect of phosphorylation-mimicking mutations on accumulation of (A) CNV (+)RNAs and (B) p33 replication protein. The relative accumulation levels of CNV RNAs are compared to wt CNV gRNA accumulation at 24 hpi (100%). The bottom line shows the ratio of sgRNA2 versus sgRNA1 in each sample. The arrowheads indicate the position of p33 in the blot.

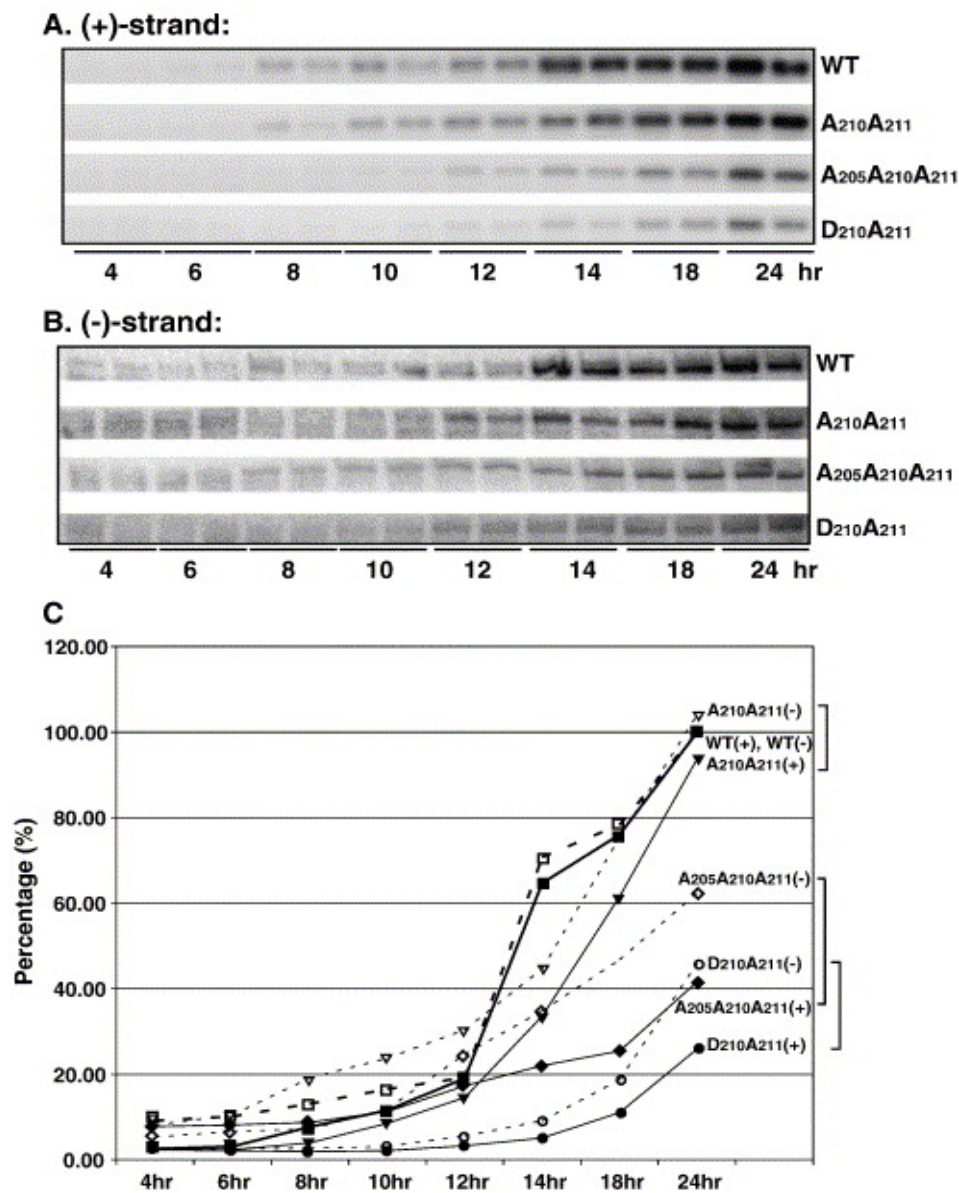


Fig. 2.7 Effect of phosphorylation-mimicking mutations on accumulation of DI-72 RNA in trans. The relative accumulation levels of (A) plus-stranded and (B) minus-stranded DI-72 RNAs are compared to infections containing the wt CNV gRNA accumulation at 24 hpi [100% separately for both (+) and (-)RNAs, indicated by solid and dotted lines, respectively]. (C) Graph showing the relative accumulation of (+) and (-) strands in wt and mutated CNV infections in *N. benthamiana* protoplasts.

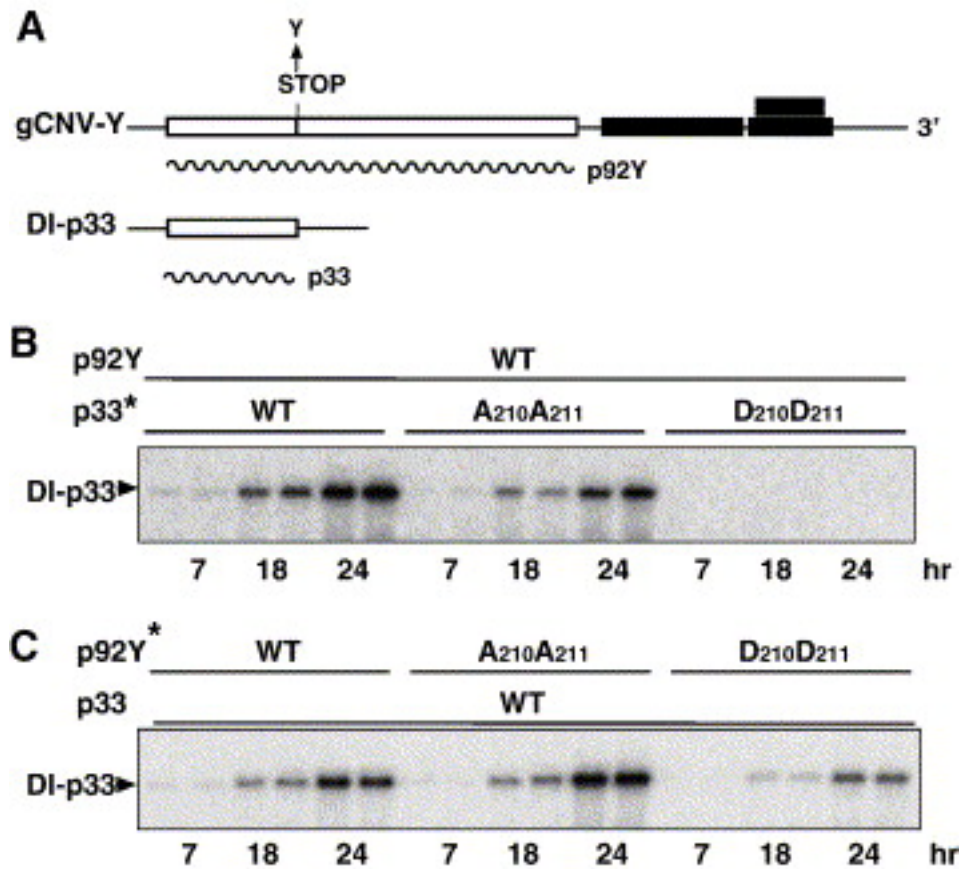


Fig. 2.8 Phosphorylation-mimicking mutations affect the function of p33, and a lesser extent, p92. (A) Schematic representation of the two constructs used in two component complementation-based replication studies. The stop codon at the end of the p33 gene in gCNV-Y was mutated to a tyrosine codon (Y) to prevent the production of p33 from this RNA. The second RNA (DI-p33) was derived from a DI RNA that carried a translation competent p33 gene. (B) Northern blot analysis of replication of DI-p33 mutants in the two-component system. The gCNV-Y RNA (2 μ g) was co-electroporated with DI-p33 (2 μ g) carrying a given mutation into *N. benthamiana* protoplasts. Sample preparation and Northern blotting was done as described in the legend of Fig. 5. The position of the DI-p33 is depicted on the left. (C) Northern blot analysis of replication of gCNV-Y mutants in the two-component system. See panel B for details.

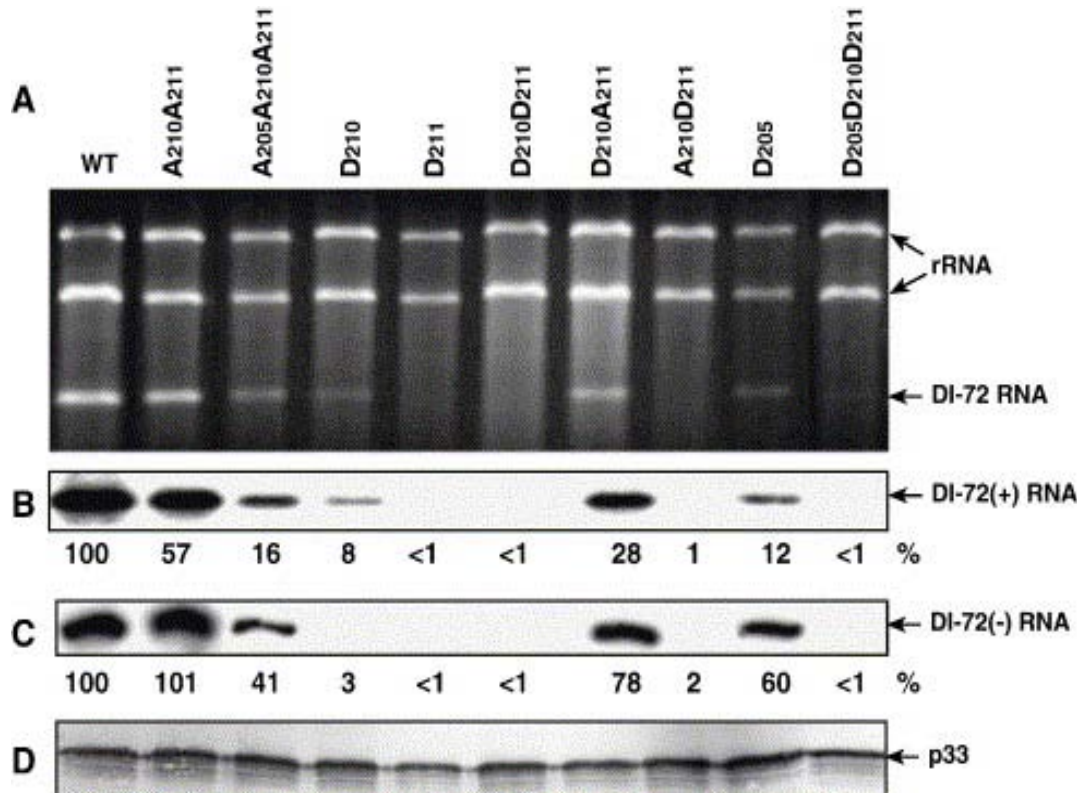


Fig. 2.9 Effect of phosphorylation-mimicking mutations on DI RNA replication in yeast. (A) Ethidium-bromide stained agarose gel showing the accumulation levels of DI-72 RNA in yeast total RNA extracts. Yeast strain Sc1 was co-transformed with three plasmids coding for full-length wt or mutated p33, wt p92Y and wt DI-72 RNA replicon. The position of the DI-72 RNA in the total RNA isolated from transformed yeast cells is shown on the right. (B) Northern blot analysis of accumulation levels of (+)DI-72 and (C) (-)DI-72 RNA in yeast. The relative level of DI-72 RNA replication in yeast [based on quantification of the Northern blot using a PhosphorImager and ImageQuant (v1.2) software from three separate experiments], is shown below the blots (100% equals with DI-72 RNA levels in yeast expressing wt p33/p92). (D) Western blot analysis of the amount of p33 present in yeast with anti-His antibody.

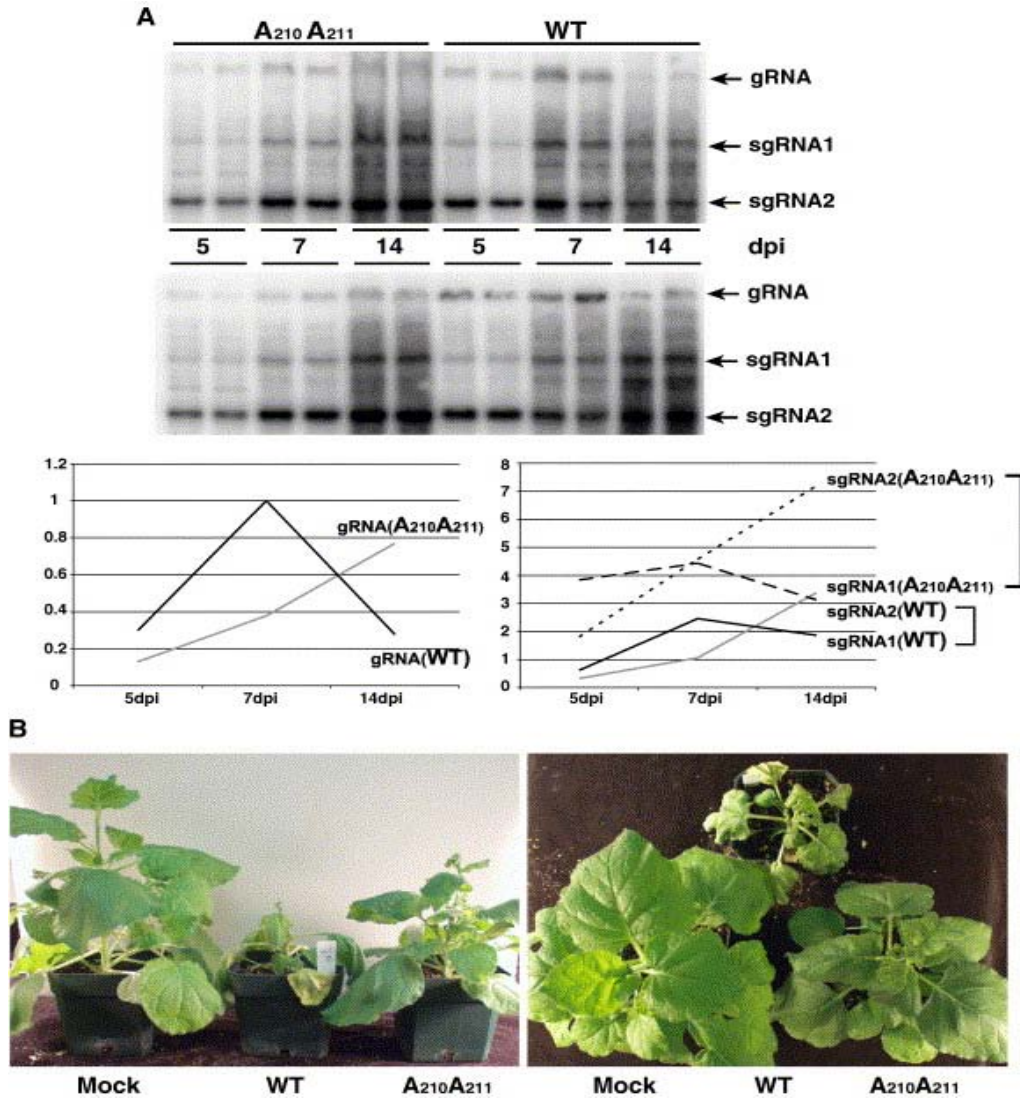


Fig. 2.10 Nonphosphorylation-mimicking mutant of CNV shows delay in gRNA accumulation and symptom formation in *N. benthamiana* plants. (A) Northern blot analysis of accumulation levels of CNV (+) RNAs in *N. benthamiana* plants. Samples were taken from two systemically infected leaves/plant and two separate plants were used in each experiment (top and bottom panels). The relative levels of gRNA, sgRNA1, and sgRNA2 are shown below the blots (100% equals with wt CNV gRNA level at 7 dpi). (B) Symptoms of mock- and CNV-infected plants at 7 dpi.

CHAPTER III

Inhibition of in vitro RNA binding and replicase activity by phosphorylation of the p33 replication protein of Cucumber necrosis tomosvirus

Introduction

Recent identification of phosphorylation-based modification of p33 (see accompanying paper by (Shapka et al., 2005) opens up the possibility that the activity of the p33 replication protein might be regulated by phosphorylation/dephosphorylation in CNV-infected plants. In vitro phosphorylation studies mapped the sites of phosphorylation in p33 to serine (S210) and threonine (T211, possibly T205) residues located adjacent to the RNA binding site (Fig. 3.1C). Neutral alanine (A) mutations, which mimic the nonphosphorylated form of p33, at these sites were found to affect the synthesis of plus versus minus strands and alter the ratio between the two subgenomic RNAs. On the contrary, the phosphorylation-mimicking aspartic acid (D) mutations that, like phosphorylation, introduced negative charges at these positions rendered the virus non-infectious in plant protoplasts.

To determine what functions of p33 might be affected by phosphorylation, in the present study, I conducted in vitro RNA binding experiments with recombinant p33 preparations. The obtained data demonstrate that D mutations in p33 at the phosphorylation sites reduced the ability of p33 to bind to viral RNA, while A mutations had lesser effects. I also found that the above D mutations in p33, but not in p92, inhibited the activity and/or the assembly of functional replicase complexes in yeast. Altogether, I propose that phosphorylation of p33 replication protein is involved in regulation of CNV replication due to affecting the ability of p33 to bind to the viral RNA.

Results

Rationale

Phosphorylation of threonine (T205 and T211) and serine (S210) residues adjacent to the arginine (R) and proline (P)-rich RPR motif (R213P214R215R216R217P218) (Fig. 3.1) is predicted to affect the ability of p33 to bind to the viral RNA. This is because phosphorylation makes these residues negatively charged that could “neutralize” the proximal positively charged R residues within the RPR motif. Therefore, the negatively charged phosphorylated residues could compete with the negatively charged RNA for binding to the positively charged RPR motif in p33. Overall, I predict that phosphorylation of p33 might affect two functions of p33: facilitating (i) binding/release of the viral RNA to/from the replicase complex during replication; and (ii) assembly/disassembly of the replicase complex, which in addition to p92, also contains the viral RNA, p33 and possible host factors. These models were tested below.

Phosphorylation of p33 adjacent to the RPR motif inhibits viral RNA binding *in vitro*

To test the effect of phosphorylation on the ability of p33 to bind to the viral RNA, first, I utilized phosphorylation-mimicking mutants of recombinant p33. The phosphorylation-mimicking mutants carried D for T/S mutations, which introduced negative charges comparable to that of phosphorylation (Waigmann et al., 2000; Jabbur et al., 2001; Freye-Minks et al., 2003; Jia et al., 2004). On the contrary, nonphosphorylated form of p33 was mimicked by A for T/S mutations, which maintain neutral charges at the phosphorylation sites. Moreover, hypo (partial)phosphorylation-mimicking mutants contained a single D mutation at either T205, S210 or T211 positions. Importantly, both D and A residues are similar in size to T/S residues, thus minimizing the sterical/structural effects caused by these mutations. However, it is important to note that D mutations only “mimic”

phosphorylation, thus results obtained with D mutants could possibly cause problems unrelated to phosphorylation.

Altogether, I generated nine p33 mutants with A and/or D mutations at the phosphorylation sites (Figs. 3.2A–D). These proteins were expressed in *E. coli* as fusion proteins with the maltose-binding protein (MBP) followed by affinity purification (Fig. 3.2E) as described (Rajendran et al., 2002; Rajendran and Nagy, 2003). Note that, instead of the full-length protein, I used a truncated version of p33, which lacked the mostly hydrophobic N-terminal domain. The N-terminal domain contains membrane-anchoring sequences, and it does not contribute to RNA binding *in vitro* (Rajendran and Nagy, 2003; Pogany et al., 2005). The purified recombinant p33 was used in a gel electrophoretic mobility-shift assay (EMSA) (Fig. 3.2) to test its binding to a ³²P-labeled RNA probe consisting of RII (+)-SL, which includes the high-affinity binding sequence p33RE (Pogany et al., 2005). The EMSA experiments demonstrated that alanine mutations (see A210A211, Fig. 3.2A), which mimic the nonphosphorylated form of p33, had no inhibitory effect on RNA binding by p33. In contrast, the phosphorylation-mimicking D210D211 p33 bound to the RNA probe poorly when compared to the nonphosphorylated p33 control (Fig. 3.2B). Thus, the phosphorylation-mimicking, but not the nonphosphorylation-mimicking mutations, inhibited the ability of p33 to bind to the p33RE-containing viral RNA *in vitro*.

To test which of the three phosphorylation sites (i.e., T205, S210 or T211) have more pronounced effect on RNA binding, I compared additional p33 mutants carrying different combinations of A/D mutations at these phosphorylation sites. The RNA binding abilities of these recombinant p33 proteins revealed that D mutation at position T211 was especially inhibitory on RNA binding (see mutants D211 and A210D211, Figs. 3.2B–C). The presence of D residue at position S210 also had inhibitory effect on RNA binding (see mutants D210 and D210A211, Figs. 3.2B–C) phosphorylation-mimicking D mutation at position 205 had lesser effect on RNA binding (compare mutant D205A210A211 with A205A210A211, Figs. 3.2D–E). I also tested the RNA binding activity of a triple phosphorylation-mimicking mutant (i.e., D205D210D211), which showed minimal RNA binding activity when compared to the nonphosphorylation-mimicking mutant (A205A210A211). Altogether, these

data suggest that each of the phosphorylation sites (T205, S210 or T211) could be involved in regulation of RNA binding by p33, and their relative effects are inverted with their distances from the RPR motif (see Discussion).

To test if the phosphorylation-mimicking mutation could affect the ability of p33 to bind to plus- and minus-stranded RNA templates, I used EMSA experiments similar to those described above except using full-length model templates representing replication-competent defective interfering RNA (termed DI-72 RNA). While the wt p33C bound efficiently to both DI-72(+) and DI-72(-) RNA, the binding of D210D211 to both RNAs was less efficient (Fig. 3.3). Altogether, these data suggest that the overall RNA binding capacity of p33 is inhibited by the presence of phosphorylation-mimicking mutations.

The second approach to test the effect of phosphorylation on the ability of p33 to bind to the viral RNA included in vitro phosphorylation of recombinant wt p33 with protein kinase C (PKC). I used PKC in this experiment because PKC has been found to phosphorylate p33 more efficiently than a plant kinase preparation in vitro (Shapka et al., 2005). EMSA performed with the kinased p33 demonstrated that the phosphorylated recombinant p33 bound to the viral RNA probe up to 3-fold less efficiently than the untreated p33 could (Fig. 3.4A). It is likely that PKC treatment had inhibitory effect on RNA binding capacity of p33 due to phosphorylation of S210 and T211 because the nonphosphorylatable A210A211 mutant of p33 did not show reduced efficiency of binding in the treated versus untreated samples (Fig. 3.4A). Accordingly, PKC has been shown to phosphorylate only S210 and T211, in p33 in vitro (see the accompanying paper by (Shapka et al., 2005).

Because treatment of p33 with PKC inhibited RNA binding only at low p33 concentrations (Fig. 3.4A, lanes 4–5), it is possible that the residual RNA binding by p33 in Fig. 3.4A (lanes 1–3) is due to incomplete phosphorylation of all p33 molecules present in solution. To test more rigorously if phosphorylated p33 maintains the ability to bind to the viral RNA probe, I developed a new EMSA assay in which p33 was ³²P-labeled (Fig. 3.4B), whereas the viral RNA [RII(+)-SL probe, Fig. 3.4B, lanes 4–5] was unlabeled. Visualization of the viral RNA with ethidium bromide staining and the p33 with Coomassie staining revealed the presence of

p33:RNA complexes (Fig. 3.4B, left and middle panels, lanes 4–5) that were not present when the mutated $\Delta C99$ RNA, which cannot bind to p33 (Pogany et al., 2005), was used as a probe (Fig. 3.4B, lanes 2–3). Importantly, the p33:RNA complexes were not labeled with ^{32}P (Fig. 3.4B, right panel, lanes 4–5), suggesting that the unphosphorylated p33 still present after PKC treatment, but not the phosphorylated p33 (^{32}P -labeled), was responsible for the observed shift in RNA:protein mobility. Based on these experiments, I conclude that the phosphorylated p33 is unlikely to bind to the viral RNA in vitro.

Phosphorylation stimulates RNA release from bound p33:RNA complexes in vitro

To test if phosphorylation of p33 could promote the release of the RNA from the p33: RNA complex, I treated the prebound p33:RNA complex with PKC (Fig. 3.4C). This experiment demonstrated that phosphorylation of p33 could promote the release, or prevents the re-binding of viral RNA from the complex. The release of RNA from the RNA:p33 complex is due to phosphorylation of S210 and T211 because RNA release after PKC treatment was not observed with the nonphosphorylatable A210A211 p33 mutant (Fig. 3.4C). In addition, I demonstrated that p33 bound to the viral RNA can be phosphorylated in vitro with PKC (Fig. 3.4D). Therefore, the obtained data are consistent with a model that phosphorylation can stimulate the release of the viral RNA from p33 and/or p33-containing replicase complexes.

Phosphorylation-mimicking p33 mutant inhibits the in vitro activity of functional CNV replicase complex

To test if phosphorylation of p33 affects the activity and/or the assembly of functional replicases in yeast host, I co-expressed one of the p33 phosphorylation-mimicking mutants with wt p92 and DI-72 RNA as described (Panavas and Nagy, 2003; Panaviene et al., 2004). To this end, I prepared two types of replicase

preparations 40 h after induction of DI-72 RNA transcription from the pYES-DI-72 expression plasmid. One of the preparations was the membrane-enriched fraction, which contained functional preassembled CNV replicase complexes that could synthesize new RNA strands using the co-purified (endogenous) DI-72 RNA template (Fig. 3.5A) (Panavas and Nagy, 2003; Panaviene et al., 2004). The second preparation was obtained by affinity purification of CNV replicase, which is able to use added (exogenous) RNA templates for complementary RNA synthesis (Fig. 3.5B) (Panaviene et al., 2004). In comparison with the control experiments including wt p33 and wt p92, which resulted in highly active CNV replicase preparations, the membrane-enriched and the affinity-purified D210D211 p33-containing CNV replicases were not functional without or with added RNA templates (Figs. 3.5A–B). The amounts of p33 present in these CNV replicase preparations were comparable to those in the wt p33-containing preparations (Figs. 3.5A–B). Thus, the stability and/or expression level of p33 is not affected by the D210D211 mutations in yeast. The simplest explanation of these observations is that the phosphorylation-mimicking D210D211 p33 inhibited the activity and/or the assembly of functional replicase complexes in yeast.

In vitro testing of the CNV replicase activity in preparations containing the nonphosphorylation-mimicking A210A211 and A205A210A211 p33 revealed reduced levels of RNA synthesis (between 29 and 45%) in both endogenous and exogenous template-containing reactions (Figs. 3.5A–B). This suggests that the nonphosphorylated p33 could participate in CNV replicase assembly. However, the assembly and/or activity of the CNV replicase containing nonphosphorylation-mimicking p33 is somewhat less efficient than those containing wt p33 (see Discussion). Additional tests revealed that the hypophosphorylation-mimicking D211 p33 supported the activity of CNV replicase by five-fold less efficiently than the wt p33 did (Figs. 3.5A–B). The amounts of p33 present in these CNV replicase preparations were comparable (Figs. 3.5A–B).

To test if a similar phosphorylation-mimicking mutation (i.e., D210D211) could affect the activity of p92 RdRp protein, I co-expressed the mutated p92 with wt p33 in yeast followed by obtaining CNV replicase preparations. These tests revealed

that phosphorylation-mimicking mutation in p92 did not inhibit the activity of the membrane-bound CNV replicase (Fig. 3.5A). This suggests that phosphorylation of p92 at positions S210 and T211 is unlikely to affect its polymerase activity in vivo.

CNV replicase containing nonphosphorylation-mimicking p33 shows reduced ratio in plus- versus minus-strand synthesis

Reduction of template activity by CNV replicase preparations containing nonphosphorylation-mimicking p33 (Fig. 3.5) suggests that phosphorylation of T205, S210 and T211 sites in wt p33 might play a role in optimal CNV replicase assembly and/or viral RNA synthesis. To test the effect of phosphorylation of p33 on RNA synthesis by the CNV replicase, first, I treated the CNV replicase with PKC prior to the replicase assay. As shown in Figs. 3.6A–B, PKC treatment had no significant effect on template activity of the CNV replicase bound to its template (endogenous RNA, Fig. 3.6A) or on the purified CNV replicase with added template (Fig. 3.6B). These data suggest that the preassembled CNV replicase: RNA complex (with the RNA likely bound to the p92 RdRp protein in the replicase complex) is not sensitive to phosphorylation in vitro.

In the second assay, I tested the ratio of in vitro synthesized (+) and (-) strands by the wt and mutated CNV replicases co-purified with their template RNAs (Fig. 3.7). Briefly, in this assay, the “membrane-enriched” replicase fraction containing the endogenous viral RNA synthesizes complementary RNA in vitro in the presence of ³²P-UTP and the three other ribonucleotides (“replicase run off” experiments). The resulting new ³²P-labeled RNA strands are then used as probes in RNA blot experiments that have the same amounts of denatured plus- and minus-strand RNA blotted on the membrane (Panaviene et al., 2004). Measuring the signal strength of the hybridized (+) and (-) strands of viral RNA, we can estimate the ratio of plus- and minus-strand templates present originally in the membrane-enriched fractions. The replicase run off experiments revealed that at the early time point (12 h) the CNV

replicase containing nonphosphorylation-mimicking p33 mutant (A205A210A211) synthesized over 10 times more minus strands than plus strands (Fig. 3.7). On the contrary, the wt replicase synthesized almost the same amounts of minus- and plus strands. At 18 h time point, the wt replicase produced not, vert, similar6 times more plus strands than minus strands, whereas the CNV replicase containing either A210A211 or A205A210A211 p33 synthesized only not, vert, similar3× and not, vert, similar1.5× more plus strands than minus strands. Interestingly, the difference in plus- and minus-strand ratio between the wt and A205A210A211 mutant replicase was still not, vert, similar7-fold at 24 h time point, suggesting that replicase with the nonphosphorylation-mimicking p33 has lower preference for plus-strand synthesis (i.e., less asymmetrical RNA synthesis) than the wt replicase.

The CNV replicase containing hypophosphorylation-mimicking p33 (i.e., D210A211) lacked detectable level of template activity at the early time points, whereas it produced not, vert, similar6-fold more plus strands than minus strands at the 30 h time point (Fig. 3.7). This suggests that the assembly of CNV replicase is inefficient in yeast expressing D210A211 p33, which could be due to inefficient RNA binding (Fig. 3.2), thus inefficient template recruitment into replication.

Discussion

In this work, I characterized the effects of phosphorylation of conserved S/T residues located adjacent to an essential RNA binding domain on the properties of tombusvirus p33 replication protein. Specifically, I found that the phosphorylated form of p33 showed reduced RNA binding *in vitro* (Figs. 3.4A–B). Moreover, phosphorylation of the p33:viral RNA complex with PKC *in vitro* promoted the release of the viral RNA from the complex (Fig. 3.4C). This was further supported by the reduced RNA binding capacity of recombinant phosphorylation-mimicking D for S/T mutants of p33 (Fig. 3.2). Altogether, these data are consistent with the model (see Fig. 3.1) that the negative charges introduced at T205, S210 and T211 adjacent to the RNA binding domain by phosphorylation can inhibit the binding of the negatively charged viral RNA to the positively charged RPR motif in p33. Based on these characteristics, phosphorylation /dephosphorylation of p33 adjacent to the RNA binding site is likely involved in regulation of p33:viral RNA interaction, and it could serve as an on/off switch in viral RNA binding/RNA release (see below).

In vitro testing of CNV replicase complexes obtained from yeast cells revealed that the purified CNV replicase containing phosphorylation-mimicking p33 (i.e., D210D211) lacked replicase activity on an added template (Fig. 3.5B). Moreover, the replicase preparation containing D210D211 p33 was also inactive on the co-purified RNA template (Fig. 3.5A). The lack of CNV replicase activity could be due to deficiency of phosphorylation-mimicking D210D211 p33 in: (i) binding/holding to the template during the *in vitro* reaction (Fig. 3.2); and/or (ii) supporting replicase assembly *in vivo* prior to replicase purification (Fig. 3.6A). This is because the viral RNA template is known to stimulate the assembly of functional replicase complexes by 40- to 100-fold in tombusviruses (Panaviene et al., 2004; Panaviene et al., 2005). On the other hand, it is unlikely that translation and/or stability of p33 were altered by these mutations because yeast cells expressed the phosphorylation-mimicking D210D211 p33 in comparable amount to wt p33 (Fig. 3.4). On the contrary, the RdRp function of D210D211 p92 was not altered by these modifications, suggesting that phosphorylation of S/T residues adjacent to the RPR motif is expected to have different effect on p92 functions than on p33 functions.

Based on the above and previous observations (Panaviene et al., 2004; Shapka et al., 2005), we propose that the CNV replicase complex in yeast expressing phosphorylation-mimicking D210D211 p33 lacks template activity likely because it (i) contains reduced amount of viral RNA due to decreased capacity of the mutated p33 in RNA binding, which in turn (ii) leads to deficiency in template recruitment (Pogany et al., 2005) and (iii) inefficient replicase assembly due to limited amount of “RNA assembly platform” for p33, p92 and putative host proteins (Panaviene et al., 2004). Altogether, inefficient replicase assembly in combination with poor template binding and increased RNA release from the replicase complex could explain the lack of detectable CNV replicase activity in membrane-enriched and purified replicase preparations obtained from yeast expressing D210D211 p33 (Figs. 3.5A–B). Altogether, I propose that phosphorylation of T205, S210 and T211 amino acid residues in p33 by a host kinase could lead to “shut down” of new replicase assembly and recruitment of viral RNA into replication during the late phase of the replication cycle. This could help in switching the role of the viral RNA from replication to other processes, such as viral RNA encapsidation and possibly cell-to-cell movement in infected hosts. In addition, early hyperphosphorylation of p33 in selected host plants could lead to resistance against tombusviruses by interference with replicase assembly and template binding.

Interestingly, the activity of preassembled replicase complex was not affected by kinase treatment in vitro (Fig. 3.6), suggesting that phosphorylation of p92 RNA-dependent RNA polymerase within the replicase complex does not alter its ability to bind to the RNA template. This could be due to the presence of two extra RNA binding regions in p92 in addition to the RPR motif (Rajendran and Nagy, 2003), thus allowing the replicase to perform RNA synthesis on templates that are present within preassembled replication complexes.

The wt nonphosphorylated recombinant p33 and the nonphosphorylation-mimicking A for S/T mutants of p33 bound to viral RNA stably in vitro (Fig. 3.2), and they also supported the assembly of functional CNV replicase complexes in yeast (Fig. 3.5). These observations are consistent with the model that the nonphosphorylated form of p33 is replication-competent, whereas the fully

phosphorylated form is replication incompetent. However, both nonphosphorylated and phosphorylated forms likely play some, albeit different, roles in tombusvirus replication. This is supported by the observation that the CNV replicase containing the phosphorylation incompetent p33 (i.e., A210A211 and A205A210A211) showed 3- to 7-fold reduction in plus- versus minus-strand synthesis when compared to the CNV replicase containing the wt p33 (Fig. 3.7). In other words, the CNV replicase containing the nonphosphorylation-mimicking p33 produced less plus-stranded RNA and/or relatively more minus-stranded RNA than the replicase with the wt p33. This could be due to the reduced release rates of viral RNA templates by the phosphorylation incompetent p33 from the replication sites or altered functionality of the CNV replicase containing A205A210A211 p33. Altogether, I propose that phosphorylation plays a role in fine-tuning of the asymmetrical replication process (see below).

The role of phosphorylation of S/T residues adjacent to the RNA binding site in p33 in the replication process could be more complex, however, due to the possible presence of partially (hypo-) phosphorylated p33 forms (see previous chapter), which might have different functions than the fully phosphorylated form of p33 in infected cells. Accordingly, hypophosphorylation-mimicking p33 mutants (i.e., D210A211, A210D211) showed reduced viral RNA binding *in vitro* (Fig. 3.2) when compared to the nonphosphorylated wt p33. In addition, CNV replicase preparations containing D210 p33 showed reduced template activity and produced small amount of plus-stranded RNA when compared to the replicase preparations with the wt p33 (Figs. 3.5A–B). Overall, hypophosphorylation of p33 could play a role in regulation of subgenomic RNA synthesis and fine-tuning of the asymmetrical replication process.

A model on the role of phosphorylation of p33 in regulation of tombusvirus replication

The p33 replication protein plays a role in selection of the viral RNA via selectively binding to a conserved stem-loop region in the p92 ORF [RII(+)-SL representing p33RE] (Monkewich et al., 2005; Panavas and Nagy, 2005; Pogany et al., 2005). This selective template binding by p33 is important for recruitment of the viral RNA from translation into replication, which takes place in membranous structures derived from peroxisomes (Navarro et al., 2004; Panavas and Nagy, 2005)). Moreover, the p33: RNA complex is essential for the assembly of the viral replicase complex (Panaviene et al., 2004), which also contains p92 and possibly host factors. Based on data presented in this chapter and the previous chapter we propose that the template selection and replicase assembly functions are performed by the nonphosphorylated form of p33, and these processes are inhibited by the phosphorylated form of p33. After the assembly of the replicase complex, hypophosphorylation of p33 (probably at S210 and T211 positions) could facilitate minus-strand and/or subgenomic RNA synthesis. Phosphorylation of p33 at T211 position (or combined phosphorylation of T205, S210 and T211 sites), however, is predicted to decrease the RNA binding capacity of p33 drastically, which could facilitate the release of newly synthesized RNA (both genomic and subgenomic) from the replication units/sites (Fig. 3.8). Because phosphorylation and dephosphorylation of p33 might take place repeatedly in cycles, one replication unit could potentially produce and release tombusviral RNA progenies multiple times. Overall, phosphorylation of p33 could help in regulating (fine-tuning) the replication and infection processes.

Cellular processes other than p33 phosphorylation (such as protein modification, protein degradation, diffusion or membrane rearrangements) could also promote the release of viral RNA from the replication units/sites, likely explaining why the nonphosphorylatable p33 (either A210A211 or A205A210A211) still could support virus replication. However, the nonphosphorylatable p33 mutants are slower in replication in single cells, and they are less potent in invading the host plants as

rapidly as the wt virus can. Altogether, these deficiencies of the nonphosphorylatable p33 in supporting tombusvirus replication could be especially detrimental in competitive environment where tombusviruses with phosphorylatable p33 are also present.

One of the proposed roles of p33 phosphorylation adjacent to the RNA binding site in fine-tuning the replication process is to regulate/stimulate the release of viral RNA from the replication sites. This might be important because the nonphosphorylated p33 binds the viral RNA rather tightly, which is advantageous for template selection during early steps of replication. On the contrary, at latter steps of replication, tight binding between p33 and the viral RNA could slow down the release of the newly made viral RNAs from the replication sites. This could be disadvantageous because the viral RNA has to participate in other processes, such as translation (i.e., sgRNAs), assembly of new replicase complexes, cell-to-cell movement and encapsidation. Altogether, the current work promotes a novel, fine-tuning role for p33 phosphorylation adjacent to the RNA binding site in tombusvirus replication.

Materials and methods

Expression and purification of recombinant replicase proteins from *E. coli*

Expression and purification of the recombinant CNV p33 replicase protein (termed p33C, lacking the hydrophobic N-terminal domain) were carried out as described earlier (Rajendran and Nagy, 2003 and Rajendran et al., 2002). Briefly, the expression plasmids carrying wt or mutated p33C sequences were transformed into *E. coli* [Epicurion BL21-CodonPlus (DE3)-RIL (Stratagene)]. Protein expression was induced at 14 °C with 0.3 mM IPTG (isopropylthiogalactopyranoside) for 8 h. The recombinant proteins were purified using amylose resin column (NEB), as described earlier (Rajendran et al., 2002; Rajendran and Nagy, 2003). All protein purification steps were carried out in a cold room. The purified recombinant proteins were analyzed in a 10% SDS-PAGE for their purity. The Bio-Rad protein assay was used to measure the amount of purified recombinant proteins.

Gel mobility shift assay (EMSA)

RNA templates were obtained using T7 RNA polymerase-based transcription on PCR templates in the presence of ³²P-labeled UTP and unlabeled ATP, CTP and GTP as described (Pogany et al., 2003; Pogany et al., 2005). After phenol/chloroform extraction and isopropanol/ammonium acetate precipitation, the obtained RNA probes were checked by 5% PAGE/8 M urea electrophoresis.

The affinity purified recombinant proteins (1 μg or as mentioned in the figure legends) were incubated with 1 ng of radioactively labeled RNA probe (see above) in a binding buffer [50 mM Tris-HCl pH 8.2, 10 mM MgCl₂, 10 mM DTT, 10% glycerol, 200 ng yeast tRNA (Sigma) and 2 U of RNase inhibitor (Ambion)] at 25 °C for 15 min (Rajendran and Nagy, 2003). After the binding reaction, the samples were analyzed by 5% non-denaturing polyacrylamide gel electrophoresis in TAE buffer performed at 200V in a cold room (Rajendran and Nagy, 2003). The gels were dried and analyzed in a PhosphorImager and quantified using ImageQuant v.1.2

(Amersham). To study the effect of phosphorylation on the RNA release from p33, we treated the prebound RNA:p33 complex (see the binding assay above) with PKC (Sigma) as described in the previous chapter prior to electrophoresis.

Yeast transformation and growth

S. cerevisiae strain INVSc1 (Invitrogen) carrying three plasmids [i.e., pGAD-His92, pGBK-His33 and pYC-DI-72(+)*Rz*, (Panaviene et al., 2004)] was grown in SC-ULT medium containing 2% galactose for 24 h at 30 °C (Panavas and Nagy, 2003a). Then, the cultures were diluted 10-fold with fresh SC-ULT medium with 2% galactose and grown at 23 °C until 0.6–0.7 OD₆₀₀ (approximately 24 h). Yeast cells were then harvested by centrifugation at 2000 × *g* for 5 min followed by washing the pellet with 20 mM Tris–HCl, pH 8.0 and centrifugation. The pelleted cells were re-suspended in 1 ml of 20 mM Tris–HCl, pH 8.0 buffer, followed by centrifugation at 21,000 × *g* for 1 min and storage of the pellet at -80 °C until further use.

CNV replicase assays

First, I obtained “membrane-enriched” CNV replicase preparations, which are suitable to test the replicase activity on the endogenous templates present within the CNV replicase preparation (Panaviene et al., 2004). Frozen yeast cells were homogenized by grinding in liquid nitrogen followed by addition of the extraction buffer (200 mM sorbitol, 50 mM Tris–HCl, pH 7.5, 15 mM MgCl₂, 10 mM KCl, 10 mM γ -mercaptoethanol, yeast protease inhibitor mix, Sigma) and centrifugation at 100 × *g* for 1.5 min at 4 °C (Panavas and Nagy, 2003a). Because no template was added to the in vitro reaction, the replicase preparation could only use the endogenous template present within the enriched membrane fraction. The RdRp products were phenol/chloroform-extracted, precipitated with isopropanol/ammonium acetate and analyzed under denaturing conditions (i.e., 5% PAGE containing 8 M urea (Pogany et al., 2003)).

The second preparation was affinity-purified CNV replicase, which can accept exogenous templates. The CNV replicase was purified via metal-affinity purification as described (Panaviene et al., 2004). Briefly, the above enriched membrane fraction was solubilized in 1% Triton X-100 and 5% SB3-10 (caprylyl sulfobetaine) (Sigma) followed by binding to ProBond resin (Invitrogen). After careful washing, the recombinant p33 was recovered from the column in the extraction buffer containing 200 mM imidazole and 0.1% Triton X-100. I used 0.5 μ g RNA templates [RI/RIII(-)] and 25 μ l of recombinant CNV replicase (Panaviene et al., 2004). The RdRp products were phenol/chloroform-extracted and analyzed under denaturing conditions (see above).

Plus- and minus-strand assay

To test the ratio of (+) versus (-) strand synthesis on the endogenous templates by the CNV replicase, I obtained the membrane-enriched fraction (see above) followed by standard replicase assay in the presence 32 P-labeled UTP and the other three unlabeled rNTPs followed by phenol/chloroform extraction and isopropanol precipitation. The obtained RNA probe and equal amounts of in vitro transcripts of DI-72(+) and (-) RNAs, prepared by T7 RNA transcription (see above), were denatured separately by heating for 5 min at 85 °C in TE buffer and formamide (in 1:1 ratio). Then, the DI-72(+) and (-)RNAs were separately blotted onto a Hybond XL membrane (Amersham) and crosslinked with UV (GS Gene Linker, Bio-Rad). Hybridization was done using ULTRAhyb solution (Ambion) at 68 °C according to the supplier's instructions. The 32 P-labeled replicase products were used as probes for hybridization.

Western blot

Aliquots (10 μ l) of the enriched membrane fraction from yeast cells or the purified p33 preparations in SDS-PAGE sample loading buffer (Sambrook et al., 1989 J. Sambrook, T. Maniatis and E.F. Fritsch, Molecular Cloning: A Laboratory Manual (2nd ed.), Cold Spring Harbor Laboratory Press, Cold Spring Harbor, N.Y. (1989).Sambrook et al., 1989) were heated for 5 min at 85 °C, electrophoresed in 10% SDS-PAGE gels and electrotransferred to a PVDF membrane (Bio-Rad). Then, CNV His-p33 was detected with monoclonal anti-His antibodies (Amersham) and secondary alkaline phosphatase-conjugated anti-mouse antibody (Sigma) as described (Pogany et al., 2005)Western blots were developed using BCIP and NBT (Sigma).

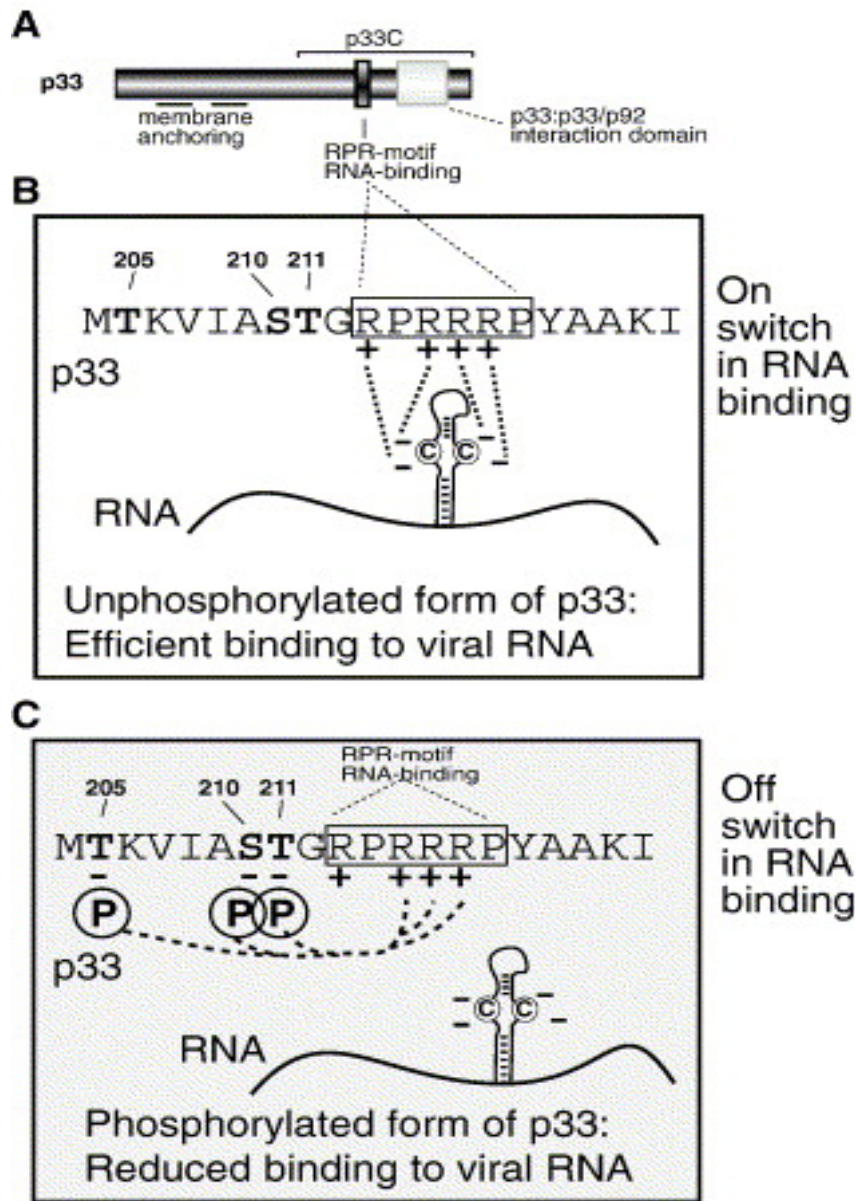


Fig. 3.1 Proposed effect of CNV p33 phosphorylation on its ability to bind to the viral RNA. (A) The known functional domains in p33 are shown schematically. (B–C) The positively charged amino acid sequence of the RPR motif involved in RNA binding and the predicted S/T phosphorylation sites are shown. The possible interactions between positively and negatively charged moieties are indicated with dotted lines. The model predicts that the nonphosphorylated p33 could bind stably to the viral RNA, whereas the phosphorylated form might not bind to the viral RNA due to the competition between the negatively charged phosphate groups and the RNA. Note that the hairpin structure illustrates RII(+)-SL with the C-C mismatch, which constitutes p33RE (Pogany et al., 2005).

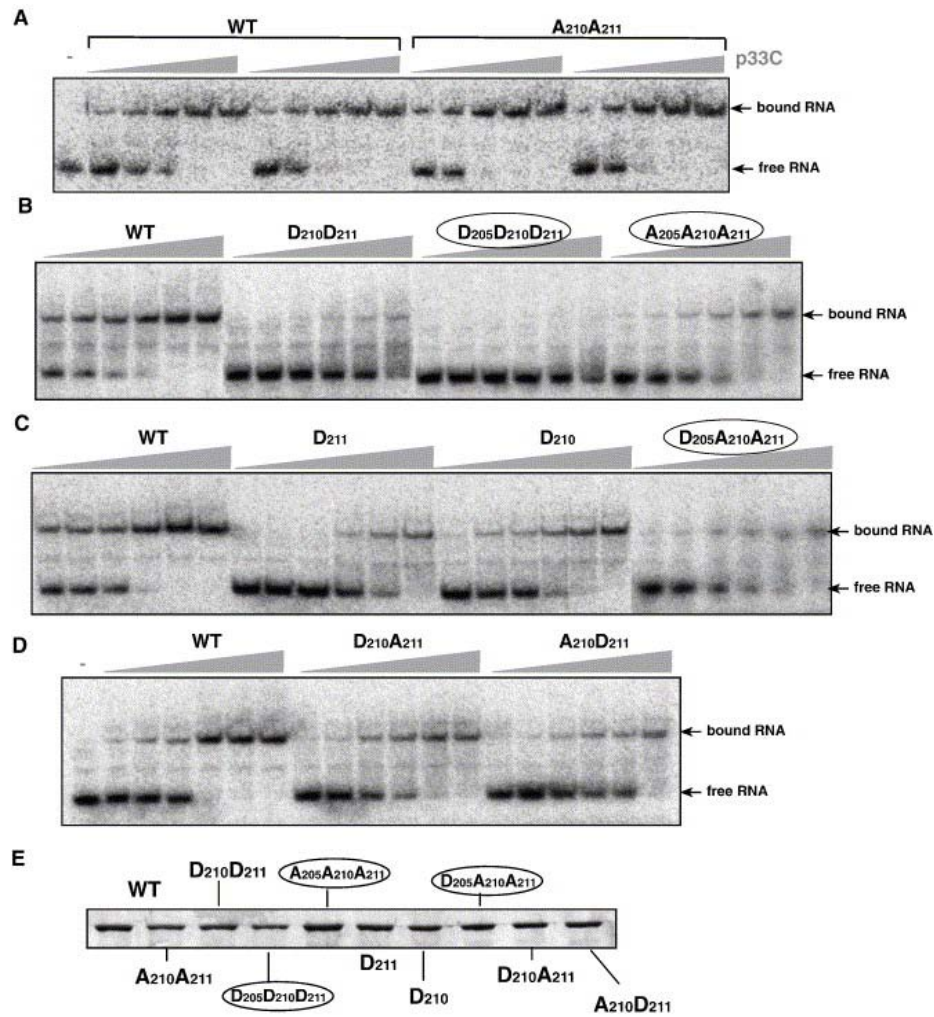


Fig. 3.2 Reduced RNA binding by the phosphorylation-mimicking p33 mutants in vitro. (A–D) EMSA was performed with various purified recombinant p33 carrying nonphosphorylation-, hypophosphorylation- and phosphorylation-mimicking mutations, respectively, at T205, S210 and/or T211 positions. The RNA probe was 32P-labeled RII(+)-SL, which includes p33RE sequence. The proteins were used in increasing amounts (2-fold increase, up to 200 μ g/ml). The migration of the unbound and bound RNAs is shown on the right of the gel images. The experiments were performed three times. (E) Coomassie-stained SDS-PAGE shows that the purified p33 preparations had comparable quantity and quality.

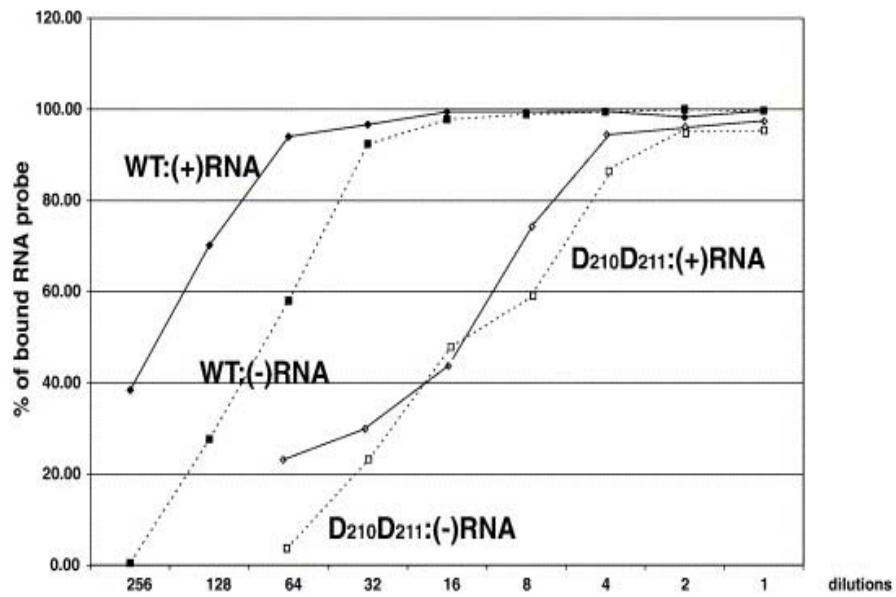
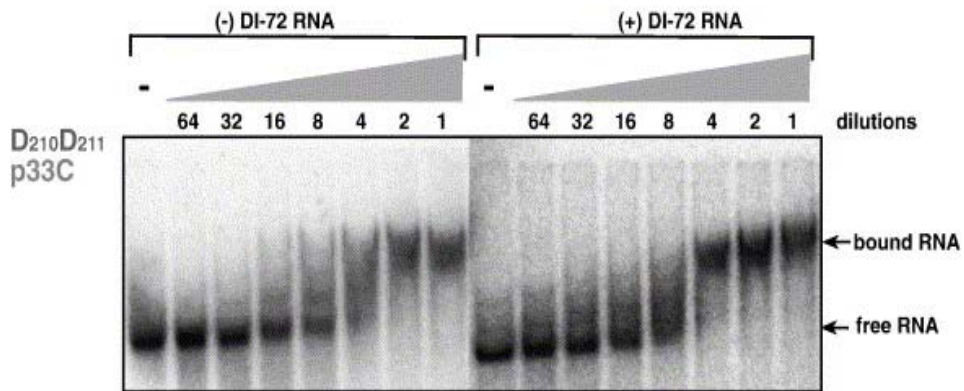
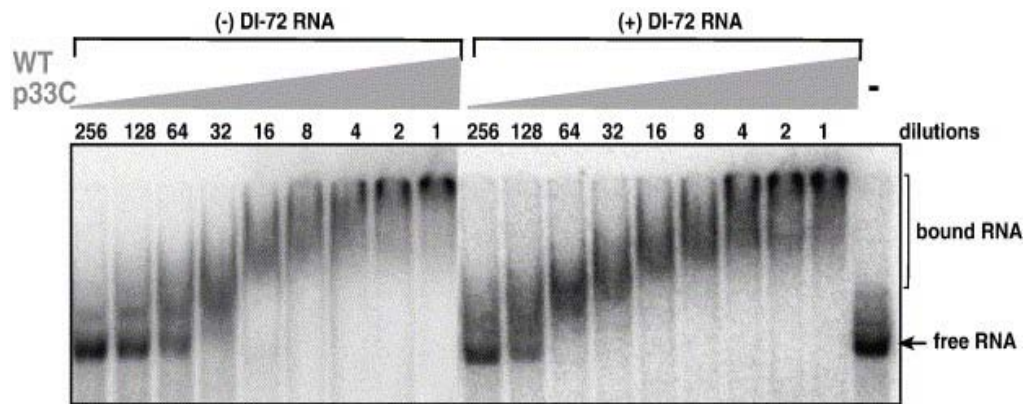
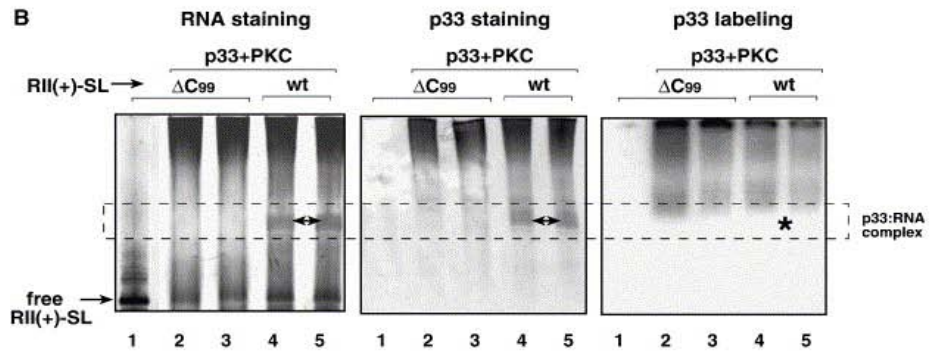
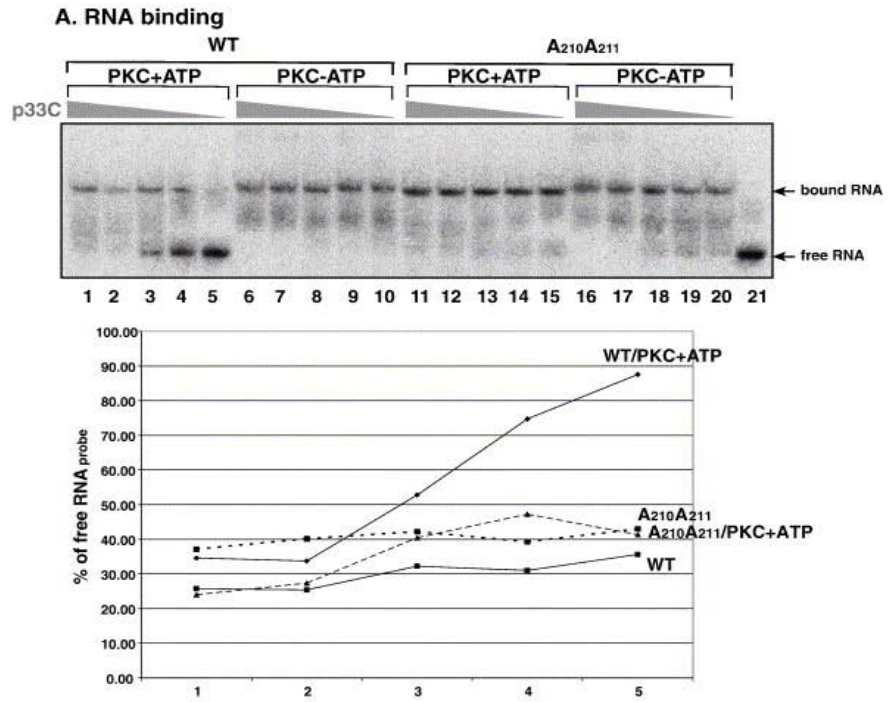
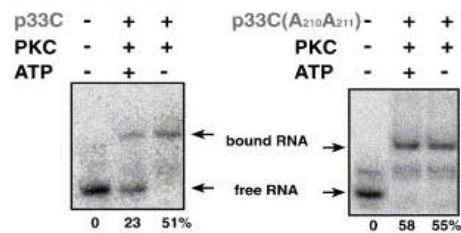


Fig. 3.3 The nonphosphorylated wt p33 binds both DI-72(+) and (-) RNA more efficiently than the phosphorylation-mimicking mutant. EMSA was performed with purified recombinant p33 preparations, either wt or D210D211 as described under Fig. 2. The p33 protein was used in increasing amounts (2-fold increase, up to 200 $\mu\text{g/ml}$), whereas the same amounts of ^{32}P -labeled DI-72(+) and DI-72(-) RNAs were applied. The percentage of bound RNA is shown graphically at the bottom. The unbound RNA probe in the absence of p33 is taken as 100%.



C. RNA release



D. phosphorylation of p33

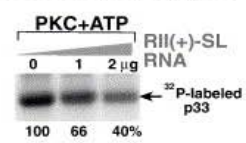
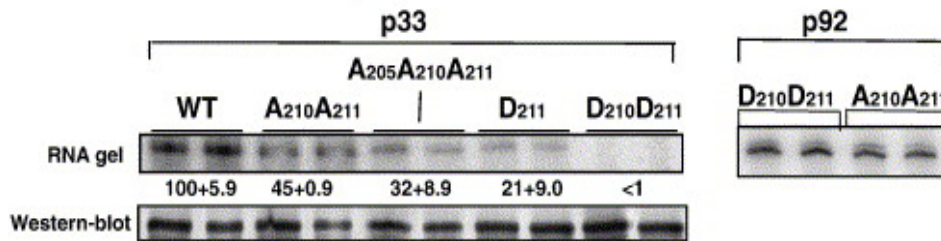


Fig. 3.4 Phosphorylation inhibits the ability of p33 to bind to the viral RNA and facilitates the release of bound RNA from the p33: RNA complex. (A) EMSA was performed with purified recombinant p33 (wt or A210A211) treated prior to RNA binding with PKC in the presence (marked as PKC + ATP) or absence of ATP (marked as “PKC-ATP”). The probe was the ³²P-labeled RII(+)-SL RNA as described in the legend to Fig. 2. The percentage of free RNA is shown graphically at the bottom. The free RNA probe in the absence of p33 is taken as 100%. (B) EMSA was performed as described in panel A, except that p33 was phosphorylated with PKC (lanes 2–5) in the presence of ³²P γ -ATP and Δ C99 (lanes 1–3) or wt RII(+)-SL (lanes 4–5) RNA probes were unlabeled. Lane 1 contains only the Δ C99 RNA probe as a marker. Left panel: the gel was stained with ethidium bromide to visualize the RNA probes (Δ C99 and wt RII (+)-SL only differ by 1 nt in length). Note the presence of a unique band in lanes 4–5, which represents the p33: RNA complex (depicted by a double headed arrow). Δ C99 RNA probe cannot bind to p33 (Pogany et al., 2005), thus there is no detectable p33: RNA complex in lanes 2–3. Middle panel: the same gel as in the left panel was stained with Coomassie blue to visualize p33. Note that the p33: RNA complex (depicted by a double headed arrow) was detected only in lanes 4–5 at the same position in the gel when compared with the left panel. Right panel: detection of ³²P-labeled p33 with a PhosphorImager from the same gel shown in the left and middle panels. Note the lack of ³²P-labeled p33 (i.e., the phosphorylated form of p33) in the area of p33: RNA complex (depicted by an asterisk). Therefore, these results suggest that the unphosphorylated form of p33, which is apparently still present after PKC treatment, is responsible for the observed RNA mobility shift visualized in the left and middle panels. (C) EMSA was performed with wt ³²P-labeled RII(+)-SL and unlabeled p33 (wt or A210A211) as described in panel A, except that the PKC treatment was done after the RNA binding reaction (i.e., after the formation of the stable p33:RNA complex). The percentage of bound RNA is shown below the gel. The free RNA probe in the absence of p33 is taken as 100%. (D) Phosphorylation of purified p33 with PKC using ³²P γ -ATP in the presence of RII(+)-SL RNA template (0, 1 or 2 μ g, as shown). Note that PKC can phosphorylate p33 even in the presence of excess amounts of RNA templates.

A. Enriched membrane preparations:



B. Purified replicase preparations:

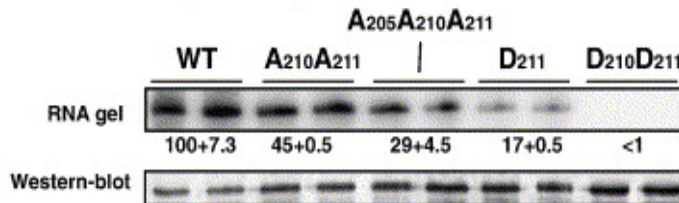
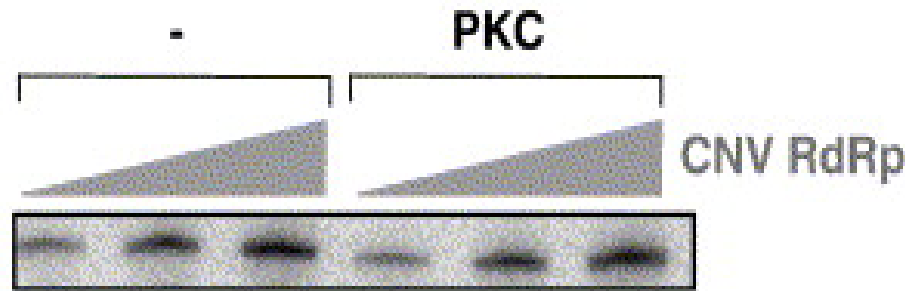


Fig. 3.5 Phosphorylation-mimicking mutations in p33 inhibit the assembly of functional CNV replicase complexes in yeast. (A) In vitro activity of CNV replicase present in membrane-enriched preparations. Each replicase preparation, obtained from yeast co-expressing p33, p92 and DI-72(+) RNA, was tested with the co-purified endogenous template (no template was added). ³²P-labeled RNA products from the above preparations were analyzed on denaturing 5% PAGE/8 M urea gels. For quantification, I measured the intensity of ³²P-labeled RNA products by using a PhosphorImager. Activity of the CNV replicase obtained from yeast expressing the wt p33 [in addition to wt p92 and DI-72(+) RNA] corresponds to 100%. Each experiment was performed three times. Western blot (at the bottom) shows the p33 levels in the membrane-enriched preparations. Similar replicase assay with membrane-enriched preparations containing mutated p92 and wt p33 is shown on the right. Note that phosphorylation-mimicking mutations in 92 (D210D211), unlike in p33, did not reduce CNV replicase activity. (B) In vitro activity of affinity purified CNV replicase preparations. Each replicase preparation, obtained from yeast co-expressing p33, p92 and DI-72(+) RNA, was tested in the presence of exogenous RI/III(-) template, which contains the minus-stranded regions I and III of DI-72 in a standard CNV replicase assay. Analysis of the replicase products and quantification were done as described in panel A. Western blot (at the bottom) shows the p33 levels in the affinity-purified CNV replicase preparations

A. with endogenous template



B. with exogenous template

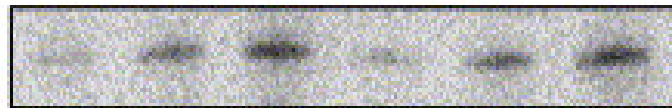


Fig. 3.6 Phosphorylation does not inhibit the activity of the preassembled functional CNV replicase complexes in vitro. (A) Enriched membrane fractions with endogenous templates, or (B) affinity-purified CNV replicase preparations programmed with RI/III(-) template, were treated with PKC prior to the replicase assay. See further details in the legend to Fig. 5.

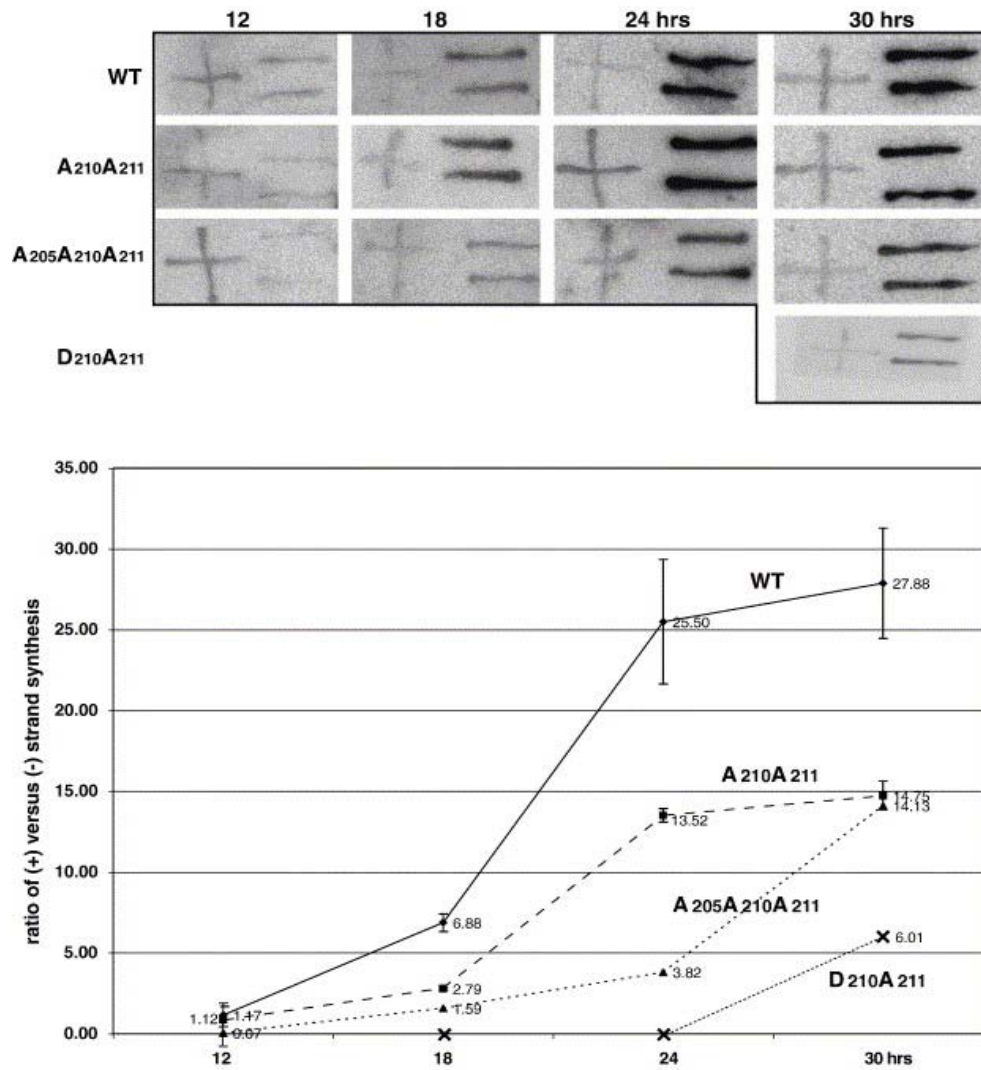


Fig. 3.7 Effect of phosphorylation site mutations in p33 on in vitro asymmetrical RNA synthesis by the CNV replicase obtained from yeast. Top: the RNA blots show the (+) and (-) strand synthesis by the in vitro CNV replicase. Unlabeled T7 RNA polymerase transcripts of DI-72(+) and DI-72(-) (400 ng each), marked as + and =, respectively, were blotted on the membrane. The blotted RNAs were then hybridized with denatured ^{32}P -labeled RNA probes, which were generated by the CNV replicase in vitro on the endogenous templates present in the enriched membrane fractions obtained from yeast. Time points for harvesting the yeast samples for isolation of enriched membrane fractions are shown on the top. Bottom: the ratio between plus- and minus-stranded RNAs in the in vitro replicase assay was calculated based on PhosphorImager analysis from three separate experiments .

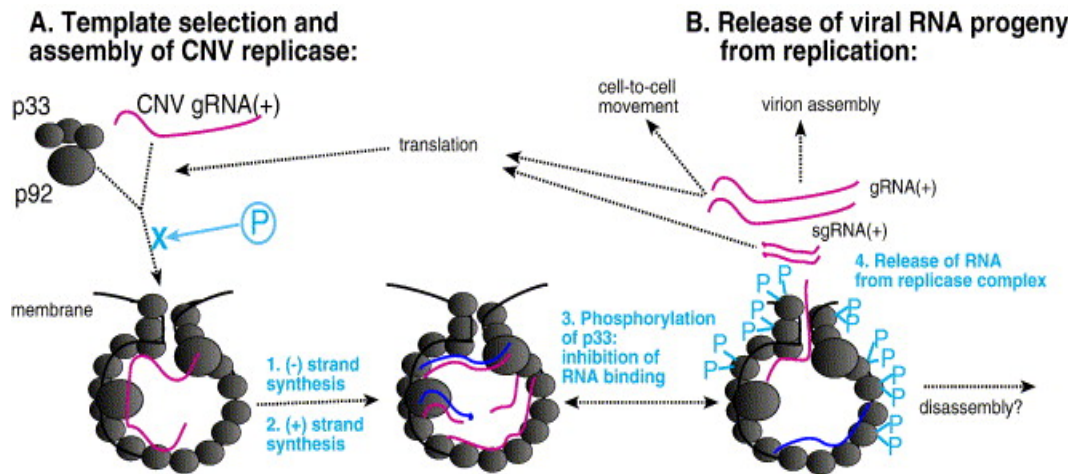


Fig. 3.8 A model on the role of phosphorylation of p33 in CNV replication. (A) At the beginning of infection, the freshly translated nonphosphorylated p33 is actively involved in the assembly of the CNV replicase, and the recruitment of the viral RNA template to membranous vesicles formed on the surfaces of peroxisomes. The single vesicle schematically shows a hypothetical replication unit, based on BMV (Schwartz et al., 2002), with numerous p33, several p92 and the (+)-stranded viral RNA (purple). Hypophosphorylation of p33 might affect the ratio of plus- versus minus-strand synthesis by the CNV replicase. (B) Phosphorylation of p33 leads to decreased RNA binding, thus facilitating the release of the newly synthesized genomic and subgenomic RNA progeny from replication. The released viral RNA will likely participate in new rounds of translation, cell-to-cell movement and/or encapsidation. However, at later time point, the phosphorylated p33 cannot participate in the assembly of new CNV replicase complexes, thus resulting in shut down of replication (indicated by an “X”). A possible role of phosphorylation in the disassembly/degradation of replicase complexes is also shown.

CHAPTER IV

RNA chaperone activity of the tombusviral p33 replication protein facilitates initiation of RNA synthesis by the viral RdRp

Introduction

RNA binding proteins, such as helicases and cofactors, have been proposed to play auxiliary roles in RNA virus replication, however (+)RNA viruses with genomes less than 6,000 nt do not code for RNA helicases (Koonin and Dolja, 1993). Accordingly, viral-coded RNA chaperones have been shown to participate in the replication of picornaviruses, coronaviruses and hepatitis delta virus (Huang and Wu, 1998; Wang et al., 2003; DeStefano and Titilope, 2006), or affect the packaging of coronaviruses, hepatitis C virus, retroviruses and minus-stranded RNA viruses (Rein et al., 1998; Cristofari et al., 2004; Levin et al., 2005; Cruceanu et al., 2006; Ivanyi-Nagy et al., 2006; Mir and Panganiban, 2006, 2006; Zuniga et al., 2007). Host-coded RNA chaperones have also been shown to affect calicivirus and viroid RNA replication (Daros and Flores, 2002; Karakasiliotis et al., 2006). The unique feature of RNA chaperones is that they do not require rNTPs for destabilizing RNA structures, but instead, they bind cooperatively to the RNA that leads to structural changes in the RNA. Thus, RNA chaperones will profoundly affect the folding process, interactions between RNAs and the accessibility of the RNA to other proteins.

One group of small plus-stranded RNA viruses, which does not code for RNA helicases, is tombusviruses. These viruses, including *Tomato bushy stunt virus* (TBSV) and *Cucumber necrosis virus* (CNV), code for an essential RNA-binding protein, termed p33, which is known to affect many steps during the infection process. For example, p33 has been shown to bind to a C•C mismatch within an internal cis-acting stem-loop element that leads to selective recruitment of the viral RNA into replication (Monkewich et al., 2005; Pogany et al., 2005). p33 is also involved in the formation of spherule-like structures on the cytoplasmic interface of peroxisomal membranes, which represent the site of viral RNA replication (McCartney et al., 2005; Panavas et al., 2005; Navarro et al., 2006). Its role in viral

pathogenesis has also been documented (Burgyan et al., 2000). In addition to the RNA-binding domain, p33 also contains two short p33:p33/p92^{pol} interaction domains that are likely important for the assembly of the viral replicase and for RNA binding, too (Panaviene et al., 2003; Rajendran and Nagy, 2004; Pogany et al., 2005). Phosphorylation close to the RNA-binding domain is thought to regulate the function of p33 during replication (Shapka et al., 2005; Stork et al., 2005). Overall, p33 seems to be the master regulator of the tombusvirus replication process (Nagy and Pogany, 2006).

Based on cooperative RNA binding ability of p33, I speculated that p33 might be able to perform many functions during infection via acting as an RNA chaperone that modifies the structure of the viral RNA to allow the participation of the viral RNA in different ribonucleoprotein complexes. To test this hypothesis, I performed biochemical experiments with purified recombinant p33 in in vitro assays. I have demonstrated that p33 can stimulate initiation of RNA synthesis by up to 5-fold by a viral RNA-dependent RNA polymerase (RdRp) in vitro. In addition, p33 made double-stranded (ds)RNA templates sensitive to S1 nuclease, it unwound short ssDNA/ssRNA hybrids and stimulated self-cleavage by a ribozyme in vitro. Interestingly, p33 required two RNA-binding regions for its RNA chaperone activity. Based on these data, I propose a role for the RNA chaperone activity of p33 during tombusvirus replication.

Results

We have shown previously that depending on the protein concentration, mutations or the composition of the buffer, the tombusvirus p33 auxiliary protein can bind to the viral RNA either specifically or non-specifically (Rajendran and Nagy, 2003; Pogany et al., 2005). The specific interaction between p33 and the viral RNA is required for the recruitment of the TBSV (+) RNA to the membrane-bound replicase complex (Monkewich et al., 2005; Pogany et al., 2005). However, after the selective (+) RNA recruitment, the function of p33 could be different within the viral replicase complex, where p33 is present in high amount, reaching ~10-20-fold excess over the p92^{pol} (Rajendran and Nagy, 2006; Serva and Nagy, 2006). The high local concentration of p33 within the replicase complex could facilitate non-specific binding of p33 to the viral RNA in cooperative manner (Rajendran and Nagy, 2003), possibly allowing p33 to function as an RNA chaperone within the replicase complex. Therefore, I tested if the tombusvirus p33 possesses RNA chaperone activity in vitro using purified components.

Strand separation activity of the recombinant p33 on short DNA oligo - RNA hybrid in vitro.

To test the possible RNA chaperone activity of p33, I used a strand separation assay (Fig. 4.1A). A short ssDNA was 5' end labeled and annealed with the unlabeled DI-72 (-)RNA, followed by the addition of purified recombinant CNV p33. I have found that 65% of ssDNA/ssRNA hybrid was separated by p33 when present in high concentration (Fig. 4.1B, lane 4). This result is in agreement with RNA chaperone-like activity of p33, which lacked ribonuclease activity (Fig. 4.1C). However, further experiments have shown that p33 could not efficiently separate 621 bp long RNA-RNA hybrids under the same conditions (not shown), suggesting that the RNA chaperone activity of p33 is not robust (not shown).

P33 replication protein renders a dsRNA template ribonuclease sensitive in vitro.

To further test if p33 can open up dsRNA structures, I developed an S1 nuclease-based assay (Fig. 4.2A). While dsDI-72 was completely resistant to S1 nuclease digestion under the in vitro conditions (Fig. 4.2B, lanes 1,5, and 9), addition of purified recombinant p33 made dsRNA S1 ribonuclease sensitive, leading to RNA degradation up to 75% (Fig. 4.2B, lanes 4,8, and 12). The same p33 preparation when applied in the absence of S1 did not lead to degradation of dsRNA, excluding the possibility that the purified recombinant p33 preparation was contaminated by a bacterial ribonuclease (Fig. 4.2C). In addition, p33 lacking the RPR RNA-binding domain (construct p33-DRPR)(Rajendran and Nagy, 2003) did not render dsDI-72 RNA S1 nuclease sensitive (Fig. 4.2D, lanes 2-4). These data are consistent with the model that the RNA-binding ability of p33 is critical to render the dsRNA template S1 nuclease sensitive.

P33 replication protein facilitates self-cleavage by a ribozyme in vitro.

Since RNA chaperones bind to the RNA nonspecifically and cooperatively, like p33 when present in high concentration (Rajendran and Nagy, 2003), they can facilitate RNA cleavage by ribozymes (Cristofari and Darlix, 2002; Zuniga et al., 2007). This property of the RNA chaperones are due to refolding of the ribozyme sequence trapped in non-active conformation. To test the effect of p33 on ribozyme activity, I used the self-cleaving ribozyme of satellite *Tobacco ringspot virus* (Buzayan et al., 1986; Panavas and Nagy, 2003) in the presence of recombinant p33 (Fig. 4.3A). I have found that p33 stimulated the ribozyme activity by ~4-fold, reducing the amount of uncleaved RNA and increasing the amount of self-cleaved RNAs (Fig. 4.3B, lane 3 versus lane 1). This finding supports the model that p33 could be involved in RNA folding in a sequence non-specific manner.

Inhibition of the RdRp-driven RNA synthesis by ssDNA complementary to the promoter is neutralized by p33.

Since the RNA chaperone activity of p33 replication protein is likely important within the viral replicase complex, I wanted to test if p33 could change the activity of a viral RdRp on RNA templates. I have chosen a heterologous RdRp derived from a related virus, *Turnip crinkle virus* (TCV). The original RdRp protein of TCV, termed p88, contains a domain similar to the tombusvirus p33 replication protein that might also function as an RNA chaperone. Therefore, I used an N-terminally-truncated p88, termed p88C, which lacks the domain similar to p33, yet it is a highly active RdRp on ssRNA templates in vitro (Rajendran et al., 2002; Panavas et al., 2006). Unfortunately, the comparable segment of TBSV or CNV p92^{pol}, termed p92C, which lacks the p33 overlapping domain, or the full-length p92^{pol} RdRp are not active in vitro (not shown), thus preventing the possibility to compare the activity of the TCV p88C and the tombusvirus p92C/p92^{pol}. Overall, the advantage of using this heterologous system is that the tombusvirus p33 does not interact directly with TCV p88C (Rajendran and Nagy, 2004), thus making it unlikely that any stimulatory effect of p33 on p88C RdRp activity would be due to direct enhancement of RdRp activity (i.e., acting like a transcription factor). Rather, p33 could likely affect RdRp activity by altering the RNA template due to its possible RNA chaperone activity.

To test for the possible RNA chaperone activity of p33 replication protein, I set up an in vitro assay based on the p88C RdRp protein and a partial ssRNA/ssDNA hybrid (Fig. 4.4A). Since previous studies have established that the accessibility of the terminal promoters by the tombusviral or TCV RdRps is a critical factor during initiation, I used a short ssDNA complementary to the very 3' end of DI-72(-) to form partial DNA/RNA hybrid within the complementary sequences. I have found that the ssDNA inhibited RNA synthesis by ~80% in the RdRp assay (Fig. 4.4B,

lanes 2, 6 versus lanes 1, 5). This observation suggests that the initiation site was much less accessible to the p88C RdRp in the presence of ssDNA than on the free RNA template.

Importantly, I have found that the addition of recombinant p33 enhanced p88C activity by ~3-fold on the partial ssRNA/ssDNA hybrid (Fig. 4.4B, lane 4 and 8). This finding supports the idea that p33 facilitates the accessibility of the cPR promoter in DI-72 (-) template by destabilizing the ssRNA/ssDNA hybrid (Fig. 4.4A).

P33 facilitates initiation of RNA synthesis on dsRNA template by p88C RdRp.

To further test the possible RNA chaperone activity of p33, I used dsDI-72 RNA in the p88C RdRp assay. Previous studies have established that p88C was inefficient in initiation of RNA synthesis on TBSV dsRNA templates when compared to the ss(-)RNA template (Panavas et al., 2006). Inefficient initiation on dsRNA templates was likely due to poor accessibility of the promoter to the RdRp in the dsRNA when compared to ssRNA. However, once initiation takes place, the RdRp can unwind the dsRNA structure during strand elongation.

Using gel-isolated dsDI-72 RNA template in p88C RdRp assay, I found that addition of increasing amounts of recombinant p33 enhanced p88C activity by more than two-fold (Fig. 4.5A-B, lanes 1-10). This enhancement is not due to stabilization of p88C by p33 because the activity of p88C on template dsDI-72(5'D69) with an unbase-paired ssRNA tail including the cPR promoter was decreased by the addition of p33 (Fig. 4.5B, lanes 11-20). Moreover, deletion of the RNA binding domain (construct p33-DRPR) of p33 eliminated the stimulatory effect of p33 on p88C with dsDI-72 template (Fig. 4.5C), suggesting that the ability of p33 to bind to the RNA is important for stimulation of the RdRp activity on dsRNA template.

To further test the possible RNA chaperone activity of p33, I used template dsDI72 (5'm3-8) (Fig. 4.5D), which has a "bubble structure" that enhances the

availability of cPR sequence by p88C RdRp by only 25% (Panavas et al., 2006). Interestingly, addition of recombinant p33 to the assay led to ~5-fold increase in template activity (Fig. 4.5E, lanes 3-4 and 7-8). Similarly, dsDI-72 (5'D11) (Fig. 4.5D), which forms a short inhibitory hairpin within the cPR sequence, was used ~2.5-fold more efficiently by p88C RdRp after addition of the recombinant p33 to the assay (Fig. 4.5E, lanes 9-16). The easiest interpretation of these data is that p33, due to its RNA chaperone activity, facilitates the initiation step for p88C RdRp by opening up the stable secondary structure within the cPR sequence in the dsRNA template.

P33 promotes initiation on (+) RNA template by the p88C RdRp.

The (+) RNA template in tombusviruses contains a silencer element that inhibits initiation of (-) RNA synthesis due to base-pairing between an internal loop sequence of a distant hairpin and the 5 nt 3' terminal sequence, which makes the initiation site poorly accessible for the viral RdRp (Fig. 4.4C) (Pogany et al., 2003). To test if the chaperone activity of p33 could promote initiation on the (+) RNA template, I used DI-72 (+) in our standard p88C RdRp assay in the presence of various amounts of recombinant p33. The RdRp assay revealed that p33 enhanced initiation on the (+) RNA template by ~2-fold (Fig. 4.4D), suggesting that p33 can facilitate opening up the base-pairs formed between the silencer and promoter, thus likely facilitating the loading of the viral RdRp on the (+) RNA template.

The C-terminal portion of p33 containing the RNA-binding region is not an active RNA chaperone in vitro.

To dissect what domains within the p33 replication protein are needed for RNA chaperone activity, first I tested p33C carrying the RPR RNA binding and the S1-S2 protein-protein interaction domains (Fig. 4.6A) (Panaviene et al., 2003; Rajendran and Nagy, 2004, 2006). Addition of p33C to the standard p88C RdRp assay with dsDI-72 template revealed a slight inhibitory effect on p88C RdRp activity (Fig.

4.6B), instead of the expected stimulatory effect. P33C also strongly inhibited p88C RdRp activity on dsDI-72 (5'D69) template (Fig. 4.6C). Based on these observations, I suggest that p33C does not have an RNA chaperone activity comparable with the full-length p33.

The N-terminal portion of p33 contains an additional RNA-binding region required for RNA chaperone activity.

The lack of RNA chaperone activity by p33C indicated that the N-terminal region in p33 might also have an RNA binding region that is necessary for RNA chaperone activity. Therefore, I tested if the N-terminal segment of p33 could bind to the viral RNA in a gel mobility shift experiment. Indeed, construct p33-N1-82 carrying the N-terminal 82 aa bound to the labeled RNA template in vitro, whereas the shorter version (termed p33-N1-72 with 72aa segment) bound less efficiently (Fig. 4.6D). These data suggested that the N-terminal portion of p33 contains ssRNA binding activity. Further experiments have demonstrated that ssRNA-binding by p33-N1-82 is non-specific and much weaker than ssRNA binding by p33C (Judit Pogany unpublished data).

To test if the N-terminal segment of p33 contributes to the RNA chaperone activity of p33, I made construct p33-D72-130, which lacked the N-proximal RNA binding region (between positions 72-82) and a transmembrane segment to increase solubility of the recombinant protein in *E. coli*. When compared with the full-length p33, the purified recombinant p33-D72-130 lacked RNA chaperone activity in the S1 nuclease sensitivity assay (Fig. 4.6E). Thus, the result with p33-D72-130 is similar to that obtained with p33C, suggesting that the N-proximal RNA binding region of p33 is likely part of the functional RNA chaperone.

Discussion

A large group of small RNA viruses codes for auxiliary replication proteins that lack helicase/ATPase motifs. Among these is the essential p33 replication protein of tombusviruses, which has essential functions in RNA replication (White and Nagy, 2004; Nagy and Pogany, 2006). The ability of p33 to bind to the viral RNA is critical during tombusvirus replication and it also affects viral RNA recombination (Panaviene et al., 2003; Panaviene and Nagy, 2003; Jaag et al., 2007). Interestingly, p33 can bind to the viral RNA in two different fashions. The first type of RNA binding by p33 is specific to a region in the plus-stranded TBSV RNA termed RII(+)-SL with a signature C•C mismatch (also termed p33 recognition element) (Monkewich et al., 2005; Pogany et al., 2005). This specific p33-RNA interaction requires small amount of p33, likely in the form of p33 dimer (Pogany et al., 2005). The above specific p33-TBSV (+)RNA interaction is critical for the selective recognition of the TBSV RNA and its recruitment into replication. The second type of RNA binding is non-specific binding of p33 to ssRNA and ssDNA, and to a lesser extent to dsRNA (Rajendran and Nagy, 2003). This non-specific nucleic acid binding by p33 requires a high concentration of p33 and occurs in a cooperative manner (Rajendran and Nagy, 2003). I envision that the non-specific RNA-binding activity of p33 is only important within the assembled, membrane-bound tombusvirus replicase complex, which contains a large amount of p33 and only the selectively recruited TBSV RNA in addition to p92^{pol} and host factors (Serva and Nagy, 2006). Within this context, the RNA chaperone activity of p33 could be important for tombusvirus replication (see below).

Based on in vitro approaches using recombinant p33, I have shown that p33 could function as an RNA chaperone. The supporting evidence for p33 RNA chaperone function includes: (i) up to 5-fold stimulation of initiation of RNA synthesis by the heterologous TCV RdRp on dsRNA templates or ssDNA/ssRNA hybrids; (ii) enhancing the level of minus-strand RNA synthesis from the minus-strand initiation promoter (gPR), which is likely due to opening up the silencer-

promoter interaction; (iii) Increasing the sensitivity of dsRNA templates to the ssRNA-specific S1 nuclease, suggesting that p33 binding to the dsRNA leads to unwinding/opening up the structure, and rendering dsRNA nuclease sensitive. (iv) Also, strand separation assay with ssDNA/ssRNA hybrids showed unwinding of the hybrid in the presence of p33; Moreover, (v) p33 stimulated self-cleavage by a ribozyme in vitro, supporting the RNA-folding ability of p33. Further evidence for the genuine RNA chaperone activity of p33 is the requirement for the RNA binding regions in p33 for RNA chaperone activity, suggesting that p33 must interact with the RNA template in order to function as a chaperone. The use of the heterologous p88C RdRp with p33 [these proteins do not interact in vitro (Rajendran and Nagy, 2004)] makes it unlikely that the stimulatory effect of p33 on TCV p88C activity on dsRNA templates is due to activation of p88C RdRp.

Many known RNA chaperones have long intrinsically disordered (unstructured) regions, which undergo disorder-to-order transitions upon binding to RNA (Ivanyi-Nagy et al., 2005). This leads to unwinding (unfolding) of the bound segment of the RNA, which then can refold to a new conformation (Tompa and Csermely, 2004). To predict if p33 replication protein contains naturally disordered regions, I used PONDR VL-XT (Romero et al., 1997; Bracken et al., 2004; Romero et al., 2004). As shown in Fig. 4.7, the p33 replication proteins of five tombusviruses were predicted to contain their two RNA-binding sequences within naturally disordered regions. The conserved naturally disordered RNA-binding regions in the p33 replication proteins further support the model that p33 functions as RNA chaperone.

Based on previous results that p33 can bind to the viral RNA in a cooperative fashion and it can also bind to dsRNA, albeit less efficiently than to ssRNA (Rajendran and Nagy, 2003), I suggest that partial coating of the RNA by p33 might help unwinding secondary structure or dsRNA form. Since p33 could not separate the dsRNA strands in the 621 bp long dsDI-72 RNA, I propose that p33 has a weak RNA chaperone activity, which might only be enough to open up dsRNA form from the end carrying the AU-rich stretch (within the plus-strand initiation promoter, Fig. 4.5) or the short silencer-promoter structure (Fig. 4.4C-D). Indeed, providing a weaker dsRNA structure in dsDI72 (5'm3-8) (Fig. 4.5D), which has a "bubble structure"

(Panavas et al., 2006), led to 5-fold enhanced RdRp activity by the TCV p88C due to the RNA chaperoning activity of p33. It is plausible that p88C is not efficient enough to bind to the dsRNA regions (i.e., leading to inefficient loading of the RdRp on the template). However, p33 might help opening up the dsRNA structure from the weaker AU-rich end, followed by loading the RdRp and then plus-strand synthesis (Fig. 4.8). Indeed, I have shown previously that both the CNV replicase and p88C can only open up the "left-side" of the dsRNA carrying the AU-rich stretch. Thus, our in vitro data indicate that the primary function of p33 as an RNA chaperone is to facilitate initiation of RNA synthesis by making the promoter regions accessible to the viral RdRp. Unwinding of additional internal RNA structures might be accomplished by the viral RdRp during RNA synthesis as demonstrated earlier (Panavas et al., 2006). Interestingly, binding of p33 or p33C to ssRNA regions actually inhibited RdRp activity (Fig. 4.5B, lanes 11-20 and Fig. 4.6C). This suggests that p33 and especially p33C bound strongly to the ssRNA might hinder RdRp activity. Based on this and other data, I propose that the RNA chaperone activity of p33 affects both plus- and minus-strand synthesis via facilitating initiation (Fig. 4.8). Future in vitro assembly approaches should help to address this and related questions.

Materials and Methods

Preparation of dsRNA templates.

First, single-stranded (ss)RNA templates were obtained by *in vitro* transcription with T7 RNA polymerase using PCR amplified DNA templates (Panavas et al., 2002; Panavas and Nagy, 2005). Second, to make the dsRNA constructs, I annealed the heat denatured ssRNA transcripts (94 °C for 5 min) in STE buffer (10 mM TRIS, pH 8.0, 1 mM EDTA, and 100 mM NaCl), followed by slow cooling (30 min) to 25 °C (Panavas and Nagy, 2005; Panavas et al., 2006). The annealed RNAs were loaded onto 5% non-denaturing polyacrylamide gels, followed by staining with ethidium bromide. After cutting out the annealed RNA band, I eluted the dsRNA into 0.6 M ammonium acetate, followed by phenol/chloroform extraction and ethanol precipitation (Panavas et al., 2006). The quality of the obtained dsRNA was checked by non-denaturing polyacrylamide gels.

Purification of recombinant proteins

TCV p88C RdRp and CNV p33 were expressed as MBP-fusion proteins in *E. coli* and purified using affinity-based chromatography as described earlier (Rajendran et al., 2002; Rajendran and Nagy, 2003), except that 2 µg RNase A was added to the sonicated cell lysate and incubated it for 15 min on ice to remove RNA. The protein concentrations were adjusted to 250 µg /ml with column buffer (Rajendran et al., 2002; Rajendran and Nagy, 2003).

In vitro replicase assays

TCV RdRp reactions were carried out for 2 h at 25°C in the RdRp buffer consisting of 50 mM Tris-HCl (pH 8.2), 10 mM MgCl₂, 10 mM dithiothreitol, 100 mM potassium glutamate, ATP, CTP, and GTP (1.0 mM each), and 0.3 µl of [³²P]UTP (0.1mCi/ml) in 50 µl volume (Rajendran et al., 2002). Each RdRp reaction mixture contained 0.5µg template (ds or ssRNA), 1.5 µg purified p88C RdRp enzyme (Panavas et al., 2006) and p33. After phenol-chloroform extraction and ammonium acetate-isopropanol precipitation, the RNA products were treated with S1 nuclease followed by another phenol-chloroform extraction and ammonium acetate/isopropanol precipitation. The samples were analyzed by electrophoresis on denaturing 5% acrylamide, gels containing 8 M urea. The gels were dried, exposed to a phosphorscreen and analyzed using Typhoon phosphorimager (GE Healthcare) and ImageQuant software .

RNA gel mobility shift assay

RI(-)probe of DI-72 RNA was labeled with [³²P]UTP using T7 RNA polymerase. Approximately 20 ng of labeled RNA was incubated with MBP-p33 mutant for 20 min at room temperature in the RdRp buffer (Rajendran et al., 2002; Rajendran and Nagy, 2003). The samples were analyzed by electrophoresis on native 5% acrylamide gels, run at 200 V for 20 min at 4°C in Tris-acetate-EDTA (TAE) buffer. Analysis was as described above.

S1 nuclease sensitivity assay

The dsRNA was obtained using [³²P]UTP-labeled (-)DI-72 RNA and unlabelled (+)DI-72 RNA in STE buffer. Different amounts (0, 0.5, 1, and 2 µg) of recombinant CNV MBP-p33 mutants were added to the dsRNA (approximately 15ng) in RdRp buffer in 10µl final volume. The samples were incubated for 15 minutes at room temperature, then 85U of S1 nuclease were added in 1.2µl 10x S1 buffer (Promega) followed by 15 minutes incubation at 37 °C. The samples were loaded on a non-denaturing 8% acrylamide gel containing 0.1% SDS.

Strand separation (unwinding) assay

Oligo #2610 (GGAAATTCTCCAGGA) was [³²P]-labeled at the 5' end with γATP (0.05 mCi) using polynucleotide kinase (Fermentas). The annealing of 4 pmol of oligo and 4 pmol of DI-72(-) RNA in STE buffer was done at 37 °C for 20 minutes. Different amounts of MBP-p33 (0, 1, and 2µg) was added to the annealed ssDNA/ssRNA hybrid in the RdRp buffer, followed by incubation at room temperature for 20 minutes. The samples were then analyzed by electrophoresis on non-denaturing 8% acrylamide gels containing 0.1% SDS [modified from (Zuniga et al., 2007)].

Ribozyme self-cleavage assay

The satellite (-) ribozyme of TRSV (Buzayan et al., 1986) fused to the 3' end TBSV RIV RNA was made by T7 polymerase. The purified recombinant MBP-p33 was included in the 20 µl T7 reaction. The DNA template for the T7 polymerase was obtained by PCR using oligos #19 (GTAATACGACTCACTATAGGAATTCCTGTTTACGAAAG) and #1069 (CCGGTCGAGCTCTACCAGGTAATATAACCACAACGTGTGT) with plasmid

pYC2/CT DI-72-Rz (Panavas and Nagy, 2003). Incubation was at 37 °C for 20 minutes, followed by a phenol chloroform extraction and ethanol precipitation. The radioactively labeled RNA was loaded to a denaturing 5% acrylamide gel/8M urea.

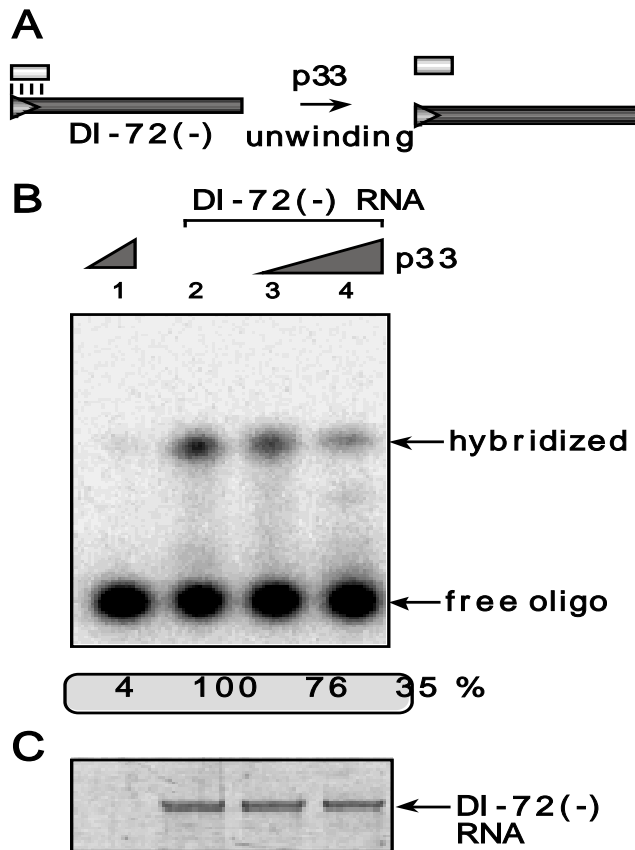


Fig. 4.1 Unwinding of the ssDNA/ssRNA hybrid by p33 in a strand separation assay. (A) Scheme of the strand separation assay showing the hybridized ssDNA/ssRNA. The 5' end labeled, 16 base ssDNA was annealed to the unlabeled DI-72(-) RNA prior to the addition of purified recombinant p33. (B) Lane 1: free ssDNA plus 2 μ g of purified MBP-p33; lane 2: annealed ssDNA/ssRNA, no p33; lane 3: annealed ssDNA/ssRNA plus 1 μ g purified recombinant p33; lane 4: annealed ssDNA/ssRNA plus 2 μ g p33. The 32 P-labeled free ssDNA and ssDNA/ssRNA hybrid were separated on nondenaturing 10% acrylamide gels. The gel contained 0.1% SDS to dissociate protein-RNA complexes. Quantification was done with ImageQuant. (C) Ethidium-bromide-stained denaturing PAGE to show the intact DI-72(-) RNA in samples treated as shown in legend B.

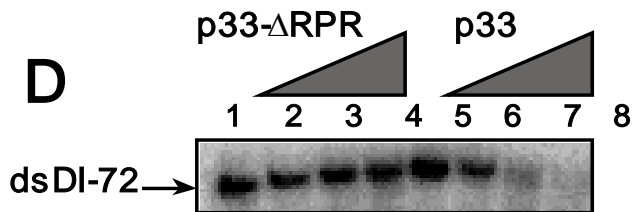
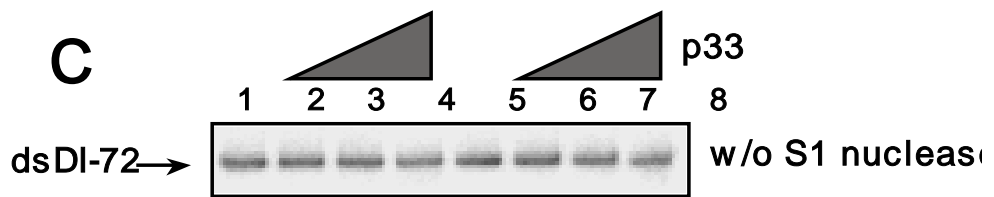
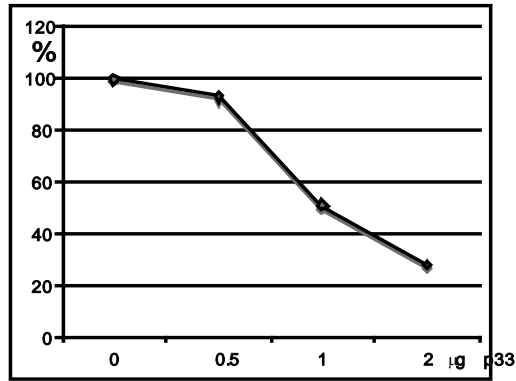
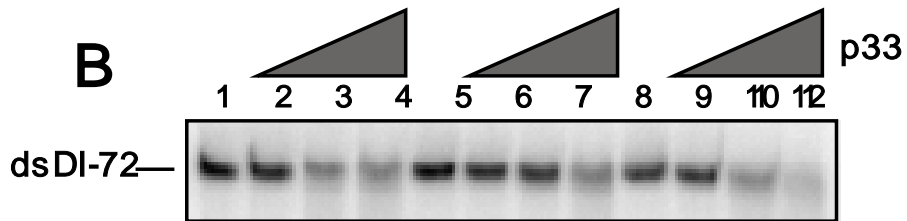
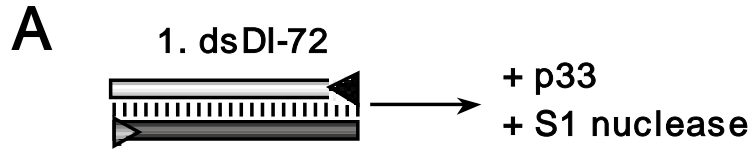


Fig. 4.2 Increased sensitivity of dsRNA to single-strand specific S1 nuclease due to the RNA chaperone activity of p33. **(A)** Schematic presentation of the dsDI-72 RNA template and the treatment applied. **(B)** Representative denaturing gel of radiolabeled RNA template (5 ng) that remained after the S1 nuclease treatment in the presence of 0, 0.5, 1 and 2 mg of purified recombinant p33 are shown. The samples were phenol/chloroform extracted prior to gel-analysis. **(C)** A control experiment showing that dsRNA template is insensitive to treatment with purified p33 in the absence of S1 nuclease. The condition during the experiments is comparable to that shown in panel B, except S1 was not added to the samples. **(D)** A control experiment showing that dsRNA template is insensitive to treatment with S1 nuclease in the presence of a p33 mutant lacking the RPR RNA-binding sequence. See further details in panel B.

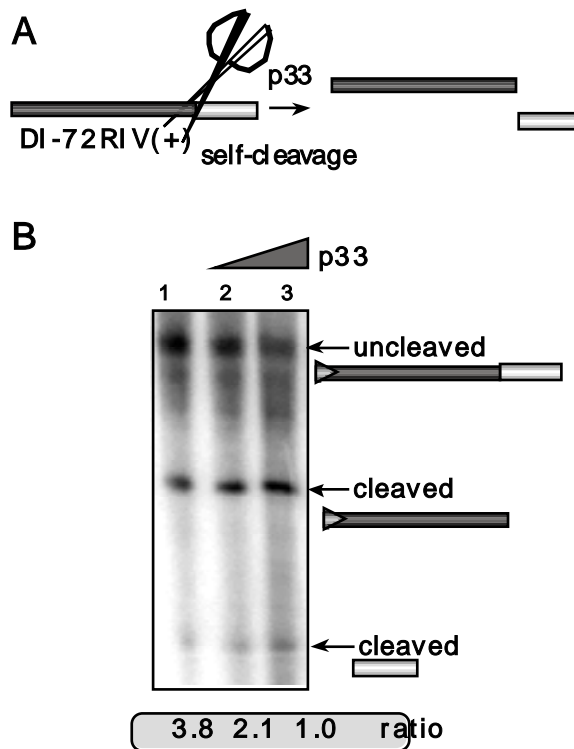


Fig. 4.3 Recombinant CNV p33 promotes the self cleavage activity of the satellite *Tobacco ringspot virus* ribozyme in vitro. (A) Schematic presentation of the RNA template carrying the ribozyme sequence before and after the self-cleavage. (B) Representative denaturing gel of ^{32}P -labeled RNA cleavage products, which are derived from the template RNA synthesized by *in vitro* transcription with T7 RNA polymerase in the presence of 0, 1 and 2 mg of purified recombinant p33 are shown.

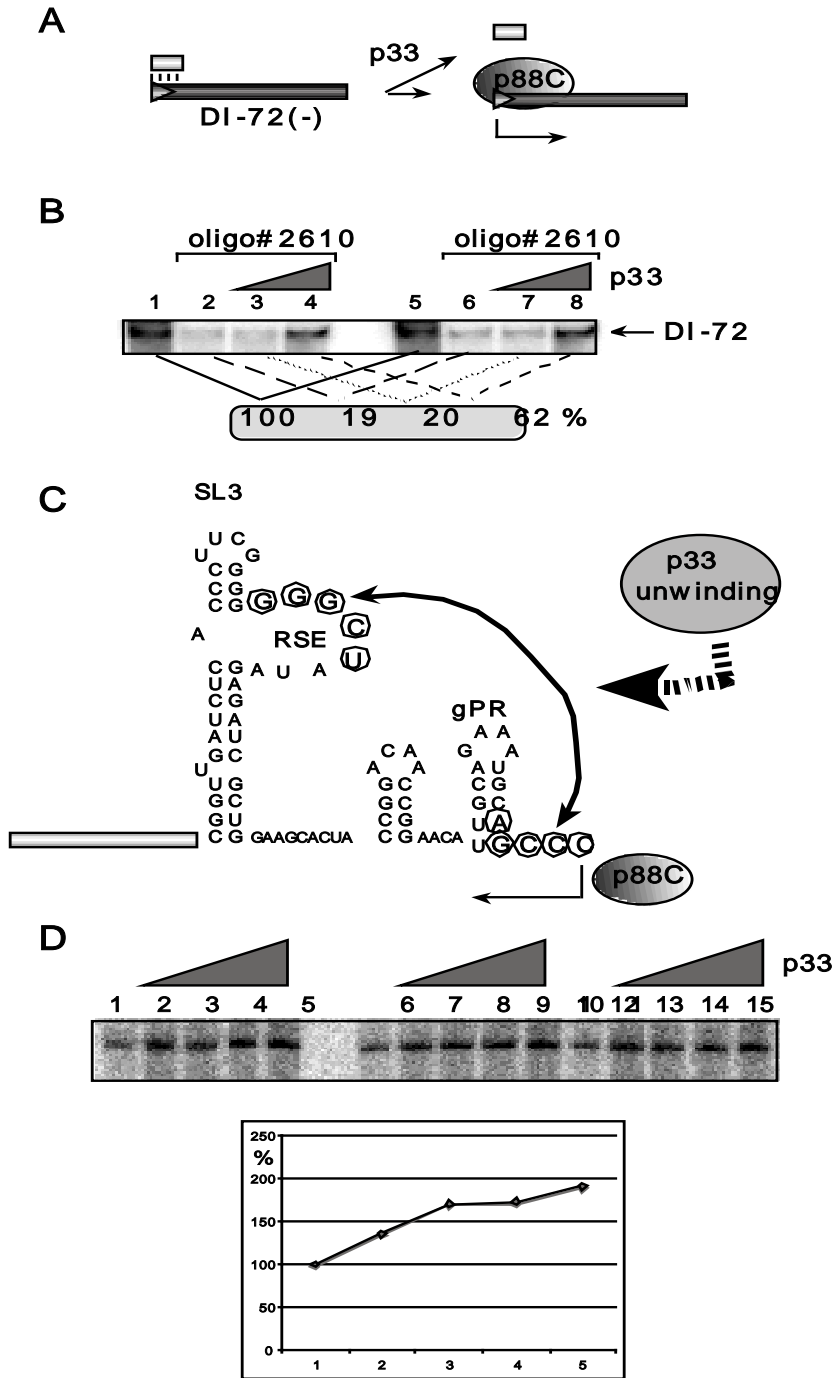


Fig. 4.4 Recombinant p33 promotes initiation on RNA templates by the RdRp. (A) Schematic presentation of the ssDNA/ssRNA hybrid template used to program the TCV p88C RdRp preparation *in vitro*. (B) Representative denaturing gel of ³²P-labeled RNA product synthesized by TCV p88C RdRp *in vitro* in the presence of 0, 1 and 2 mg of purified recombinant p33 is shown. The level of RNA synthesis was compared to that of the RdRp activity obtained in the absence of ssDNA and p33 (100%). The samples were treated with S1 nuclease to exclude terminal transferase-based labeling of DI-72(-) RNA, which might be present in the affinity-purified TCV p88C or CNV p33 preparations. Each experiment was repeated three times. (C) Schematic presentation of the 3' terminus of the (+)DI-72 RNA template used to program p88C RdRp *in vitro*. The base-pairing interaction between the replication silencer (RSE) and the minus-strand initiation promoter (gPR) is indicated with a double-headed arrow. The site of initiation of complementary RNA synthesis is marked below the sequence. (D) Representative denaturing gels of radiolabeled RNA products synthesized by p88C RdRp in the presence of 0, 0.5, 1, 2 and 4 mg of purified p33 are shown. The samples were treated with S1 nuclease.

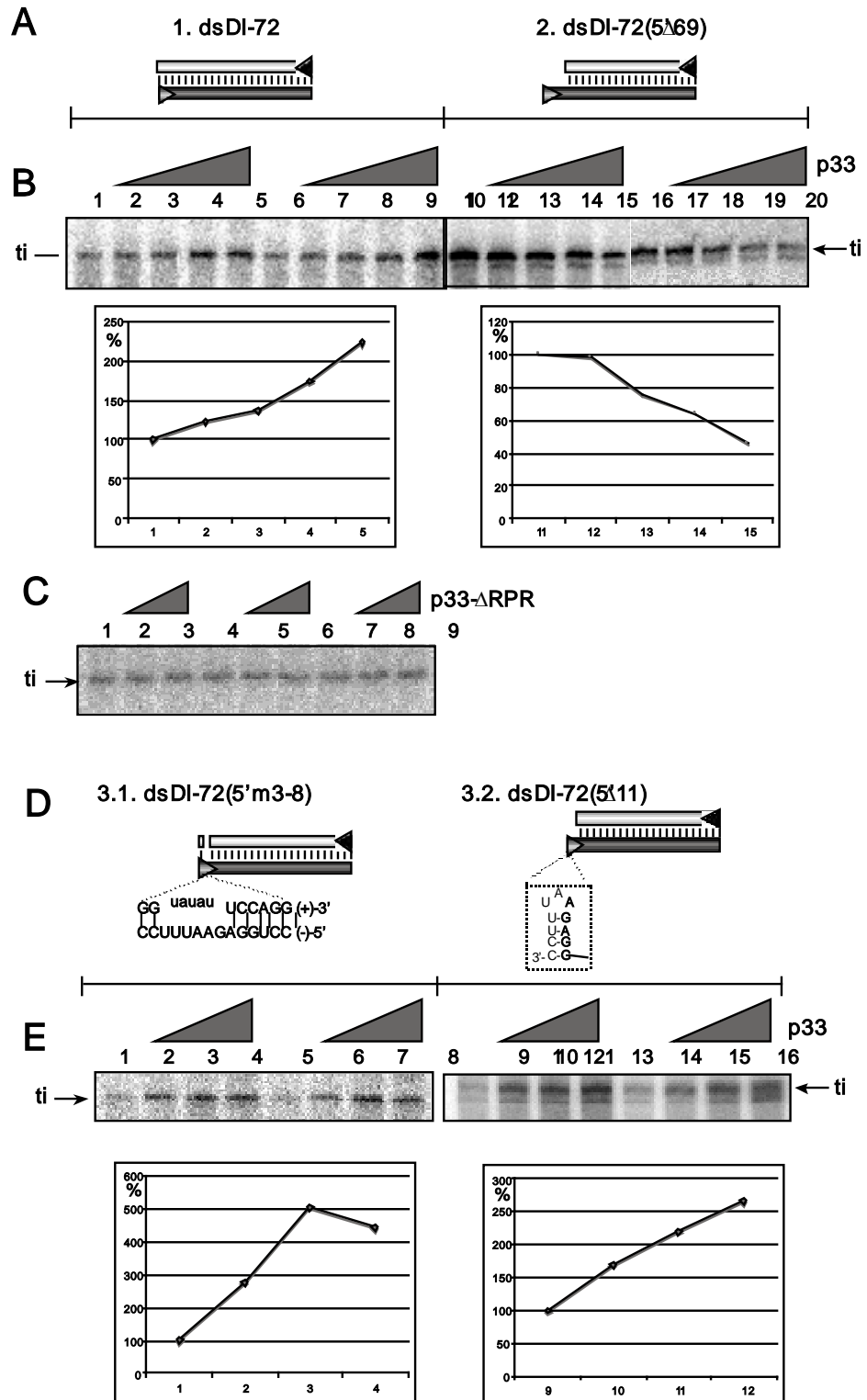


Fig.4.5 Recombinant CNV p33 promotes initiation on dsRNA template by the recombinant TCV RdRp. (A) Schematic presentation of the two dsRNA templates used to program the TCV p88C RdRp preparation *in vitro*. (B) Representative denaturing gels of ³²P-labeled RNA products synthesized by *in vitro* transcription with TCV p88C RdRp in the presence of 0, 0.5, 1, 2 and 4 mg of purified recombinant p33 are shown. The dsRNA templates were gel isolated after annealing of plus- and minus-stranded RNAs (in 1:1 ratio), and they were used in equal amounts (0.5 mg per sample). The level of RNA synthesis was compared to that of the RdRp activity obtained in the absence of p33 (100%). The samples were treated with S1 nuclease to exclude terminal transferase-based labeling of dsDI-72, which might be present in the affinity-purified TCV p88C or CNV p33 preparations. Each experiment was repeated three times. (C) Representative denaturing gels of radiolabeled RNA products synthesized by *in vitro* transcription with TCV p88C RdRps in the presence of 0, 1 and 2 mg of a p33 mutant are shown. The p33 mutant lacked the RPR sequence involved in RNA binding. See Fig. 5B for further details. (D) Schematic presentation of the two RNA templates used to program the TCV p88C RdRp preparation *in vitro*. See Fig. 5A for further details. (E) Representative denaturing gels of radiolabeled RNA products synthesized by *in vitro* transcription with p88C RdRp in the presence of 0, 0.5, 1 and 2 mg of purified recombinant p33 are shown. The samples were treated with S1 nuclease. See Fig. 5B for further details.

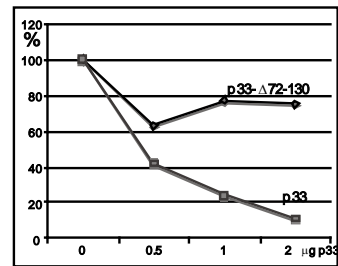
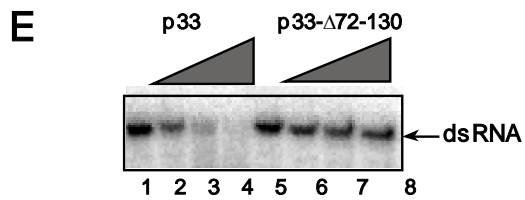
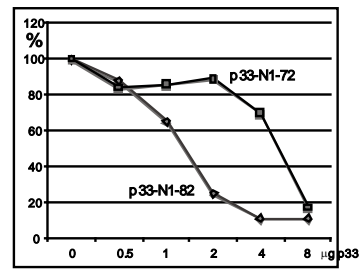
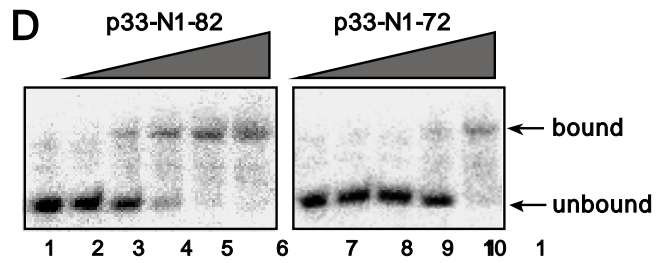
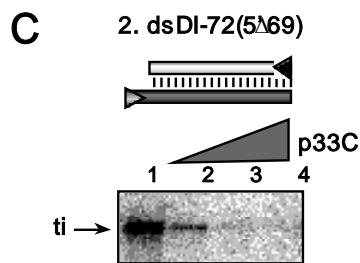
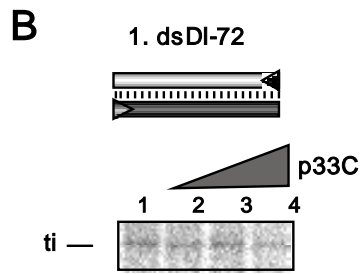
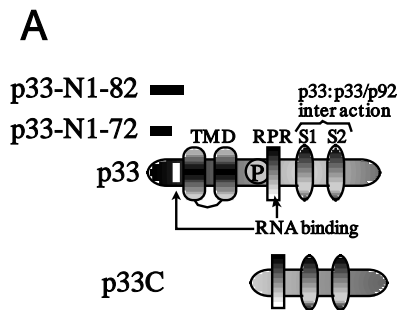
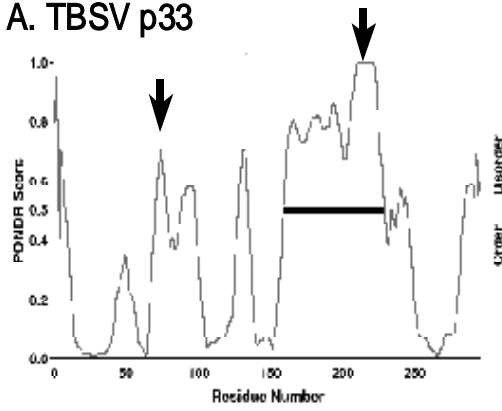
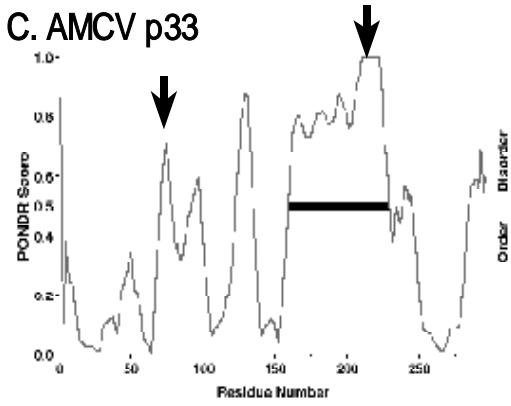


Fig. 4.6 The lack of RNA chaperone activity of p33 mutant missing the N-terminus *in vitro*. (A) Schematic presentation of CNV p33 and mutants with known functional domains. The only previously known function of the N-terminal sequence was its involvement in the localization of p33 to the peroxisomal membrane (including the trans-membrane domains, TMDs). The C-terminal sequence carries the Arginine-proline-rich (RPR) domain involved in RNA binding and the S1 and S2 subdomains involved in p33:p33/p92 interaction. (B) Representative denaturing gels of radiolabeled RNA products synthesized by *in vitro* transcription with p88C RdRp in the presence of 0, 0.5, 1 and 2 mg of purified recombinant p33C are shown. The samples were treated with S1 nuclease. See Fig. 5B for further details. (D) Gel-mobility shift assay that shows RNA binding by the truncated p33 variants. The ³²P-labeled probe (20 ng) was used with 0, 0.5, 1, 2, 4 and 8 mg of purified recombinant p33-N1-82 and p33-N1-72. The free RNA and the shifted band representing the RNA-protein complex are marked with arrows. The amount of free RNA left in the samples was quantified and shown as % of the total probe in the absence of protein (lanes 1 and 7). (E) Representative denaturing gels of ³²P-labeled dsRI RNA template that remained after the S1 nuclease treatment in the presence of 0, 0.5, 1 and 2 mg of purified recombinant p33 mutant lacking the second RNA binding sequence are shown. The samples were phenol/chloroform extracted and precipitated prior to gel-analysis. Note that I used a p33 mutant with increased solubility in *E. coli* due to the missing hydrophobic TMD domain.

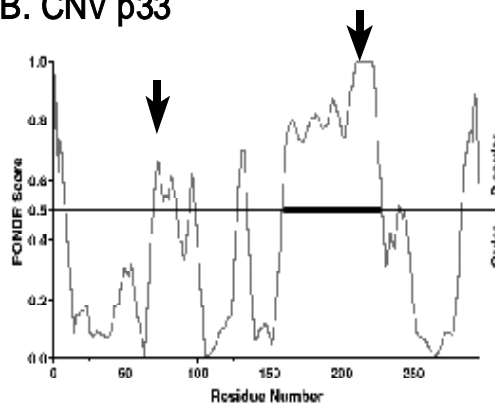
A. TBSV p33



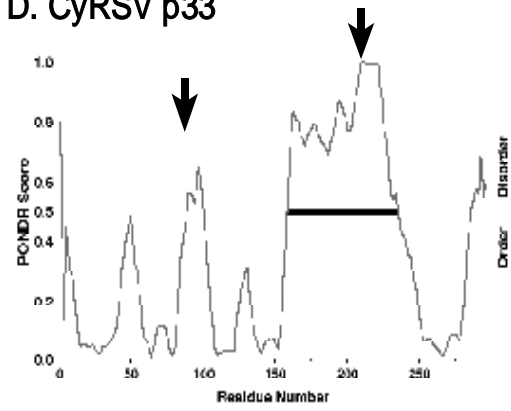
C. AMCV p33



B. CNV p33



D. CyRSV p33



E. CIRV p33

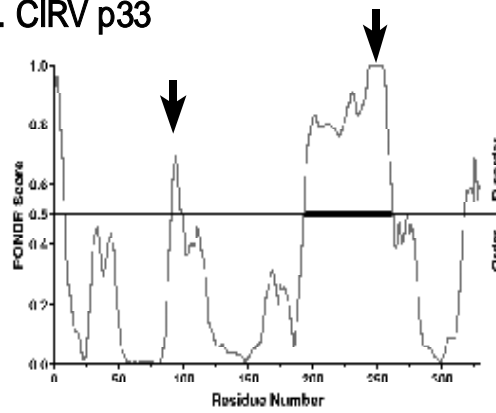


Fig. 4.7 The RNA binding sequences are predicted to be present within intrinsically disordered (unstructured) regions in p33 replication proteins of five tombusviruses. The probability of disorder is shown graphically in p33 based on analysis with PONDR-VL-XT. Amino acids with disorder value (PONDR score) of more than 0.5 are considered "disordered", whereas below 0.5 are considered "ordered". Arrows point at the two RNA-binding regions.

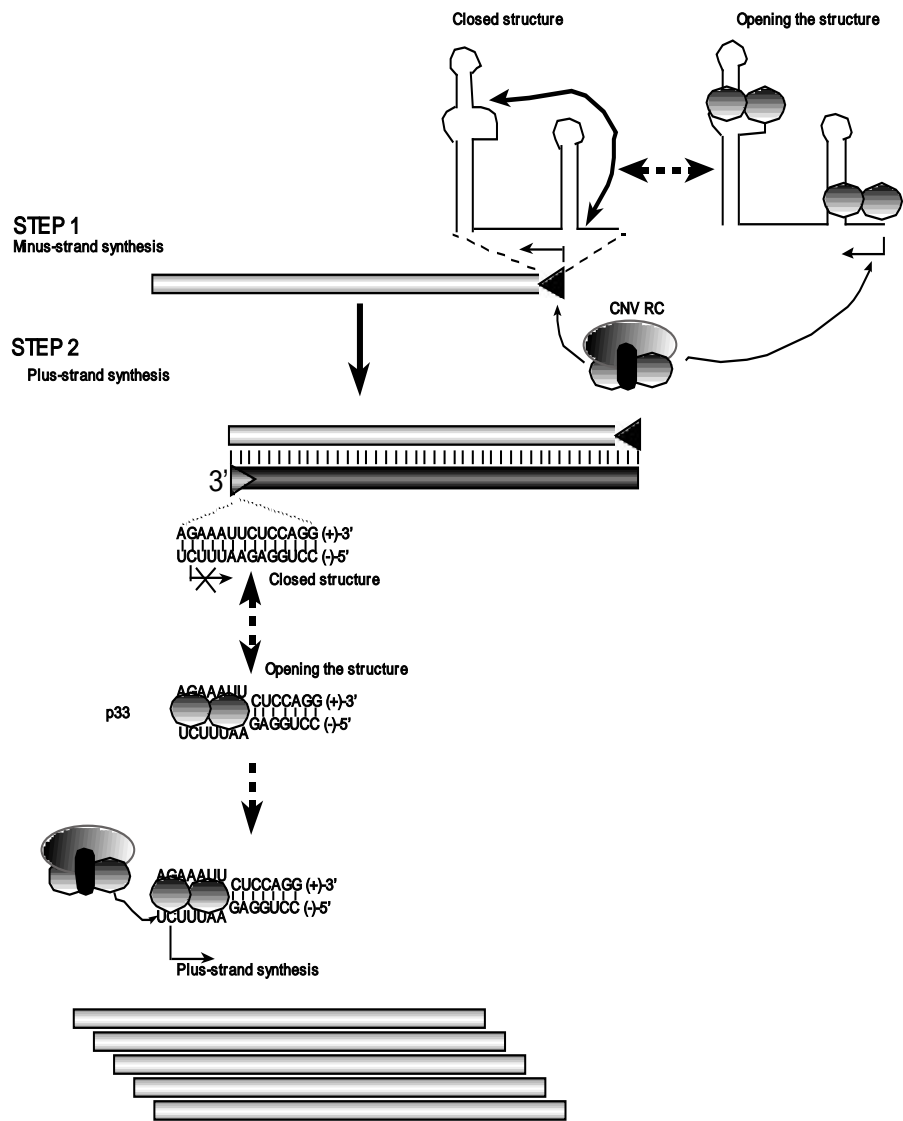


Fig. 4.8 A model on the possible role of the RNA chaperone activity of p33 in tombusvirus replication. I predict that p33 is involved in opening the closed silencer-promoter structure, which then leads to minus-strand synthesis by the tombusvirus replicase (Step 1). Also, p33 might be involved in opening up the AU-rich terminus of the putative dsRNA intermediate (Step 2). I propose that binding of p33 to dsRNA could facilitate loading of the replicase to the open end, followed by initiation of plus-strand synthesis (bottom). It is likely that binding of p33 could stabilize the open structure within the AU-rich stretch in the cPR promoter as shown. After initiation, the tombusvirus replicase can efficiently unwind the remaining part of the dsRNA template during RNA synthesis as demonstrated earlier (Panavas et al., 2006).

CHAPTER V

Role of a host HSP70 protein in viral replication

Introduction

Viral replicases are the key enzymes in the replication of positive stranded RNA viruses. Replicase complexes are often associated with proteins from the host organism (Panavas and Nagy, 2003). For instance, the viral replicase complex consists of virus-encoded proteins, the RNA-dependent RNA polymerase (RdRp) and auxiliary viral protein(s), as well as a suite of host proteins and the viral RNA template (Serva and Nagy, 2006)). The replicase complexes are assembled on intracellular membranes, including the peroxisomal membrane in case of TBSV and CNV (Panavas et al. 2005; Jonczyk, Nagy 2007). Recent studies have unveiled the role of a host protein in the peroxisomal localization of the viral replicase proteins ((Jonczyk et al., 2007). However, in general little is known about the membrane translocation of viral proteins.

P33 and p92 the replication proteins of the CNV are membrane proteins with the membrane spanning domain located between two hydrophilic regions. During the transport of the proteins through the cytosol the membrane spanning domain have to be in a conformation when it faces to the center of the protein transportation complex. At the target membrane the membrane-spanning domain has to be inserted into the membrane. No study was published about the mechanism of the membrane insertion of the proteins.

Ssa1/2p were found to be associated with the viral replicase complex. The overexpression of Ssa1p enhanced, while the deletion of *Ssa1and 2* decreased the RDRP activity in the yeast membrane fraction (Serva, Nagy 2006). These experiments indicated that Ssa1 and/or 2p are integral part of the viral replicase complex. Ssa is known to play a role in the translocation of precursor proteins into mitochondria and the ER in an ATP dependent manner (Deshaies et al. 1988).

Ssa is a member of the heat shock protein 70 family in yeast . The family consist of four subfamily Ssa, Ssb, Ssc and Ssd. The Ssa subfamily has four members Ssa 1 and 2 is expressed constitutively while 3 and 4 is expressed from a heat inducible promoter (Werner Craig 1987)

Results

Ssa is needed for *in vitro* replicase activity

Recombinant p33 and p92 expressed in *E. coli* were not active in a previously developed in an *in vitro* RDRP assay (Rajendran and Nagy, 2003). However, if expressed in yeast, the co-purified CNV p33 and p92 showed *in vitro* RDRP activity (Panaviene Nagy 2003). To establish the mechanism rendering the replication proteins active in yeast, a novel system was developed using recombinant p33 and p92 expressed in *E. coli* and cell free yeast extract by Dr. Judit Pogany in our lab. In this cell-free assay, the recombinant viral proteins expressed in *E. coli* were able to replicate the viral template RNA. The membrane fraction of the yeast cell-free extract, however, was incapable of viral RNA synthesis in the presence of added recombinant p33 and p92 and the viral RNA template. Based on these data, I hypothesized that a yeast soluble (cytosolic) protein(s) is needed to form the active viral replicase complex in the cell-free extract. To identify the host protein involved in the assembly/activation of the replicase complex, I centrifuged the cell free yeast extract (15000 RPM for 10 minutes) to divide the membrane bound and soluble proteins. As expected, the membrane only (pellet) fraction showed reduced replicase activity compared to the combined membrane+soluble fractions.

Since Ssa1p is part of the tombusvirus replicase complex (Serva and Nagy, 2006), I wanted to test if the activator protein is the Ssa1p. For this test, I used the soluble fraction of Ssa1\2p deleted mutant yeast strain to rescue the replicase activity of the membrane fraction of the cell free extract. Yeast extract prepared from yeast carrying mutated, nonfunctional *ssa1/ssa2* genes activated the replicase four fold less efficiently in vitro than the cell-free extract prepared from wild type yeast did (fig 5.1).

To further investigate the role of Ssa1/Ssa2p in activation of the tombusvirus replicase, I replaced the soluble fraction with various amounts of FLAG-tag affinity purified Ssa1p from yeast in an in vitro assay also containing the membrane fraction

of the cell free extract in addition to p33/p92/repRNA. I found that the added purified recombinant Ssa1p was able to rescue the replicase activity in vitro. To find out whether the Ssa1p or a copurified protein is responsible for the activation, I performed a high salt washing step to reduce the amount of co-purified yeast proteins in the Ssa1p preparation. Additionally, an extra washing step was added to the assay with high (1.2 M NaCl) salt concentration aimed at removing additional proteins bound to the resin in a non-specific manner (via the peptide binding domain of Ssa1p). The high salt washing of Ssa1p did not reduce the replicase activity in the cell free extract assay (fig. 5.1). To further demonstrate that Ssa activated the *E. coli* expressed viral replicase proteins, I made two point mutations separately in the ATP binding socket of the Ssa1p, namely K69Q and G199D. These mutations inactivate the ATPase activity of Ssa 1 p, rendering the protein defective (McClellan and Brodsky, 2000). Accordingly, both Ssa1p mutants were unable to activate the bacterial expressed viral replication proteins in the membrane fraction of the cell free extract.

Ssa1/2p are needed for viral replication in yeast

Previous work showed that the deletion of *ssa1/ssa2* significantly decreased the accumulation of viral replicon in yeast (Serva and Nagy, 2006). To further study the effect of *ssa1/ssa2* deletion on viral replication, I used a temperature sensitive mutant *Ssa1*. While deletion of all four *Ssa* genes is lethal in yeast (Boorstein et al., 1994), researchers constructed a yeast strain with *ssa2/ssa3/ssa4* deleted in combination with *Ssa1* is a temperature sensitive allele (Becker et al., 1996). This strain was used to study the viral replication in the absence of SSA2/3/4 function. Transformation of the above temperature sensitive *Ssa1* strain and wild type *Ssa1* strain with plasmids encoding the viral replicase proteins and DI72 repRNA regulated by galactose inducible promoters showed that the yeast strain expressing the temperature sensitive Ssa1p was not able accumulate detectable amount of viral RNA at the restrictive temperature. Meanwhile, the same strain at the permissive temperature and the control strain expressing wild type Ssa1p accumulated viral

repRNA efficiently (Fig. 5.2). The expression of the viral protein demonstrated by western blot analysis was as high in the nonpermissive versus permissive temperatures, suggesting that the defect at nonpermissive temperature is not due to the lack of expressed p33.

There are several steps in viral replication, which could be affected by Ssa1p. To determine whether Ssa1p is involved in the early or the late steps, I induced the viral replication at the permissive temperature for six hours, and then changed the media to glucose to shut down the expression of viral proteins and repRNA. At the same time, I raised the temperature to the nonpermissive to inhibit the tsSsa1p function. After 18 hours, examination of the viral repRNA accumulation by northern blot showed that both the temperature sensitive and wild type Ssa1p containing strain were able to accumulate viral RNA to a comparable level at the permissive temperature (fig 5.2). This suggested that the viral proteins and replicon in the temperature sensitive and wild type Ssa1p bearing strains at permissive temperature allowed the viral replicase complex to assemble and start replication. On the contrary, we found no TBSV repRNA accumulation at the nonpermissive temperature in yeast expressing tsSsa1p (Fig. 5.3). Purification of the membrane fraction from these strains showed that the *in vitro* RDRP activity at the permissive 25 °C and non-permissive 37 °C temperature were comparable (fig 5.3).

Ssa is needed for the membrane localization of p92 and p33

p33 is localized in the cytosol in the absence of Ssa function (Robert Wang unpublished data). To find out whether Ssa is needed for the viral proteins to be membrane bound a flag purified recombinant Ssa expressed in yeast, MBP fusion p33 and p92 expressed in *E. coli* and cell free yeast extract. I collected the membrane fraction from the cell free yeast extract by centrifugation, washed it to obtain HSP 70 free yeast membrane. To the membrane I added the purified Ssa and viral proteins together with ATP incubated the reaction for two hours then collected the membrane

fraction. After washing three times to remove the water soluble proteins I studied the membrane fraction by western blot.

There were significantly more viral proteins membrane bound in the samples with Ssa and ATP added than in the samples without Ssa, ATP or with mutant K69Q and G199D Ssa.

Discussion

Earlier work revealed that Ssa1\Ssa2 yeast HSP70s are associated with the viral replicase complex (Serva and Nagy, 2006). Pull down experiments showed that Ssa binds to p33 *in vitro*. The deletion of the Ssa1/2 inhibited, overexpression of Ssa1\Ssa2 enhanced viral replication. These experiments established that Ssa plays a crucial role in viral replication in yeast, but the mode of action remained unclear. Since the deletion of all four Ssa results in lethality, a temperature sensitive Ssa1 allele was developed to study Ssa in a ssa2-3-4 deletion background. The aim was to determine whether Ssa function is necessary for viral replication in yeast. Induction of viral protein expression at non-permissive temperature did not result in detectable viral RNA accumulation. In contrast, the replication was not inhibited *in vivo* at non-permissive temperature if the viral replication proteins were expressed at permissive temperature. The *in vitro* results too showed no significant difference in RDRP activity at permissive and non-permissive temperature, if the viral replication proteins were expressed at permissive temperature. These results suggested that Ssa plays a role in the early steps of viral replication.

Laser scanning confocal microscopy experiments showed that the misslocalization of viral proteins were consistent with the lack of Ssa function.

P33 was cytosolic at non-permissive temperature if expressed in ts Ssa1, ssa2, ssa3, ssa4 yeast (Robert Wang unpublished data). Published data demonstrates that Ssa facilitates transporting membrane proteins through the cytoplasm. Ssa binds to the hydrophobic regions of the proteins keeping them in soluble form and preventing coagulation and precipitation of the highly hydrophobic proteins. This way the membrane proteins can be transported from the site of translation to the target membrane (Boorstein et al., 1994). Tombusviruses utilize the peroxisomal membrane to form a “pocket” where the replication takes place. Our confocal microscopy data showed that the viral replication protein does not target the peroxisomal membrane without Ssa function (Robert Wang unpublished data). Rather, the protein distribution

observed as fluorescence was seen evenly throughout the cytosol. The “doughnut shape” localization of the protein shows that it is in a soluble form, even if it has long highly hydrophobic regions. Our earlier data showed that p33 precipitates if expressed in bacteria-which lacks the Ssa proteins-with his tag (Judit Pogany unpublished data). The solubility of p33 in the temperature sensitive mutant at non permissive temperature suggests that the interaction between p33 and tm Ssa is not disrupted by the Ssa mutation. The point mutation, which makes Ssa temperature sensitive, is in the ATP binding domain of the protein. Since the peptide-binding domain is not affected Ssa can bind to p33 keeping it in soluble form. This suggests that the proper localization of p33 requires the ATPase activity of Ssa. Previous work demonstrated that Ssa stimulates the post-translational translocation of wheat-germ-translated PP α f into microsomes (Chirico et al., 1988).

Examination of the membrane localization of viral proteins in presence and absence of Ssa and/or ATP showed that when both Ssa and ATP were present, there was approximately a four-fold increase in membrane bound p33 compared to the reactions when either ATP or Ssa was not added to the reaction mixture. Based on this result and in combination with the findings of Chirico , the most plausible explanation is that Ssa functions as a molecular ratchet pulling the hydrophilic portion of p33/92 through the membrane. Alternatively, as yet unknown proteins are interacting with Ssa are key to the replication process. Results stemming from these experiments establish that Ssa is needed for the activation of recombinant p33

purified from *E. coli*. *In vitro* studies showed that recombinant p92 and p33 expressed as an MBP-fusion protein in *E. coli* have no RDRP activity, if expressed in baker’s yeast with his tag have RDRP activity. In this case the main difference between the bacterial and yeast expression is the lack of the peroxisomal membrane and Ssa function in the bacteria. The peroxisomal membrane serve as a platform to assemble the tombusvirus replicase complex (Jonczyk et al., 2007), and Ssa is needed for the membrane insertion of the replicase protein.

Based on this results I propose a model: Ssa p binds to the hydrophobic portions p33/92 at the ribosome, keeping them in soluble form during the transport to the peroxisomal membrane where it inserts them into the membrane in an ATP

dependent manner. The membrane insertion renders the proteins functional. This way the replication takes place only inside the membrane structure formed by the replicase complex, and not in the cytosol where the double-stranded viral RNA would be exposed to the plant defense system activating the PTGS.

Materials and methods

Yeast strains

Saccharomyces cerevisiae strain InvSc1 (Invitrogen) was used as the wild type (wt). The double deletion (*ssa1 ssa2*) strain MW123 (*his3 leu2 lys2 trp1 ura3 ssa1::HIS3 ssa2::LEU2*; (Wernerwashburne et al., 1987)), the temperature sensitive mutant a1-45 (*ssa1ts ssa2 ssa3 ssa4*) and its wild type (*SSA1 ssa2 ssa3 ssa4*) (Becker et al., 1996) was kindly provided by Elizabeth A. Craig.

Plasmid constructs

To express the viral replicase proteins and DI-72, I used pGBK -p33, pGAD-his-p92, pYES-DI-72 plasmids (Panaviene et al., 2004)). For the dual expression of p33 and Di-72 from a single plasmid, I used the plasmid pESC-His-p33-DI-72 (Jonczyk et al., 2007) that use the galactose inducible *GALI* and *GAL10*. For overexpression of Flag-tagged Ssa1p, I used the plasmid pYC-HFSSA (Serva Nagy 2006) carrying *GALI* promoter. Two mutants of Ssa1, namely K69Q and *ssa1-103* (G199D), were obtained using the Quick-Change site-directed mutagenesis kit (Stratagene). For obtaining K69Q, I used the primer pair of 5'-CCGTTTTTCGACGCTCAGCGTTTGATCGG-3' and 5'-CCGATCAAACGCTGAGCGTCGAAAACGG-3', for G199D: 5'-GATTTTCGACTTGGGTGATGG TACTTTC GATGTC-3' and 5'-GACATCGAAAGTACCATCACCCAAGTC GAAAATC-3' (McClellan and Brodsky, 2000).

RNA blot analysis of total RNA from yeast cells

Total RNA extraction from yeast was performed as described earlier (Panavas and Nagy, 2003). Briefly, equal volumes of buffer (50 mM sodium acetate [pH 5.2], 10 mM EDTA, 1% SDS) and water-saturated phenol were added to the yeast cells pelleted by centrifugation and resuspended by vortexing. After incubation for 4 min at 65°C, and for 2 min on ice, the samples were centrifuged at 21,000 x g for 5 min at room temperature (RT). The total RNA was precipitated by adding 2 volumes of 95% ethanol to the aqueous phase, followed by centrifugation at 21,000 x g for 15 min at 4°C. The pelleted RNA samples were washed with 70% ethanol, dried and dissolved in Tris-EDTA buffer (50 mM) and formamide (in 1:1 ratio). The samples were heated for 5 min at 85°C, electrophoresed in 1% agarose gels, and transferred to Hybond XL membrane (Amersham), and cross-linked to the membrane using UV (Bio-Rad). Hybridization to the ³²P-labeled RNA probe was done in ULTRAhyb solution (Ambion) at 68°C according to the supplier's instructions. The ³²P--labeled complementary DI-72 RNA probe was obtained via T-7 transcription.

Western blot analysis

For total protein extract from yeast I harvested yeast cells by centrifugation from 1 ml culture, the cell were dissolved in 0.2 ml 100 mM NaOH and vortexed for 5 minutes. The samples were centrifuged for 2 minutes at 21000 g and the NaOH solution was carefully removed, 0.2ml SDS-PAGE sample loading buffer (Sambrook et al. 1989) was added to the protein samples, followed by heating for 5 min at 85°C, electrophoresis in SDS-8% PAGE gels, and electro-transfer to a polyvinylidene difluoride membrane (Bio-Rad). The membrane was incubated in 5% nonfat dry milk

solution in Tris-buffered saline (TBS) buffer (Sambrook et al. 1989) containing 0.1% Tween 20 (TTBS) for one hour to avoid nonspecific binding of antibodies. The membrane was washed three times with TTBS buffer and incubated with monoclonal anti-His antibodies (Amersham) for 1 h at room temperature, washed again three times for 10 min with TTBS buffer, and then the membrane was incubated for 1 h at room temperature with secondary antibody (alkaline phosphatase-conjugated, Sigma). After three 10 min washes with TTBS, proteins on the membrane were visualized using 5-bromo-4-chloro-3-indolylphosphate and nitroblue tetrazolium (Sigma).

***In vitro* replication assays using cell free yeast extract**

The cell free yeast extract for the replication assay was obtained as published earlier (Pogany, Nagy 2008). Briefly: the selected yeast strains were grown in 200 ml glucose media until reaching \sim OD=1, then harvested by centrifugation at 4000 rpm for 4 min at 4°C. The pellet was washed twice with water and twice with buffer A (0.3 ml of 1 M HEPES-KOH pH 7.4, 1 ml of 1 M potassium acetate, and 0.02 ml of 1M magnesium acetate). Then, 0.5 g of pellet was suspended in 0.75 ml buffer A containing 1.5 μ l 1M DTT and 3 g pre-chilled glass beads. The yeast cells were broken by shaking for 5 min, followed by centrifugation at 500 x g at 4 °C for 5 min in a swinging bucket rotor. The supernatant was then moved to a new tube, followed by centrifugation at 500 x g at 4 °C for 5 min. The supernatant was stored at -80C until use. The above yeast cell-free extract (1 μ l) was pre- incubated on ice for 10 min in 10 μ l cell-free replication (CFR) buffer containing [50 mM HEPES-KOH pH 7.4, 150 mM potassium acetate, 5 mM magnesium acetate, 0.2 M sorbitol and 0.4 μ l Actinomycin D (5 mg/ml)]. Then, the reaction volume was adjusted to 20 μ l with 1x CFR buffer also containing 2 μ l of 150 mM creatine phosphate, 2 μ l of 10 mM ATP, CTP, GTP and 0.25 mM UTP, 0.3 μ l of 32P-UTP, 0.2 μ l of 10 mg/ml creatine kinase, 0.2 μ l of RNase inhibitor, 0.2 μ l of 1 M DTT, and 0.5 μ g RNA transcript. The reaction was incubated at 25 °C for 3 hours. The reaction was terminated by adding 110 μ l stop buffer (1% SDS and 0.05M EDTA pH 8.0), followed by phenol/chloroform extraction, isopropanol/ammonium acetate precipitation, a

washing step with 70% ethanol as described earlier (Nagy et al. 2000). For testing the replicase activity in the membrane-enriched fraction from yeast extract, we centrifuged the cell-free extract for 10 min at 21,000 x g at 4 °C to separate the membrane-enriched and soluble fractions. The membrane-enriched fraction dissolved in buffer A was used in the *in vitro* replication assays with the addition of the soluble fraction of the appropriate yeast strains or affinity (Flag-tag) purified recombinant proteins (Ssa1p or mutant Ssa1p) expressed in yeast.

Flag-tag purification

For expression of Flag-tagged Ssa1p, I used plasmid pYC-HFSSA (Serva and Nagy, 2006)). To express the Ssa1p without a tag, I used pYES2/NT-Ssa, which was obtained by cloning the *SSA1* sequence into pYES2/NT plasmid between the restriction sites *Hind* III and *Xho* I. I then PCR- amplified the *SSA1* sequence using the primer pair of 5'-GGC AAG CTT ATG TCT AAA GCT GTC GGT ATT, and 5'-GGC CTC GAG TTA ATC AAC TTC TTC GAC AGT. To express the viral replicase protein p92, I used pGAD-His92 plasmid (Panaviene et al., 2004). *Saccharomyces cerevisiae* strain InvSc1 (Invitrogen) was used for expression of the recombinant proteins. Yeast was co-transformed with plasmids pYC-HFSSA, pGAD-His92, pESC-His-p33-DI-72 and pYES2/NT-Ssa, pGAD-His92, pESC-His-p33-DI-72. The yeast was grown in 10ml SC-ULH 2% glucose medium for 24 hours, and the cells were harvested by centrifugation at 100 × g for 5 min, washed and resuspended in 200ml SC-ULH 2% galactose medium. The yeast culture was then grown until reaching OD 0.8 (approximately 8 hours) at 23 °C.

Cells were harvested by centrifugation and the membrane proteins were obtained as described earlier (Panaviene et al., 2004)). Briefly, yeast cells were ground in a mortar in liquid nitrogen. The obtained 1 volume yeast powder was dissolved in ten-volume extraction buffer (200 mM sorbitol, 50 mM Tris-HCl [pH 7.5], 15 mM MgCl₂, 10 mM KCl, 10 mM β-mercaptoethanol, yeast protease inhibitor mix; Sigma). Cell debris was removed by centrifugation at 100 × g for 1.5 min at

4°C. Membrane fraction was obtained from the extract by centrifugation at 21,000 × g for 15 min at 4°C.

The enriched membrane fraction was resuspended in 500 µl extraction buffer containing 1% Triton X-100 by gentle rotation for 1 h at 4°C, followed by centrifugation at 21,000 × g for 15 min at 4°C. 30 µl anti-FLAG M2-agarose affinity gel (Sigma) was added to supernatant and rotated for 1 h at 4°C. The FLAG resin was washed twice with 1ml RDRP buffer (50 mM Tris-HCl (pH 8.2), 10 mM MgCl₂, 10 mM dithiothreitol, 100 mM potassium glutamate), then eluted with 100µl RDRP buffer containing 5µg/ml FLAG peptide. 25µl of the eluted proteins were added to the *in vitro* replication assay. The *in vitro* replication assay was performed at 25 °C for two hours. I used 0.5 µg of external/added RNA templates for the 50 µl reactions (Nagy and Pogany, 2000)). The RdRp products were phenol-chloroform extracted and loaded on denaturing PAGE gel (i.e., 5% PAGE containing 8 M urea). Then the gels were dried and exposed to phosphorscreen and evaluated with Typhoon imager and Imagequant software.

***In vitro* replication assays based on recombinant viral proteins expressed in yeast**

For this replication assay, I obtained the membrane fraction from yeast as it is described in the FLAG-tag-based purification method above, with the difference that I added 5% SB3-10 (caprylyl sulfobetaine) to the extraction buffer. The obtained membrane fraction was considered enriched membrane fraction, which was resuspended in the extraction buffer and used in the *in vitro* replicase reactions as it is described below.

To affinity purify the CNV replicase preparation from yeast, the enriched membrane fraction was resuspended in the extraction buffer containing 1.2 M NaCl, followed by gentle rotation for 20 min at 4°C and centrifugation at 21,000 x g for 15 min at 4°C. The obtained pellet was resuspended in the extraction buffer containing 1% Triton X-100 and 5% SB3-10 (caprylyl sulfobetaine) (Sigma) by gentle rotation for 1 h at 4°C, followed by centrifugation at 21,000 x g for 15 min at 4°C. The

obtained supernatant was considered the solubilized membrane fraction. This preparation was tested in the *in vitro* replicase assay as described below.

To prepare the samples for the 6xHis tag-based metal affinity purification, the solubilized the enriched membrane fraction in the solubilization buffer (extraction buffer plus 1% Triton X-100, 5% SB3-10, and 0.5 M KCl) was centrifuged to remove insoluble materials, and then the supernatant was applied to a column containing ProBond resin (Invitrogen) equilibrated with the solubilization buffer. The column was then rotated for 1 h, followed by washing with two column volumes of the solubilization buffer, washing with the extraction buffer containing 1% Triton X-100 and 5% SB3-10, and then a second wash with the extraction buffer containing 1% Triton-100, 5% SB3-10, and 2 mM imidazole. The recombinant proteins were recovered from the column in the extraction buffer containing 150 mM imidazole, 1% SB3-10, and 0.1% Triton X-100 in a two-step elution (each in a half-column volume). The purity of the obtained recombinant protein-containing preparations was tested by sodium dodecyl sulfate-polyacrylamide gel electrophoresis (51, 57), while the amount of the recombinant proteins in various samples was compared by using Western blotting with monoclonal anti-His tag antibody (GE Healthcare).

Purification of p33 and p92 proteins from *E. coli*.

The expression and purification of the recombinant TBSV proteins were carried out as described (Rajendran and Nagy, 2003). Briefly, protein expression plasmids were transformed into Epicurion BL21-CodonPlus (DE3)-RIL (Stratagene). The overnight cultures from the transformed bacterial cells were diluted to 1:100 in rich growth medium (10 g of tryptone, 5 g of yeast extract, 5 g of NaCl) containing 0.2% glucose and 100 µg of ampicillin per ml and grown at 37°C until the optical density reached 0.6 to 0.8. Protein expression was then induced at 14°C with 0.3 mM IPTG (isopropyl-β-D-thiogalactopyranoside) for 8 to 10 h. The induced cells were harvested at 4,000 x g at 4°C for 10 min, resuspended in ice-cold column buffer (10 mM Tris-HCl [pH 7.4], 1 mM EDTA, 25 mM NaCl, 10 mM β-mercaptoethanol), sonicated on ice to disrupt the cells, and centrifuged at 21,000 x g for 10 min at 4°C.

The supernatant was added to an equilibrated amylose resin column (New England Biosciences), washed thoroughly with 20 volumes of column buffer, and eluted with 10 mM maltose in column buffer. All protein purification steps were carried out at 4°C. The purified recombinant proteins were analyzed in SDS-8% polyacrylamide gel electrophoresis (SDS-PAGE) for their purity. The protein concentrations were then adjusted to 250 µg/ml using the Bradford assay.

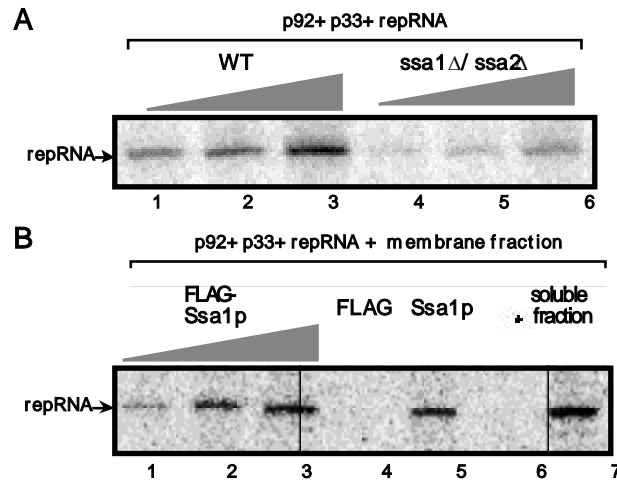


Fig 5.1 RDRP activity of yeast cell free extract membrane fraction with added MBP p33 and p92

- A.) lanes 1-3 WT yeast
lanes 4-6 *ssa1,ssa2,Ssa3,Ssa4* yeast strain
- B.) lanes 1-3 FLAG-tag affinity purified Ssa1 protein in increasing concentration
lane 4 FLAG resin purified yeast extract
lane 5 Ssa protein
lane 6 yeast membrane without Ssa
lane 7 yeast membrane with the soluble fraction of the yeast

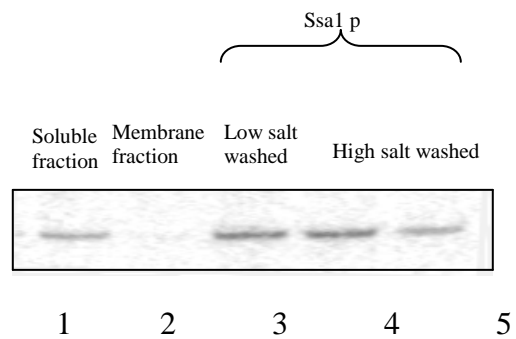


Fig 5.2 Effect of high concentration (1.2 M) salt washing during affinity purification of Flag tagged Ssa1 p on RDRP activity of yeast cell free extract membrane fraction with added MBP p33 and p92

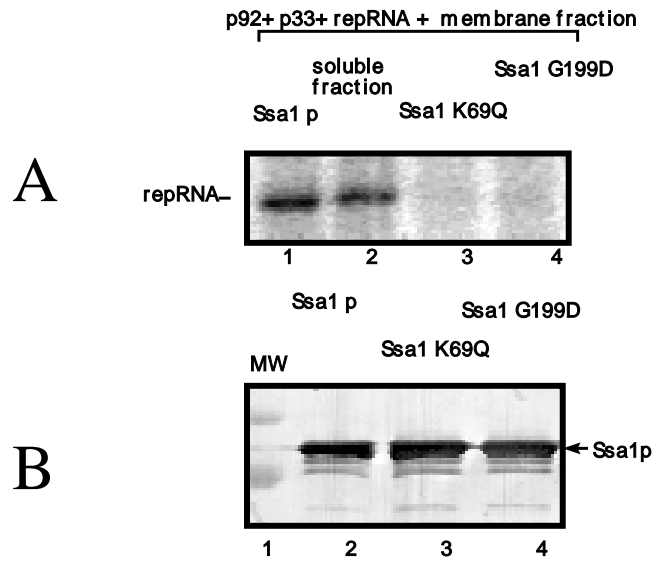


Fig 5.3 RDRP activity of yeast cell free extract membrane fraction with added mutant and wt Ssa1 p

- A.) lane 1 Flag tag affinity purified Ssa1
lane 2 Soluble fraction of the yeast cell free extract
lane 3 Flag tag affinity purified K69Q mutated Ssa 1 P
lane 4 Flag tag affinity purified G199D mutated Ssa 1 P
- B.) Western blot analysis of Flag tag affinity purified wt and mutated Ssa1p used in the assay

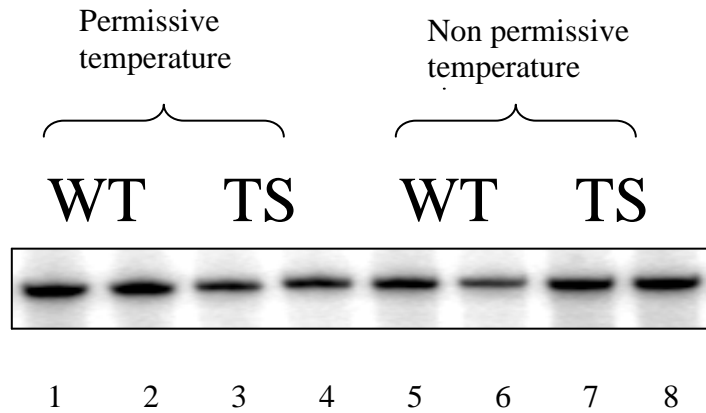


Fig 5.4 RDRP activity of membrane enriched fractions obtained from wt Ssa 1 ssa 2, 3, 4 and ts Ssa 1 ssa 2, 3, 4 yeast strains grown at permissive temperature.

RDRP reactions were performed at 25° C and 37° C using yeast membrane enriched fractions obtained from wt Ssa 1 ssa 2, 3, 4 and ts Ssa 1 ssa 2, 3, 4 (the yeast cells were grown at 23° C)

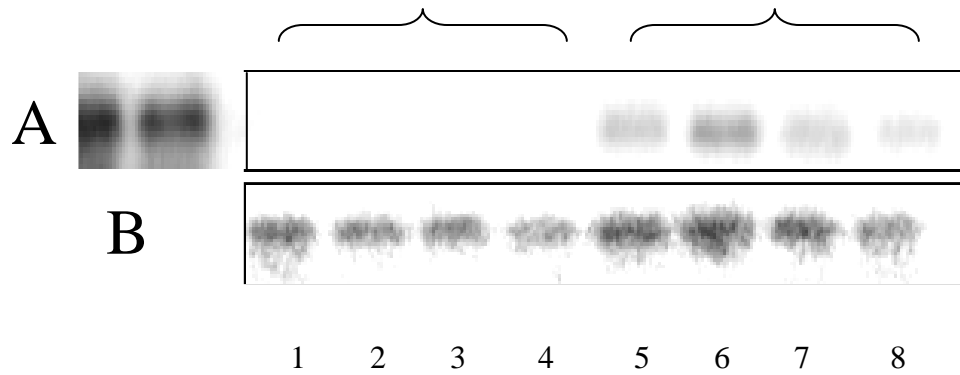
lanes 1,2 wt Ssa at 25° C;

lanes 3,4 ts Ssa 25° C;

lanes 5,6 wt Ssa at 37° C;

lanes 7,8 ts Ssa at 37°

RNA accumulation



Protein expression

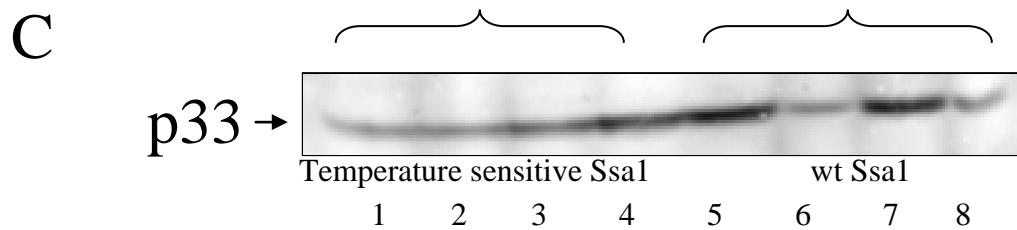


Fig 5.5 Northern blot analysis of the replicon RNA isolated from wt Ssa 1 ssa 2, 3, 4 and ts Ssa 1, ssa 2, ssa 3, ssa 4 yeast strains grown at different temperatures.

- A. Yeast strains were pre-grown in media containing glucose at permissive temperature, then shifted the temperature to the non-permissive 36°C, and at the same time changed the media to induce the expression viral replication proteins and replicon. After 18 hours of induction RNA was isolated from the yeast cells examined by northern blot
- B. Replication was induced at the permissive temperature for six hours, then the media was changed to glucose to shut down the expression of viral proteins and replicon. At the same time the temperature was raised to the non-permissive to kill the Ssa function, after 18 hours the viral RNA accumulation was examined by northern blot.
- C. Western blot analysis of p33 protein expression during assay A

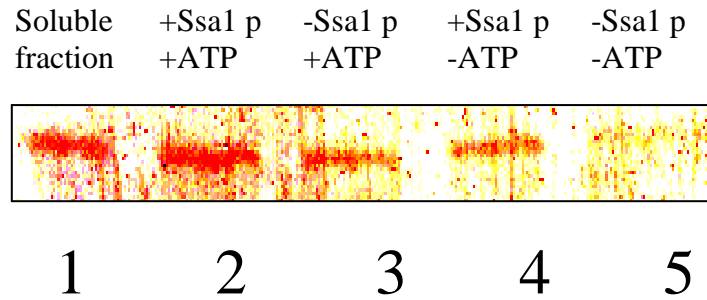


Fig 5.6 Western blot analysis of membrane fractions of yeast cell free extract membranes incubated with

- 1.) the soluble fraction of the yeast cell free extract
- 2.) Flag tag affinity purified Ssa 1 p and ATP
- 3.) ATP only
- 4.) Flag tag affinity purified Ssa 1 p only
- 5.) RDRP buffer with no ATP or Ssa 1P

CHAPTER VI

Summary

The tombusvirus p33 is a multifunctional replication protein that is essential for the viral replication (Panaviene et al., 2004). The read through product of p33, namely p92 replication protein, contains the RDRP motif essential for RNA polymerization. At the beginning of my thesis work, the roles/functions of p33 replication co-factor during the viral replication process were unclear. During the course of my studies our lab have discovered several functions of p33, such as RNA binding (Rajendran 2003), recruitment of the viral RNA (Pogany 2005), assembly of the viral replicase complex (Panaviene et al., 2004, 2005).

My work on p33 focused on the area of posttranslational modification (phosphorylation) of p33, the RNA chaperone-like activity of p33, and its interaction with the heat shock protein 70 (Ssa1p, a yeast homolog). The results of the phosphorylation chapters suggest the significance of a phosphorylation sites in the vicinity of the RNA binding domain. The phosphorylation of these sites results in reduced RNA binding. Sequence comparison with other related viruses showed predicted phosphorylation sites at approximately the same position. The presence of a conserved phosphorylation sites suggests that the phosphorylation-unphosphorylation cycle of serine, threonine residues in the vicinity of the RNA binding domain plays a major role in positive strand RNA virus life cycle. Phosphorylation sites are predicted in the vicinity of the arginin rich domain of the HIV Tat protein too by Netphos phosphorylation prediction program, suggesting that other viruses may use phosphorylation to reversibly disrupt RNA binding.

My results suggest that p33 act as a weak RNA chaperone. Positive strand RNA virus replication produces approximately 100 more positive strand RNA than negative strand RNA. During the replication the newly synthesized positive strand RNA has to be removed from the negative strand, in order to make the negative strand available as a template. Although the TCV replicase can unwind double stranded structures, it requires the promoter to be single stranded. P33 facilitated the initiation of TCV replicase on fully double stranded RNA templates, suggesting that by binding to the double stranded RNA it can de-stabilize the double stranded structure exposing the promoter to the replicase.

My work with the host factor Ssa showed that the Ssa1 and/or Ssa2 protein plays a role in p33 transportation through the cytoplasm to the target membrane and also facilitates the membrane translocation of the p33 protein. Other viruses might use heat shock proteins for similar function.

My contribution to the better understanding of the role p33 plays in the replication can be summarized in a single model. After translation, p33 is transported to the peroxisomal membrane by Pex19p host protein (Pathak et al, 2008). During the intracellular transportation of p33, the host HSP70 binds and covers the highly hydrophobic regions of the p33 protein. The interaction between the host HSP70 and p33 renders the protein complex hydrophilic, thus preventing the formation of p33 aggregates and promoting the transport from the cytoplasm to the peroxisome membranes. At the

destination the host HSP70 facilitates the membrane integration of p33 in an ATP-dependent manner. The integration of p33 into the membrane contributes to the proper folding of p33, with its C and N terminal ends carrying the RNA binding site and the protein interaction domains exposed towards the cytosolic surface of the membrane. This conformation is the “active” form of p33. Acting like a pair of pliers p33 facilitates the proper folding of the viral RNA for replication by weakening the RNA-RNA interaction between the silencer and the genomic promoter elements, thus facilitating the initiation of replication by the viral replicase complex.

After the new RNA is synthesized, a series of phosphorylation sites adjacent to the central RNA binding site are getting phosphorylated that weakens the RNA - p33 interactions. This facilitates the release of the newly synthesized viral (+)RNA from the viral replicase complex.

Future directions

In all three areas of my research there are unanswered questions:

The plant kinase, which phosphorylates p33, is currently unknown. The yeast genome wide screen identified kinases, which alters the accumulation of viral RNA. Examining their plant analogs might lead to the identification of the host kinase(s), which phosphorylates the p33 in the native plants.

Another possible approach to identify the kinase(s) would be the chemical inhibition of the different kinase families, and examine the ability of the plant extract to phosphorylate the p33 at the predicted phosphorylation sites. This way we can narrow down the search to a distinct group of kinases.

Finding the cellular localization of the kinase would be another way which can lead to the identification of the kinase(s). Using ultracentrifugation techniques we can separate plant cell organelles and make protein preparations from them which can be tested in the in vitro phosphorylation experiments.

I focused my research on only two phosphorylation sites adjacent to the RNA binding motif of p33, but there are other phosphorylation sites predicted in the protein by the NetPhos prediction program. Examining the possible role of them may lead to a better understanding of the viral replication process.

The experiments to demonstrate the RNA chaperone activity of the p33 showed weak chaperone activity. Taking advantage of the new tools developed since the original experiments were made (yeast cell free extract, MBP fusion protein replication system) one can develop an experimental system to show stronger evidence. At the time I did the experiments we did not have a recombinant CNV replicase system. The CNV replicase we had was purified from infected plants and obviously we did not have a way to adjust p33-p92 ratio like we did in the recombinant TCV replicase system. Since then we developed a yeast membrane based system adding recombinant MBP fusion p92 and p33 expressed in *E. coli*.

Using the new system one can adjust the p92-p33 ratio, and examine the effects on the RDRP activity. The new experimental system can show stronger evidence than the heterologous TCV replicase-CNV p33 system.

Dissecting the role of HSP70 family proteins, in plant-virus interactions is important. I showed the importance of yeast HSP70 in viral replication in vitro. The observation that Ssa is part of the viral replicase complex suggests that Ssa plays other roles during the replication. HSP 70-s usually makes short term interactions with the target proteins, and after re-folding them search for new substrate. The functions of Ssa I demonstrated in the fifth chapter require short term interactions. The fact that Ssa co-purifies with the viral replicase complex suggests that Ssa plays other roles during the replication, which require long term interaction. Identifying the host HSP70 proteins in plants, which play a role in viral replication is important, not just for the better understanding of the virus-host interactions, but for chemical and/or biological inhibition of the host HSP70 functions. I think that this approach could lead to the discovery of novel antiviral drugs or other antiviral approaches.

References

- Ahlquist P** (2002) RNA-dependent RNA polymerases, viruses, and RNA silencing. *Science* **296**: 1270-1273
- Ahlquist P, Noueir AO, Lee WM, Kushner DB, Dye BT** (2003) Host factors in positive-strand RNA virus genome replication. *Journal of Virology* **77**: 8181-8186
- Barik S, Banerjee AK** (1992) Phosphorylation by cellular casein kinase-II is essential for transcriptional activity of vesicular stomatitis-virus phosphorylation-P. *Proceedings of the National Academy of Sciences of the United States of America* **89**: 6570-6574
- Becker J, Walter W, Yan W, Craig EA** (1996) Functional interaction of cytosolic hsp70 and a DnaJ-related protein, Ydj1p, in protein translocation in vivo. *Molecular and Cellular Biology* **16**: 4378-4386
- Boorstein WR, Ziegelhoffer T, Craig EA** (1994) Molecular evolution of the HSP70 multigene family. *Journal of Molecular Evolution* **38**: 1-17
- Bracken C, Iakoucheva LM, Romero PR, Dunker AK** (2004) Combining prediction, computation and experiment for the characterization of protein disorder. *Curr Opin Struct Biol* **14**: 570-576
- Brand SR, Kobayashi R, Mathews MB** (1997) The Tat protein of human immunodeficiency virus type 1 is a substrate and inhibitor of the interferon-induced, virally activated protein kinase, PKR. *Journal of Biological Chemistry* **272**: 8388-8395
- Buck KW** (1996) Comparison of the replication of positive-stranded RNA viruses of plants and animals. *In Advances in Virus Research, Vol 47, Vol 47*. Academic Press Inc, San Diego, pp 159-251
- Burgyan J, Hornyik C, Szitty G, Silhavy D, Bisztray G** (2000) The ORF1 products of tombusviruses play a crucial role in lethal necrosis of virus-infected plants. *J Virol* **74**: 10873-10881
- Buzayan JM, Hampel A, Bruening G** (1986) Nucleotide sequence and newly formed phosphodiester bond of spontaneously ligated satellite tobacco ringspot virus RNA. *Nucleic Acids Res* **14**: 9729-9743
- Chirico WJ, Waters MG, Blobel G** (1988) 70K Heat-shock related proteins stimulate protein translocation into microsome. *Nature* **332**: 805-810
- Cristofari G, Darlix JL** (2002) The ubiquitous nature of RNA chaperone proteins. *Prog Nucleic Acid Res Mol Biol* **72**: 223-268
- Cristofari G, Ivanyi-Nagy R, Gabus C, Boulant S, Lavergne JP, Penin F, Darlix JL** (2004) The hepatitis C virus Core protein is a potent nucleic acid chaperone that directs dimerization of the viral (+) strand RNA in vitro. *Nucleic Acids Res* **32**: 2623-2631
- Cruceanu M, Urbaneja MA, Hixson CV, Johnson DG, Datta SA, Fivash MJ, Stephen AG, Fisher RJ, Gorelick RJ, Casas-Finet JR, Rein A, Rouzina I, Williams MC** (2006) Nucleic acid binding and chaperone properties of HIV-1 Gag and nucleocapsid proteins. *Nucleic Acids Res* **34**: 593-605
- Daros JA, Flores R** (2002) A chloroplast protein binds a viroid RNA in vivo and facilitates its hammerhead-mediated self-cleavage. *Embo J* **21**: 749-759

- DeStefano JJ, Titilope O** (2006) Poliovirus protein 3AB displays nucleic acid chaperone and helix-destabilizing activities. *J Virol* **80**: 1662-1671
- Evans MJ, Rice CM, Goff SP** (2004) Phosphorylation of hepatitis C virus nonstructural protein 5A modulates its protein interactions and viral RNA replication. *Proceedings of the National Academy of Sciences of the United States of America* **101**: 13038-13043
- Fouts DE, True HL, Cengel KA, Celander DW** (1997) Site-specific phosphorylation of the human immunodeficiency virus type-1 Rev protein accelerates formation of an efficient RNA-binding conformation. *Biochemistry* **36**: 13256-13262
- Freye-Minks C, Kretsinger RH, Creutz CE** (2003) Structural and dynamic changes in human annexin VI induced by a phosphorylation-mimicking mutation, T356D. *Biochemistry* **42**: 620-630
- Gao Y, Greenfield NJ, Cleverley DZ, Lenard J** (1996) The transcriptional form of the phosphoprotein of vesicular stomatitis virus is a trimer: Structure and stability. *Biochemistry* **35**: 14569-14573
- Gao Y, Lenard J** (1995) Cooperative binding of multimeric phosphoprotein (P) of vesicular stomatitis-virus to polymerase (L) and template-pathways of assembly. *Journal of Virology* **69**: 7718-7723
- Gunnery S, Mathews MB** (1998) RNA binding and modulation of PKR activity. *Methods-a Companion to Methods in Enzymology* **15**: 189-198
- Havelda Z, Dalmay T, Burgyan J** (1995) Localization of Cis-acting sequences essential for cymbidium ringspot tomosvirus defective interfering RNA replication. *Journal of General Virology* **76**: 2311-2316
- Hericourt F, Blanc S, Redeker V, Jupin I** (2000) Evidence for phosphorylation and ubiquitinylation of the turnip yellow mosaic virus RNA-dependent RNA polymerase domain expressed in a baculovirus-insect cell system. *Biochemical Journal* **349**: 417-425
- Hillman BI, Carrington JC, Morris TJ** (1987) A Defective interfering RNA that contains a mosaic of a plant-virus genome. *Cell* **51**: 427-433
- Huang LY, Sineva EV, Hargitta MRS, Sharma SD, Suthar M, Raney KD, Cameron CE** (2004) Purification and characterization of hepatitis C virus non-structural protein 5A expressed in *Escherichia coli*. *Protein Expression and Purification* **37**: 144-153
- Huang ZS, Wu HN** (1998) Identification and characterization of the RNA chaperone activity of hepatitis delta antigen peptides. *J Biol Chem* **273**: 26455-26461
- Hunter T, Karin M** (1992) The regulation of transcription by phosphorylation. *Cell* **70**: 375-387
- Ivanov KI, Puustinen P, Gabrenaite R, Vihinen H, Ronnstrand L, Valmu L, Kalkkinen N, Makinen K** (2003) Phosphorylation of the potyvirus capsid protein by protein kinase CK2 and its relevance for virus infection. *Plant Cell* **15**: 2124-2139
- Ivanov KI, Puustinen P, Merits A, Saarma M, Makinen K** (2001) Phosphorylation down-regulates the RNA binding function of the coat protein of potato virus A. *Journal of Biological Chemistry* **276**: 13530-13540
- Ivanyi-Nagy R, Davidovic L, Khandjian EW, Darlix JL** (2005) Disordered RNA chaperone proteins: from functions to disease. *Cell Mol Life Sci* **62**: 1409-1417

- Ivanyi-Nagy R, Kanevsky I, Gabus C, Lavergne JP, Ficheux D, Penin F, Fosse P, Darlix JL** (2006) Analysis of hepatitis C virus RNA dimerization and core-RNA interactions. *Nucleic Acids Res* **34**: 2618-2633
- Jaag HM, Stork J, Nagy PD** (2007) Host transcription factor Rpb11p affects tombusvirus replication and recombination via regulating the accumulation of viral replication proteins. *Virology* **368**: 388-404
- Jabbur JR, Huang P, Zhang W** (2001) Enhancement of the antiproliferative function of p53 by phosphorylation at serine 20: An inference from site-directed mutagenesis studies. *International Journal of Molecular Medicine* **7**: 163-168
- Janda M, Ahlquist P** (1993) RNA-Dependent replication, transcription, and persistence of Brome Mosaic-virus RNA replicons in *Saccharomyces-cerevisiae*. *Cell* **72**: 961-970
- Jia JH, Tong C, Wang B, Luo LP, Jiang J** (2004) Hedgehog signalling activity of Smoothed requires phosphorylation by protein kinase A and casein kinase I. *Nature* **432**: 1045-1050
- Jonczyk M, Pathak KB, Sharma M, Nagy PD** (2007) Exploiting alternative subcellular location for replication: Tombusvirus replication switches to the endoplasmic reticulum in the absence of peroxisomes. *Virology* **362**: 320-330
- Kann M, Gerlich WH** (1994) Effect of core protein-phosphorylation by protein-kinase-C on encapsidation of RNA within core particles of hepatitis-B virus. *Journal of Virology* **68**: 7993-8000
- Kann M, Sodeik B, Vlachou A, Gerlich WH, Helenius A** (1999) Phosphorylation-dependent binding of hepatitis B virus core particles to the nuclear pore complex. *Journal of Cell Biology* **145**: 45-55
- Karakasiliotis I, Chaudhry Y, Roberts LO, Goodfellow IG** (2006) Feline calicivirus replication: requirement for polypyrimidine tract-binding protein is temperature-dependent. *J Gen Virol* **87**: 3339-3347
- Karpova OV, Rodionova NP, Ivanov KI, Kozlovsky SV, Dorokhov YL, Atabekov JG** (1999) Phosphorylation of tobacco mosaic virus movement protein abolishes its translation repressing ability. *Virology* **261**: 20-24
- Kim SH, Palukaitis P, Park YI** (2002) Phosphorylation of cucumber mosaic virus RNA polymerase 2a protein inhibits formation of replicase complex. *Embo Journal* **21**: 2292-2300
- Kim SJ, Kim JH, Kim YG, Lim HS, Oh JW** (2004) Protein kinase C-related kinase 2 regulates hepatitis C virus RNA polymerase function by phosphorylation. *Journal of Biological Chemistry* **279**: 50031-50041
- King RW, Deshaies RJ, Peters JM, Kirschner MW** (1996) How proteolysis drives the cell cycle. *Science* **274**: 1652-1659
- Kong QZ, Wang JL, Simon AE** (1997) Satellite RNA-mediated resistance to turnip crinkle virus in Arabidopsis involves a reduction in virus movement. *Plant Cell* **9**: 2051-2063
- Koonin EV, Dolja VV** (1993) Evolution and taxonomy of positive-strand RNA viruses: implications of comparative analysis of amino acid sequences. *Crit Rev Biochem Mol Biol* **28**: 375-430
- Lee JY, Lucas WJ** (2001) Phosphorylation of viral movement proteins - regulation of cell-to-cell trafficking. *Trends in Microbiology* **9**: 5-8

- Lenard J** (1999) Host cell protein kinases in nonsegmented negative-strand virus (mononegavirales) infection. *Pharmacology & Therapeutics* **83**: 39-48
- Levin JG, Guo J, Rouzina I, Musier-Forsyth K** (2005) Nucleic acid chaperone activity of HIV-1 nucleocapsid protein: critical role in reverse transcription and molecular mechanism. *Prog Nucleic Acid Res Mol Biol* **80**: 217-286
- Li ZH, Barajas D, Panavas T, Herbst DA, Nagy PD** (2008) Cdc34p ubiquitin-conjugating enzyme is a component of the tombusvirus replicase complex and ubiquitinates p33 replication protein. *Journal of Virology* **82**: 6911-6926
- Macdonald A, Crowder K, Street A, McCormick C, Harris M** (2004) The hepatitis C virus NS5A protein binds to members of the Src family of tyrosine kinases and regulates kinase activity. *Journal of General Virology* **85**: 721-729
- McCartney AW, Greenwood JS, Fabian MR, White KA, Mullen RT** (2005) Localization of the tomato bushy stunt virus replication protein p33 reveals a peroxisome-to-endoplasmic reticulum sorting pathway. *Plant Cell* **17**: 3513-3531
- McClellan AJ, Brodsky JL** (2000) Mutation of the ATP-binding pocket of SSA1 indicates that a functional interaction between Ssa1p and Ydj1p is required for post-translational translocation into the yeast endoplasmic reticulum. *Genetics* **156**: 501-512
- Mir MA, Panganiban AT** (2006) Characterization of the RNA chaperone activity of hantavirus nucleocapsid protein. *J Virol* **80**: 6276-6285
- Mir MA, Panganiban AT** (2006) The bunyavirus nucleocapsid protein is an RNA chaperone: possible roles in viral RNA panhandle formation and genome replication. *Rna* **12**: 272-282
- Monkewich S, Lin HX, Fabian MR, Xu W, Na H, Ray D, Chernysheva OA, Nagy PD, White KA** (2005) The p92 polymerase coding region contains an internal RNA element required at an early step in Tombusvirus genome replication. *J Virol* **79**: 4848-4858
- Nagy PD** (2008) Yeast as a model host to explore plant virus-host interactions. *Annual Review of Phytopathology* **46**: 217-242
- Nagy PD, Pogany J** (2000) Partial purification and characterization of Cucumber necrosis virus and Tomato bushy stunt virus RNA-dependent RNA polymerases: Similarities and differences in template usage between tombusvirus and carmovirus RNA-dependent RNA polymerases. *Virology* **276**: 279-288
- Nagy PD, Pogany J** (2006) Yeast as a model host to dissect functions of viral and host factors in tombusvirus replication. *Virology* **344**: 211-220
- Nagy PD, Pogany J, Simon AE** (2001) In vivo and in vitro characterization of an RNA replication enhancer in a satellite RNA associated with Turnip crinkle virus. *Virology* **288**: 315-324
- Naito T, Kiyasu Y, Sugiyama K, Kimura A, Nakano R, Matsukage A, Nagata K** (2007) An influenza virus replicon system in yeast identified Tat-SF1 as a stimulatory host factor for viral RNA synthesis. *Proceedings of the National Academy of Sciences of the United States of America* **104**: 18235-18240
- Narayan M, Kusuhara K, Green PL** (2001) Phosphorylation of two serine residues regulates human T-cell leukemia virus type 2 Rex function. *Journal of Virology* **75**: 8440-8448

- Navarro B, Rubino L, Russo M** (2004) Expression of the Cymbidium ringspot virus 33-kilodalton protein in *Saccharomyces cerevisiae* and molecular dissection of the peroxisomal targeting signal. *Journal of Virology* **78**: 4744-4752
- Navarro B, Russo M, Pantaleo V, Rubino L** (2006) Cytological analysis of *Saccharomyces cerevisiae* cells supporting cymbidium ringspot virus defective interfering RNA replication. *J Gen Virol* **87**: 705-714
- Oster SK, Wu BD, White KA** (1998) Uncoupled expression of p33 and p92 permits amplification of tomato bushy stunt virus RNAs. *Journal of Virology* **72**: 5845-5851
- Panavas T, Hawkins CM, Panaviene Z, Nagy PD** (2005) The role of the p33 : p33/p92 interaction domain in RNA replication and intracellular localization of p33 and p92 proteins of Cucumber necrosis tomosvirus. *Virology* **338**: 81-95
- Panavas T, Hawkins CM, Panaviene Z, Nagy PD** (2005) The role of the p33:p33/p92 interaction domain in RNA replication and intracellular localization of p33 and p92 proteins of Cucumber necrosis tomosvirus. *Virology* **338**: 81-95
- Panavas T, Nagy PD** (2003) The RNA replication enhancer element of tomosviruses contains two interchangeable hairpins that are functional during plus-strand synthesis. *Journal of Virology* **77**: 258-269
- Panavas T, Nagy PD** (2003) Yeast as a model host to study replication and recombination of defective interfering RNA of Tomato bushy stunt virus. *Virology* **314**: 315-325
- Panavas T, Nagy PD** (2003) Yeast as a model host to study replication and recombination of defective interfering RNA of Tomato bushy stunt virus. *Virology* **314**: 315-325
- Panavas T, Nagy PD** (2005) Mechanism of stimulation of plus-strand synthesis by an RNA replication enhancer in a tomosvirus. *J Virol* **79**: 9777-9785
- Panavas T, Pogany J, Nagy PD** (2002) Internal initiation by the cucumber necrosis virus RNA-dependent RNA polymerase is facilitated by promoter-like sequences. *Virology* **296**: 275-287
- Panavas T, Stork J, Nagy PD** (2006) Use of double-stranded RNA templates by the tomosvirus replicase in vitro: Implications for the mechanism of plus-strand initiation. *Virology* **352**: 110-120
- Panaviene Z, Baker JM, Nagy PD** (2003) The overlapping RNA-binding domains of p33 and p92 replicase proteins are essential for tomosvirus replication. *Virology* **308**: 191-205
- Panaviene Z, Nagy PD** (2003) Mutations in the RNA-binding domains of tomosvirus replicase proteins affect RNA recombination in vivo. *Virology* **317**: 359-372
- Panaviene Z, Panavas T, Nagy PD** (2005) Role of an internal and two 3'-terminal RNA elements in assembly of tomosvirus replicase. *Journal of Virology* **79**: 10608-10618
- Panaviene Z, Panavas T, Serva S, Nagy PD** (2004) Purification of the Cucumber necrosis virus replicase from yeast cells: Role of coexpressed viral RNA in stimulation of replicase activity. *Journal of Virology* **78**: 8254-8263
- Pawson T, Scott JD** (1997) Signaling through scaffold, anchoring, and adaptor proteins. *Science* **278**: 2075-2080

- Pogany J, Fabian MR, White KA, Nagy PD** (2003) A replication silencer element in a plus-strand RNA virus. *Embo J* **22**: 5602-5611
- Pogany J, White KA, Nagy PD** (2005) Specific binding of tombusvirus replication protein p33 to an internal replication element in the viral RNA is essential for replication. *J Virol* **79**: 4859-4869
- Puustinen P, Rajamaki ML, Ivanov KI, Valkonen JPT, Mäkinen K** (2002) Detection of the potyviral genome-linked protein VPg in virions and its phosphorylation by host kinases. *Journal of Virology* **76**: 12703-12711
- Raghavan V, Malik PS, Choudhury NR, Mukherjee SK** (2004) The DNA-A component of a plant geminivirus (Indian mung bean yellow mosaic virus) replicates in budding yeast cells. *Journal of Virology* **78**: 2405-2413
- Rajendran KS, Nagy PD** (2003) Characterization of the RNA-binding domains in the replicase proteins of tomato bushy stunt virus. *J Virol* **77**: 9244-9258
- Rajendran KS, Nagy PD** (2004) Interaction between the replicase proteins of Tomato bushy stunt virus in vitro and in vivo. *Virology* **326**: 250-261
- Rajendran KS, Nagy PD** (2006) Kinetics and functional studies on interaction between the replicase proteins of Tomato Bushy Stunt Virus: requirement of p33:p92 interaction for replicase assembly. *Virology* **345**: 270-279
- Rajendran KS, Pogany J, Nagy PD** (2002) Comparison of turnip crinkle virus RNA-dependent RNA polymerase preparations expressed in *Escherichia coli* or derived from infected plants. *J Virol* **76**: 1707-1717
- Rein A, Henderson LE, Levin JG** (1998) Nucleic-acid-chaperone activity of retroviral nucleocapsid proteins: significance for viral replication. *Trends Biochem Sci* **23**: 297-301
- Rochon DM** (1991) Rapid denovo generation of defective interfering RNA by cucumber necrosis virus mutants that do not express the 20-KDA nonstructural protein. *Proceedings of the National Academy of Sciences of the United States of America* **88**: 11153-11157
- Romero, Obradovic, Dunker K** (1997) Sequence Data Analysis for Long Disordered Regions Prediction in the Calcineurin Family. *Genome Inform Ser Workshop Genome Inform* **8**: 110-124
- Romero P, Obradovic Z, Dunker AK** (2004) Natively disordered proteins: functions and predictions. *Appl Bioinformatics* **3**: 105-113
- Rubino L, Russo M** (1998) Membrane targeting sequences in tombusvirus infections. *Virology* **252**: 431-437
- Salonen A, Ahola T, Kaariainen L** (2004) Viral RNA replication in association with cellular membranes. *In Membrane Trafficking in Viral Replication*, Vol 285. Springer-Verlag Berlin, Berlin, pp 139-173
- Scholthof KBG, Scholthof HB, Jackson AO** (1995) The Tomato bushy stunt virus replicase proteins are coordinately expressed and membrane-associated. *Virology* **208**: 365-369
- Serva S, Nagy PD** (2006) Proteomics analysis of the tombusvirus replicase: Hsp70 molecular chaperone is associated with the replicase and enhances viral RNA replication. *J Virol* **80**: 2162-2169

- Serva S, Nagy PD** (2006) Proteomics analysis of the tombusvirus replicase: Hsp70 molecular chaperone is associated with the replicase and enhances viral RNA replication. *Journal of Virology* **80**: 2162-2169
- Shapka N, Stork J, Nagy PD** (2005) Phosphorylation of the p33 replication protein of Cucumber necrosis tombusvirus adjacent to the RNA binding site affects viral RNA replication. *Virology* **343**: 65-78
- Sokolova M, Pruffer D, Tacke E, Rohde W** (1997) The potato leafroll virus 17K movement protein is phosphorylated by a membrane-associated protein kinase from potato with biochemical features of protein kinase C. *FEBS Letters* **400**: 201-205
- Song CZ, Simon AE** (1994) RNA-dependent RNA polymerase from plants infected with turnip crinkle virus can transcribe (+)-strands and (-)-strands of virus-associated RNAs. *Proceedings of the National Academy of Sciences of the United States of America* **91**: 8792-8796
- Stork J, Panaviene Z, Nagy PD** (2005) Inhibition of *in vitro* RNA binding and replicase activity by phosphorylation of the p33 replication protein of Cucumber necrosis tombusvirus. *Virology* **343**: 79-92
- Street A, Macdonald A, Crowder K, Harris M** (2004) The hepatitis C virus NS5A protein activates a phosphoinositide 3-kinase-dependent survival signaling cascade. *Journal of Biological Chemistry* **279**: 12232-12241
- Takacs AM, Barik S, Das T, Banerjee AK** (1992) Phosphorylation of specific serine residues within the acidic domain of the phosphoprotein of vesicular stomatitis-virus regulates transcription *in vitro*. *Journal of Virology* **66**: 5842-5848
- Tompa P, Csermely P** (2004) The role of structural disorder in the function of RNA and protein chaperones. *FASEB J* **18**: 1169-1175
- Trutnyeva K, Bachmaier R, Waigmann E** (2005) Mimicking carboxyterminal phosphorylation differentially effects subcellular distribution and cell-to-cell movement of Tobacco mosaic virus movement protein. *Virology* **332**: 563-577
- Waigmann E, Chen MH, Bachmaier R, Ghoshroy S, Citovsky V** (2000) Regulation of plasmodesmal transport by phosphorylation of tobacco mosaic virus cell-to-cell movement protein. *EMBO Journal* **19**: 4875-4884
- Wang CC, Chang TC, Lin CW, Tsui HL, Chu PB, Chen BS, Huang ZS, Wu HN** (2003) Nucleic acid binding properties of the nucleic acid chaperone domain of hepatitis delta antigen. *Nucleic Acids Res* **31**: 6481-6492
- Wang RYL, Nagy PD** (2008) Tomato bushy stunt virus co-opts the RNA-binding function of a host metabolic enzyme for viral genomic RNA synthesis. *Cell Host & Microbe* **3**: 178-187
- Wernerwashburne M, Stone DE, Craig EA** (1987) Complex interactions among members of an essential subfamily of HSP70 genes in *Saccharomyces-cerevisiae*. *Molecular and Cellular Biology* **7**: 2568-2577
- White KA, Morris TJ** (1994) Enhanced competitiveness of tomato bushy stunt virus defective interfering RNAs by segment duplication of nucleotide insertion. *Journal of Virology* **68**: 6092-6096
- White KA, Morris TJ** (1994) Recombination between defective Tombusvirus RNAs generates functional hybrid genomes. *Proceedings of the National Academy of Sciences of the United States of America* **91**: 3642-3646

- White KA, Nagy PD** (2004) Advances in the molecular biology of tombusviruses: gene expression, genome replication, and recombination. *Prog Nucleic Acid Res Mol Biol* **78**: 187-226
- White KA, Nagy PD** (2004) Advances in the molecular biology of tombusviruses: Gene expression, genome replication, and recombination. *In Progress in Nucleic Acid Research and Molecular Biology, Vol 78, Vol 78*. Academic Press Inc, San Diego, pp 187-226
- Younis I, Green PL** (2005) The human T-cell leukemia virus Rex protein. *Frontiers in Bioscience* **10**: 431-445
- Zuniga S, Sola I, Moreno JL, Sabella P, Plana-Duran J, Enjuanes L** (2007) Coronavirus nucleocapsid protein is an RNA chaperone. *Virology* **357**: 215-227

VITA

Name: Jozsef Stork

Place of birth: Budapest, Hungary

Date of birth: 06 06 1970

Educational institutions attended: University of Godollo, Godollo Hungary

Professional publications:

A key role for heat shock protein 70 in localization and insertion of the tombusvirus replication proteins to intracellular membranes.

Wang RY, Stork J, Nagy PD.

J Virol. 2009 Jan 19. [Epub ahead of print]

In vitro assembly of the Tomato bushy stunt virus replicase requires the host Heat shock protein 70.

Pogany J, Stork J, Li Z, Nagy PD.

Proc Natl Acad Sci U S A. 2008 Dec 16;105(50):19956-61. Epub 2008 Dec 5.

Host transcription factor Rpb11p affects tombusvirus replication and recombination via regulating the accumulation of viral replication proteins.

Jaag HM, Stork J, Nagy PD.

Virology. 2007 Nov 25;368(2):388-404. Epub 2007 Aug 8.

Use of double-stranded RNA templates by the tombusvirus replicase in vitro: Implications for the mechanism of plus-strand initiation.

Panavas T, Stork J, Nagy PD.

Virology. 2006 Aug 15;352(1):110-20. Epub 2006 Jun 12.

Inhibition of in vitro RNA binding and replicase activity by phosphorylation of the p33 replication protein of Cucumber necrosis tomosvirus.

Stork J, Panaviene Z, Nagy PD.

Virology. 2005 Dec 5;343(1):79-92.

Phosphorylation of the p33 replication protein of Cucumber necrosis tomosvirus adjacent to the RNA binding site affects viral RNA replication.

Shapka N, Stork J, Nagy PD.

Virology. 2005 Dec 5;343(1):65-78.